

List of relevant changes of the manuscript GMD-2016-47

Will et al. , “Coupling of the regional climate model COSMO-CLM using OASIS3-MCT with regional ocean, land surface or global atmosphere model: description and performance”

Abstract

Adapted to the revised presentation of results

1. Introduction

No major changes

2. Description of model components

Line 135: more detailed description of the content of the article

Line 162: clarification of model versions used added

3. Description and optimization of COSM

Line 607: function used for relaxation in CCLM+MPI-ESM added

Line 660ff: Clarification of the physics of coupling.

4. Computational Efficiency

Line 719: Introduction to presentation of the results improved

Line 761: Clarification about the configurations of model physics and dynamics

Line 790 ff: Section strategy for finding an optimum configuration now section 4.3 with several clarifications of the strategy suggested

Line 864: Difference between SMT and ST mode described more precisely

Line 950ff. Result presentation now in two sections

- New section ‘Optimum configuration’ applies the strategy of finding it to different couplings and presents the results
- Section ‘extra time and cost’ describes the analysis of these cost in a more systematic way. All numbers are now directly comparable. See also table 8, section 3.3.
- In Section “coupling cost reduction’ the mapping of processes on cores is described in more detail to improve understanding.

Line 1222: The description of potential improvement of CCLM+MPI-ESM is removed

5. Conclusions

The more detailed analysis of extra cost of coupling is summarised.

Appendix A: Source code availability

- New description of source code availability

-

Appendix B: Model time step organization

- No changes

Figures

Fig.1: new

Fig.2-4: improved visibility of “optimum configuration“

Fig. 7-13: Same layout for all figures

Tables

Table 1: additional acronyms CCLM_OC to CCLM_sa,OC

Table 8: section 3.3.1-3.3.5 new

Response to GMD-2016-47-SC1 (Editor)

Dear authors,

In my role as Executive editor of GMD, I would like to bring to your attention our Editorial version 1.1:

<http://www.geosci-model-dev.net/8/3487/2015/gmd-8-3487-2015.html>

This highlights some requirements of papers published in GMD, which is also available on the GMD website in the 'Manuscript Types' section:

http://www.geoscientific-model-development.net/submission/manuscript_types.html

In particular, please note that for your paper, the following requirement has not been met in the Discussions paper:

- "The main paper must give the model name and version number (or other unique identifier) in the title."

Please add the version number of COSMO-CLM in the title upon your revised submission to GMD.

Answer: This was done and the number 4.8 added in the title

Additionally, I ask you to revise the Code Availability Section.

First of all it should be clearly made as an individual section. But the type-setting of copernicus will ensure that anyway, but, secondly, the content of the Code Availability section is somewhat confusing: On the one hand side code parts not discussed in the article (COSMO-ART) are named. If it is not used in your article it should not be mentioned here. On the other hand side you write about a lot of other climate system models which are coupled to COSMO-CLM via OASIS3-MCT. Therefore the availability of these models should also be clarified in the Code Availability section. Last but not least, a kind reader would be interested how to access the COSMO-CLM version including OASIS3-MCT. For the latter it would be enough to say that it is available by contacting one of the authors and will be part of a future official COSMO(-CLM) version.

Answer: The availability of all components is now specified in Appendix A as "source code availability". The sentence related to COSMO-ART was removed.

Response to GMD-2016-47-RC1 (anonymous)

Introduction

Coding and technical aspects of coupling Earth System Models are often relegated to institutional reports seldom referenced or widely read, and outcomes of work in coupling and load balancing are often blindly used by physical and biogeochemical modeling groups. Therefore I commend the authors for documenting their expansive coupling work, and for submitting it to be reviewed for a journal with a readership that bridges the coupler development and physical modeling communities. I do, however, have reservations about the final results, methods, and one comment about the scope of the cited literature.

Answer: we appreciate that the effort we made to document our technical work could be hosted by the journal. In this revision, we try to answer the referee questions, adding details, without overloading the article too much.

Significance of this paper in the context of other work

The manuscript's introduction could extend the perceived reach of the work if it were to illustrate its international significance. There are several latest-generation regional coupled earth system models in development in the U.S. and Canada, some of which use MCT and takes advantage of the work of Craig et al. (2012) that could have been cited and have appeared in the reviewed literature in recent years. The reason I mention these publications is to say that the introductory argument perhaps could be further enhanced, since work on load balancing high-resolution regional coupled earth system models is taking place in many parts of the Earth System Modeling community. This helps to widen the appeal of the current manuscript, and its significance.

Answer: the referee rightly emphasises that load balancing is not a new issue in our community. Studies based on CESM model, for example, are familiar to the authors (Craig 2012 is cited in the article, line 385). We have also mentioned Dennis et al. 2012 (line 88) and Alexeev et al. 2014 (line 90) in our introduction. We added a reference to Balaprakash et al 2014 (line 809) in chapter "4.3 Strategy for finding an optimum configuration" and we have mentioned that, in our case, "due to the heterogeneity of our coupled systems, a single algorithm cannot be proposed (as in Balaprakash et al, 2014)". Unless the CESM package, the OASIS library allows an unlimited kind of component combination in coupled systems. For the moment, it is rather complicated to propose an automatic load balancing tool that could deliver an optimal solution for all combinations. We hope that the present article will help the OASIS community to develop an ability to better balance their systems and, in a second step, propose solutions that may be gathered in a single tool.

Efficiency versus accuracy

This paper discusses a considerable number (five) of different coupled model configurations using CCLM, however only scant information is provided on each one of these configurations. It would be particularly useful to view maps of model domains to demonstrate the individual configurations for each of the coupled model systems in Table 2.

Answer: Model domains are shown now in Figure 1.

This would help make it clear exactly how much ocean, land and sea ice exist in the respective model domains. Such details can have a large impact on scalability and parallel efficiency, especially in the cryosphere (sea ice and snow). Therefore I suggest providing greater detail on the physical configuration of each of the models chosen, because this, too, has an enormous impact on the model solution.

Answer: We fully agree with the reviewer that details on the physical configuration have an impact on individual performances of components, and consequently, on performances of the whole coupled system. However, the article is not investigating the physical

performance of the coupled systems. It is rather focussing on presentation of the coupling method, the computational performance in COSMO-CLM reference configuration and finding of an “optimum configuration”. It is thus out of scope to discuss in detail the amount of ice and snow in the model domain and the impact on computational performance. It is also out of scope to discuss physical and dynamical parameters that could influence the computing performance. This remains for future work. Further below we propose an improved definition of our component characteristics by parameters relevant for computing performances. We also answer the referee’s questions about CICE.

To illustrate this point, I focus here on the implementation of CICE Version 5 for CCLM+TRIMNP+CICE. The computational efficiency of the solution in CICE is heavily dependent upon the total number of sea ice thickness categories used, the number of tracers needed, for example, by melt pond and ice-age tracking and biogeochemistry, and most importantly, the sea ice mechanics solution. If CICE 5 has been configured to use anisotropic (Elastic Anisotropic Plastic; EAP) sea ice mechanics, then it will definitely be expensive, and, could take as much as 30% of the total model execution time in pan-arctic fully coupled regional models, if a highly converged plastic sea-ice solution is required (2-second sub-cycling). However, if using the Elastic Viscous Plastic (EVP) sea ice rheology with 10-second sub-cycling, the time to solution of the sea ice model greatly improves, with only slight degradation of the plastic solution. In this configuration, the sea ice model could take only 10% of the total core time of running the model. It is still unknown as to which of the two variants is physically more accurate. This is precisely the same CICE Version 5.1 code, in the same coupled framework, using MCT, but with two different namelist settings yet to be fully explored in the literature. Further issues with the CICE coupling are discussed in the appendix.

Answer: EVP was used ($k_{dyn}=1$). However, CICE domain covers only the Baltic Sea and Kattegat, not the pan-arctic. The sea ice which appears in a relatively small domain like the Baltic Sea and disappears totally in summer has less complicated features compared to the Arctic. However, we cannot say how much different the calculations would be if EAP was chosen, as no sensitivity tests about these parameters have been conducted. The scope of the paper was to present a strategy of analysis of the computational performance of the coupled system in comparison to stand-alone performance. A deeper analysis is out of scope of the paper and remains for future work. We highlight the relevance and the opportunities of such an analysis in the result section for the CCLM+MPI-ESM coupling (line 1111 ff).

This CICE anecdote drives at my main criticism of this paper as it currently stands: It seems to be a vacant conclusion to discuss model efficiency without discussing model accuracy. The most efficient model one can design is a constant number, but seldom is this model the most accurate. The only way this limitation in the current manuscript can be remedied is to explicitly state the configurations used for each particular model in the tests presented, including graphically representing the domains used. However, due to the number of different models and model configurations used, this may balloon the paper to unmanageable proportions. However, as the paper currently stands, there is too little information available for it to be useful for other groups trying to address coupled model efficiency in their particular configurations.

Answer: The aim of the paper is to analyse the performance of the coupled systems using a configuration common for climate applications. Therefore, the analysis of computational performance was conducted using well tested and recommended climate modelling configurations for each component model without any idealisation, e.g. the I/O is the same as in standard climate applications. This is described in section 4.1, line 746 ff.. We agree with the reviewer that a detailed description of all configuration would balloon the paper and

hope having found an appropriate compromise concentrating on configuration details specific for the couplings described in chapter 2.

However, the computing performances of the coupled system necessarily depends on the performances of each component. We agree with the referee that the choice of an additional component cannot only depend of its computing cost. Obviously, the model accuracy (or model skill) is the most important criterion. The article does not say anything about component accuracy in stand alone mode or, what we consider to be even more important, component accuracy in coupled mode. This article addresses the usability of configurations, which is a prerequisite of scientific analysis described in other papers, as for example Pham et al. 2016 (CCLM+NEMO-NORDIC) or Davin et al. 2016 (CCLM+CLM).

Nevertheless, we agree that more information is usefull to facilitate the comparison of component costs and to estimate the cost of possible other configurations (e. g. with other resolutions). An interesting suggestion is the computing performance metrics described in Balaji et al. 2017, particularly the 2 parameters describing the models: resolution and complexity. "Resolution" -G- is measured as the number of grid points (or more generally, spatial degrees of freedom) NX,NY,NZ per component. "Complexity" -V- is measured as the number of 3D prognostic variables per component (to be able to compare 3D models, like atmosphere, with 2D models, like land models, it is assumed that V of 2D models are equal to 1). These 2 parameters are added in Table 3.

G and V are key parameters to explain why some components are more costly than others (MPI-ESM, with highest G and V, is also the one which induces the highest coupling cost). This information is emphasised in § 4.5 "Extra time and costs", line 1005 ff. It can also be used for users who would like to estimate the extra cost induced by changes in a coupled component, like a resolution increase (horizontal or vertical) or a complexity increase (additional calculations like biogeochemistry in the ocean or chemistry in the atmosphere ...)

Conclusion

In some respects, the scope of this paper is too large and should be refined. The concluding arguments would be far more compelling, and, I believe, interesting to the modeling community, if it explored individual coupled configurations, and efficiency related to a group of relatively standard model settings in each component model. However, this is probably beyond the scope intended by the authors, and therefore one way to make sure the good work already done is published would be to: 1) Provide greater details of each of the models used to produce the results, including model domain maps, of the model configuration tables, the latter in an appendix; and 2) Provide at least some indication of the accuracy of the solutions. Otherwise, one is left to wonder as to how exactly the results were produced.

Answer: As already stated, (1) we use recommended and overall tested model configurations for climate application over Europe. (2) a map is added in Figure 1 showing the model domains and (3) metrics are added in Table 3 to better estimate the model accuracy. Furthermore, the results of computational performance are revised and presented in a more consistent way. Figures 5 and 6 together with table 8 provide consistent results. In table 8 the section 3.3 shows a systematic analysis of extra costs of coupling for all couplings investigated at optimum configuration. The components are described in lines 920 ff.

Currently the paper fails the reproducibility test, because insufficient information is provided to repeat the experiments. This, alone, is grounds for significant revision, which I hope the authors will undertake.

Answer: We thank the reviewer for this comment. The reproducibility of results is an important aspect of community work in the CLM Community and we hope to be able to show it in the following. We added details on how to get the model versions and configurations used for the performance analysis presented in the Appendix under “source code availability”, line 1135 ff. At the moment, the model versions used are not official CLM-Community model versions but available from the model developers. An implementation into an official CLM-Community released version is ongoing. Hereby we follow the procedure of source code development introduced in the COSMO and CLM Community. Each experiment can be repeated with the set up information from the article and using the model input files. To get the individual coupled systems, model input files and configuration details the authors have to be contacted as described in the Appendix.

All results presented and the original model output files used are available from the lead author, following the rules of good scientific practice.

However, the machine blizzard is not available anymore. Thus the results are, strictly speaking, not reproducible. This, however, is not the responsibility of the authors and true for each numerical model result after some years. The authors believe that the results highlighted are robust and can be obtained on a similar machine as well.

Appendix – CICE configuration and coupling

This appendix addresses technicalities of the CICE setup that were puzzling to the reviewer. First, the authors may be interested to know that there were important bug fixes in the code between version 5.0 and 5.1 of CICE (update is in Hunke et al., 2015), however these would be unlikely to influence computational performance. Setting this aside, there are further improvements in the computational performance of the model using EAP that are being updated by the University of Reading at the current time. It is impossible to know whether or not this affects the results in this paper, because the CICE configuration used in this paper is never made clear. Also, and perhaps I missed it in the text, whether or not the namelist option “distribution_type” is changed in CICE is not discussed. This affects computational performance.

Answer: Parameters used in CICE and TRIMNP are the same as in real climate simulations for Europe. They are listed and discussed in the following but not included in as much detail in the paper.

CICE:

```
+ kitd = 1; ktherm = 2; conduct = 'MU71'
+ kdyn = 1 (means EVP is used); ndte = 60; revised_evp = .false.; advection = 'upwind'
+ shortwave = 'dEdd'; albedo_type = 'default'
+ tr_brine = .false.; skl_bgc = .false.; bgc_flux_type = 'Jin2006'
+ formdrag = .false.
+ tr_iage = .true.; tr_FY = .true.; tr_lvl = .true.; tr_pond_cesm = .false.; tr_pond_topo =
.false.; tr_pond_lvl = .true.; tr_aero = .false.
+ distribution_type = "cartesian"; processor_shape = "square-pop"; distribution_wght =
"latitude"; ew_boundary_type = "open" ; ns_boundary_type = "open"
```

The original formula of category boundary (kcatbound = 0) with the thickness boundaries for five thickness categories and the linear remapping of the ice thickness distribution (kitd = 1) are configured in this study. The thermodynamics option new “mushy” formulation (ktherm=2) is applied in which salinity evolves (Turner et al., 2013). For each thickness category, CICE computes changes in the ice and snow thickness and vertical temperature profile resulting from radiative, turbulent, and conductive heat fluxes. The ice has a temperature-dependent specific heat to simulate the effect of brine pocket melting and freezing. The standard thermal conductivity option used is ‘MU71’ following Untersteiner (1964) and

Maykut and Untersteiner (1971). The explicit melt pond parameterisation uses the delta-Eddington radiation scheme with the default (ccsm3) shortwave parameterisation which incorporates melt ponds implicitly by adjusting the albedo based on surface conditions. The revised Elastic Viscous Plastic (EVP) sea ice rheology and the upwind advection algorithm are applied.

The distribution type option is the standard Cartesian distribution of blocks which allows redistribution via a 'rake' algorithm for improved load balancing across processors, and redistribution based on space-filling curves. The processor shape is square-pop. The 'latitude' option weights the blocks based on latitude and the number of ocean grid cells they contain. The Neumann boundary conditions are set up for both east-west and north-south boundary type.

TRIMNP:

hdif_u=50., hdif_v=50., hdif_w=0., hdif_s=25., hdif_t=25., hdif_q=0.,

The dynamics of the free surface are discretised semi-implicitly, and the resulting linear equation system is solved with a pre-conditioned conjugate gradient method. The vertical mixing and friction including non-linear bottom friction and surface wind stress are also solved with a semi-implicit method. The vertical mixing and friction coefficients are parameterised using prognostic equations for turbulent kinetic energy and dissipation (Umlauf and Burchard 2005). For horizontal diffusion, harmonic terms are used with scale dependent constants. The lateral diffusion and the viscosity constants are 25 m²/s and 50 m²/s, respectively. Advection for all time-dependent variables is done with a Semi-Lagrangian method, where at the end of each time step the values of the variables at the corresponding grid points (the arrival points) are determined by following a trajectory backwards in time for one time step interval to the departure points. The values of the variables at the departure points are determined by trilinear interpolation. For details see Cheng et al. (1993).

Most importantly, however, is the information within Table 5 on how CICE is coupled to CCLM. My understanding is that the U symbol indicates fluxes being passed from CCLM to CICE. If this is the case, there is only one feedback from CICE to CCLM in Table 5 (SST), which draws into question the physical consistency of the coupling. If this were to be a fully coupled model, then there must be more feedbacks that just surface temperature to the atmosphere. For sea ice, the most important feedback is either albedo or reflected shortwave radiation, passing back from the sea ice model to the atmosphere, but neither is listed, which leads one to assume that albedo is being calculated in the atmospheric model independently. Given the sophistication of the Delta-Eddington albedo parameterization in CICE, this seems odd. This inconsistency should be addressed before publication.

It is also odd that the atmosphere is calculating sensible and latent heat fluxes, given that the CICE configuration has five sea ice thickness categories each calculating an independent surface temperature upon which turbulent fluxes are based. Hence the turbulent heat fluxes must be inconsistent with the surface stress term, which is being calculated internally in CICE in the configuration given. When this calculation is done within CICE, assuming Monin-Obukhov stability calculations are being performed, the drag coefficient accounts for the individual surface temperature of each of the five sea ice thickness categories. If this calculation is not being performed in CICE, then the only alternative would be for the sea ice model to use only neutral drag, which would also be inconsistent with the sensible and latent heat flux components of turbulent transfer being passed from the atmosphere.

The only way to remedy this is either to specify surface stress from the atmospheric model, or to fully use the turbulent transfer calculations in CICE, and pass the sensible and latent heat fluxes back to the atmosphere from the sea ice model. This is the reverse of what is currently being done, or at least described in this manuscript. This inconsistency should also be addressed before publication.

Answer: We agree that the inconsistency exists and needs to be improved in the future. We explain this inconsistency in the paper now (chapter 3.4, line 630 ff). In the experiment CCLM+TRIMNP+CICE, only SSTs are passed to the atmosphere as in the version of CCLM used at the time when the experiment was conducted for this study the partial sea ice cover, snow on sea ice and water on sea ice are not considered. In a water grid box of CCLM, the albedo parameterisation switches from ocean to sea ice if surface temperature is below a freezing temperature threshold of -1.7°C . We would have passed sea ice fraction to CCLM as it was done for NEMO-Nordic. However, we think that careful checks e.g. for reflected shortwave radiation should be made for the coupled system model CCLM+TRIMNP+CICE if sea ice fraction and albedo from CICE are sent to CCLM. These checks remain for future work.

In the current study, no sea ice information from CICE was passed to CCLM. But they were sent to TRIMNP. In TRIMNP the surface temperature is calculated as a combination of SSTs from TRIMNP and the sea ice skin temperatures from CICE, weighted by the sea ice concentration before the combined surface temperature is passed to CCLM. In Table 5, "surface temperature over sea/ocean" is used instead of SST to avoid a potential misunderstanding in case of sea ice existence.

We also think that even if sea ice fraction from CICE is sent to CCLM, the latent and sensible heat fluxes in CCLM are still different to those in CICE due to different turbulent schemes of the two models CCLM and CICE. The inconsistency can be removed only if all models use the same energy fluxes, calculated in one model at the highest resolution, for example in CICE model, as the reviewer suggested. This strategy could be applied in future studies considering the result of this performance study, that exchanging much more fields has a small impact on cost.

References:

- Alexeev, Y., Mickelson, S., Leyffer, S., Jacob, R., and Craig, A., 2014: The Heuristic Static Load-Balancing Algorithm Applied to the Community Earth System Model, in: 28th IEEE International Parallel and Distributed Processing Symposium, no. 28 in Parallel & Distributed Processing Symposium Workshops, pp. 1581–1590, IEEE, doi:10.1109/IPDPSW.2014.177
- Balaji, V., Maisonnave, E., Zadeh, N., Lawrence, B. N., Biercamp, J., Fladrich, U., Aloisio, G., Benson, R., Caubel, A., Durachta, J., Foujols, M.-A., Lister, G., Mocavero, S., Underwood, S., and Wright, G., 2017: CPMIP: Measurements of Real Computational Performance of Earth System Models in CMIP6 , *Geosci. Model Dev.*, **46**, 19-34, doi:10.5194/gmd-10-19-2017
- Balaprakash, P., Alexeev, Y., Mickelson, S. A., Leyer, S., Jacob, R. L. and Craig, A. P., 2014: Machine learning based load-balancing for the CESM climate modeling package, in Proceedings for 11th International Meeting on High-Performance Computing for Computational Science (VECPAR 2014)
- Davin, E. L., Maisonnave E. and Seneviratne, S. I., 2016: Is land surface processes representation a possible weak link in current Regional Climate Models ? , *Environ. Res. Lett.*, **11** 074027
- Dennis, J. M., Vertenstein, M., Worley, P. H., Mirin, A. A., Craig, A. P., Jacob, R., and

Mickelson, S., 2012: Computational performance of ultra-high-resolution capability in the Community Earth System Model, *Int. J. High Perf. Comp. Appl.*, 26, 5–16, doi:10.1177/1094342012436965

- Cheng, R., Casulli, V., Gartner, J., 1993. Tidal, Residual, Intertidal Mudflat (TRIM) Model and its Applications to San Francisco Bay, California. *Estuarine, Coastal and Shelf Science*, 36, 235–280
- Jin, M., Deal, C. J., Wang, J., Shin, K. H., Tanaka, N., Whittedge, T. E., Lee, S. H., and Gradinger, R. R., 2006. Controls of the landfast ice-ocean ecosystem offshore Barrow, Alaska. *Ann. Glaciol.*, 44:63–72.
- Maykut G. A. and Untersteiner N., 1971. Some results from a time dependent thermodynamic model of sea ice. *J. Geophys. Res.*, 76:1550–1575.
- Pham, Trang Van, J. Brauch, B. Früh, B. Ahrens, 2016: Simulation of snowbands in the Baltic Sea area with the coupled atmosphere-ocean-ice model COSMO-CLM/NEMO. *Met. Z.*, DOI: 10.1127/metz/2016/0775
- Souverijns, N., Gossart, A., Demuzere, M., Lhermitte, S., Gorodetskaya, I., Van Lipzig, N., 2016: Evaluation of a default COSMO-CLM simulation over Antarctica with a focus on accumulation and the surface mass balance, *Cosmo Assembly*, Lüneberg, 20-23 September 2016
- Turner, A. K., Hunke, E. C., and Bitz, C. M., 2013. Two modes of sea-ice gravity drainage: a parameterization for large-scale modeling. *J. Geophys. Res.*, 118:2279–2294, doi:10.1002/jgrc.20171.
- Umlauf, L., Burchard, H., 2005. Second-order turbulence models for geophysical boundary layers. A review of recent work. *Cont. Shelf Res.*, 25, 795–827.
- Untersteiner, N., 1964. Calculations of temperature regime and heat budget of sea ice in the Central Arctic. *J. Geophys. Res.*, 69:4755–4766.

Response to GMD-2016-47-RC2 (Sophie Valcke)

Dear Ms. Valcke,

we thank you for the constructive and detailed comments and questions and hope to give an easy to follow and satisfactory answer. We tried to consider all of your points and some more with the article revision. We also kept some redundancy of the basic aims in order to facilitate following the idea of the article.

Please, keep in mind that all references to the paper given in the following are references to the revised version of the article. Your comments are given in black, our answers in blue.

Best regards, Andreas Will

.

General comments

This paper present a detailed analysis of the performance of coupling configurations involving the COSMO-CLM regional model. An extensive literature exists on the performance analysis of individual models or codes but there is much less published on the performance of the coupled system and on the coupling aspects per se. This paper addresses this gap and as the work onto which it is based is sound, it deserves publication. However, I consider it needs major revisions before being published.

Answer: We are very pleased to know that our paper is interesting from your point of view and we did the best to answer your questions.

Specific comments

My first main concern is about the way the results on the optimum configurations (p.25, section 4.4, Fig. 5 and Table 8) are presented ; currently, they are difficult to appreciate because there is, on one hand, a lot of information (sometimes superfluous), and on the other hand, some missing details.

Answer: Thank you for that comment. We revised chapter 4, improved the figure description, separated figures 3-4 “time to solution” and “cost” from figure 5 “parallel efficiency” , which belongs to finding of optimum configuration, we introduced a separation of extra cost in 5 components and revised table 8 accordingly considering the reviewer comments. In particular, the last section 3.3 of table 8 is revised and all numbers are presented in a consistent and unique way as % of cost of optimum configuration of CCLM stand-alone. We removed the figures and the discussion of possible improvements of CCLM+MPI-ESM.

First of all, I do not understand why the cost of the CCLM part of CCLM-CLM and CCLM+VEG3D are about doubled compared to the costs of the CCLM stand alone or compared to the CCLM-NEMO-MED12 coupling. On p.25, l.854, it is stated “The corresponding costs are about double the costs of the stand-alone reference: 512.0 and 473.6 CHPSY, respectively”. Can you give an explanation? Is it linked to the fact that CCLM runs in SMT non-alternating mode in stand-alone and in the CCLM-NEMO-MED12 coupling where as it runs in SMT alternating mode in the CCLM-CLM and CCLM+VEG3D couplings? If so, it should be stated in the text.

Answer: We agree with the reviewer that it is difficult to follow the discussion and improved it (hopefully). You find a new paragraph (section 4.5. line 927 ff) clarifying which the dominating components of extra cost of coupling are. It turned out, it is mainly due to using ST instead of SMT mode and of the double number of cores.

“On p.25, l.854, it is stated “The corresponding costs are about double the costs of the stand-alone reference: 512.0 and 473.6 CHPSY, respectively”. Can you give an explanation? Is it linked to the fact that CCLM runs in SMT non-alternating mode in stand-alone and in the CCLM-NEMO-MED12 coupling where as it runs in SMT alternating mode in the CCLM-CLM and CCLM+VEG3D couplings?”

Answer: You are right to a wide extend. See previous answer.

The fact that the COSMO version used for CCLM+CLM is different from the COSMO version used for CCLM+VEG3D and that the results presented for CCLM+VEG3D are in fact not the optimum ones (128 cores were chosen to be able to compare with CCLM-CLM) is disturbing and the paragraph p.25 l-843-855 is difficult to understand (same thing for p.27, l922-923). I am not sure on how to correct this but this should be simplified maybe simply by removing results for CCLM-CSM?

Answer: Thank you for the comment. We conducted additional measurements comparing `cosmo_5.0_clm1` used in CCLM+CLM and `cosmo_4.8_clm17` used in CCLM+VEG3D (on another machine since blizzard is not available anymore). This exhibited 45% higher cost of 5.0. We revised the result presentation and in particular this paragraph .

It is not clear on figure 5 if the time to solution includes or not the OASIS interpolations. Can you clarify this? It is written in Table 8 caption that it does not but it should be stated either in Fig 5 captions and in the text, stressing that the interpolation time is relatively small anyway (as quantified in Table 8). Can you also specify that the OASIS interpolation times are provided directly by the Lucia tool in table 8 captions (even if this is mentioned in the text on p.21)

Answer: The “computing time” measured by LUCIA and by the “time” function includes interpolation time. We introduced a clear analysis of extra cost, corrected the caption of table 8 and extended the caption of (now) Figure 6. The OASIS interpolation is now given clearly for each coupling.

My second concern is about the definition of the criteria to identify the optimum configuration, which are not clear:

In section 4.2, please specify what you mean by “each component’s gain in speed, Compared to its speed on one node, outweighs the increase in costs.” The units of speed are not the same as the units of cost so they cannot be compared directly. Are you considering the relative gain in speed (in %) is compared to the relative increase of cost (in %)? To help the understanding, one practical example with numbers should be given (maybe at the beginning of current section 4.4?), for example the steps that lead to the identification of the optimum configuration for the CCLM

Answer: Thank you for this comment. We agree that the description of the strategy was not sufficient to understand and reproduce the results presented. We revised (now) section 4.3 describing the strategy and give the numbers in the new section 4.4 describing the application of the strategy.

The optimum configuration is always a compromise between efficiency (depending on models scalability) and availability of resources or time to solution and cost. It is maybe not possible to give an objective definition of what this compromise should be. Thus we introduced a parameter for that compromise, the parallel efficiency: “The optimum configuration is found by starting the measuring of the computing time on one node for all components, doubling the resources and measuring the computing time again and again as long as all component parallel efficiencies remain above 50%. The threshold of 50% is subjective and can be defined by the user, i.e. one could decide to stop at a higher parallel efficiency if costs are a limiting factor.” This definition is the same for both concurrent and sequential

configurations. An additional criterion is introduced, if the increase of cost has no impact on time to solution, in other words, if there is no scalability. In this case the parallel efficiency down to 50% is not used.

I think section 4.2 would be better to place just before 4.4 (i.e switching current 4.2 and 4.3 sections)

Answer: we follow the advice and switched the two §

p.22, l.749: This constraint is effective only for sequential coupling so it should be moved to the paragraph currently starting in line 754.

Answer: We have rewritten the sentence considering the reviewers suggestion (line 826 ff).

p.22 l.763 & l.779: It is not clear who or what decides if the costs are a limiting factor or not. Did you consider the costs was a limiting factor in your identification of the optimum? If so, what was the limit? This should be clarified.

Answer: Thank you for the comment. We rewrote the paragraph (line 836-849). We didn't introduce any other criterion but 50% parallel efficiency and, lowest cost, if no scalability is found. The application of the criteria is described in section 4.4 for each coupling in detail.

My third major concern is about section 4.5.2. I find this section not really relevant in the context of this paper. Of course, one can always get better fictive results by neglecting costly or badly written parts of the code!

Answer: We thank the reviewer for this suggestion. Section 4.5.2 is removed. Figure 6 and 7 are removed. Instead the extra cost of coupling for CCLM-MPIESM are discussed in section 4.5. line 984 ff and in section 4.6.

Then I have the following major remarks:

In general, I think the text is quite heavy with many repetitions. I suggest to make it lighter and more "right-to-the-point". In particular, section 2 describing the components could be reduced and the appendix A, that is not essential to the understanding of the paper could be given as supplementary material.

Answer: We would like to thank the reviewer for highlighting this important aspect of readability. The authors discussed this aspect again. Interestingly, reviewers 1 and 2 have dissenting opinions. You suggest reduction of the content and focusing on finding of an optimum configuration. The second reviewer suggests adding more details on configuration for asserting reproducibility and adding a discussion of the impact of configuration of model physics and dynamics on cost and time to solution. Considering the online publication form, we would like to keep section 2 in the paper. We revised the introductions of the sections in chapter 2 indicating that it is not essential for readers interested in the strategy of finding an "optimum configuration" only. The text is kept as it was with minor corrections. The introduction of the Appendix 1 is revised as well. It is essential for understanding of the coupling physics and dynamics and it is kept as appendix of the article since it does not increase the size of the PDF significantly and allows to keep everything in one document.

With which version of COSMO were the CCLM stand-alone tests done? Is it cosmo_4.8_clm19 like for all coupling but CCLM-CLM? This should be clarified in the text.

Answer: Yes, see our answer below. We modified § 2.1, line156, and § 2.6 accordingly.

p.3, l.69: Please give some details on why the MESSy approach was not considered.

Answer: The CCLM couplings available with MESSy and OASIS are different. A comparison between MESSy and OASIS is planned for CCLM+MPI-ESM couplings. This requires additional developments for a fair comparison which are not finished yet.

p.5, l.597: You mention a “coupling weight” increasing to 1 with time but this coupling weight is not described. Can you explain with more details how it works?

Answer: Thank you for this suggestion. The function used is given now in the text, line 601-605..

p.21, l.724: can you justify the formula used to approximate the time for 40 levels based on the time for 45 levels; why not simply use : $T_{40} = T_{45} \times 40/45$

Answer: The scaling of 80% of the computing time (and not 100% as suggested by your comment) is already explained in the footnote.4, line 760.

p.24, 806-807: I do not understand how one can conclude that “COSMO-CLM inv ST and SMT mode exhibits a very similar PE for the same number of processes ...” The curves are distinct. Do you mean that we should compare the SMT results for a specific number of cores with the ST results with twice as many cores (to get to the same number of processes)?

Answer: Yes, this is what we wanted to say. We agree that the explanation is weakly understandable and improved it. See line 808 ff.

p.24, l.808: you write “an increased loss of PE between 160 and 80 grid points per process.” but the reader cannot directly infer the number of grid points per process given the number of cores (which is the information provided on the figure), so the corresponding number of cores should be mentioned to help the reader.

Answer: We thank the reviewer for this comment and revised the paragraph for a better explanation. See line 814.

16. p.24, l.813-814: I do not fully understand this sentence. First I am not sure what the “component interface” is. Is it the coupling interface? If so, I do not understand how to reconcile this with the fact that the coupling interface time probably includes the time for interpolations (which are done either on the source side before the sending or on the target side after the receiving) and that the “time to solution” does not.

Answer: We thank the reviewer for raising this point. We agree that this sentence is not correct. We revised this paragraph and moved this explanation to “extra time and costs” in §4.5 , line 1009.

p.24, l.815-819: I do not understand the meaning of the sentence “Hereby, the number of cores and the threading mode (ST or SMT) are kept constant.” I propose to remove this sentence and rewrite the following ones as: “ COSMO-CLM components of concurrent couplings should be compared to stand-alone COSMO-CLM in SMT mode because in both cases two threads per core are used to run COSMO-CLM. Conversely, COSMO-CLM components of sequential couplings should be compared to stand-alone COSMO-CLM in ST mode because in both cases only one thread per core is used to run COSMO-CLM.” if I am right in my interpretation.

Answer: Thank you for this suggestion. The reference for each coupling is described now as suggested in section 4.4

p.24, l.826-827: It is written “However, as mentioned in section 2.6 CLM is coupled to cosmo_5.0_clm1 model version which is a more recent version than cosmo_4.8_clm19 used for all other couplings “ but I don’t see this mentioned in section 2.6.

Answer: We thank the reviewer for this remark. We corrected section 2.6 accordingly.. “The model version `cosmo_4.8_clm19` is the recommended version of the CLM-Community (Kotlarski et al., 2014) and it is used as basis of the development of the couplings. CCLM as part of the CCLM+CLM coupled system is used in a slightly different version (`cosmo_5.0_clm1`). The way this affects the performance results is presented in section 4.5, line 954 ff. In addition, the reviewer can see, in the figure below, a scalability comparison between the 2 versions. This reveals (even though the machine is not the same than the one used in the article) the cost of the 5.0 version are 45% higher than for 4.8.

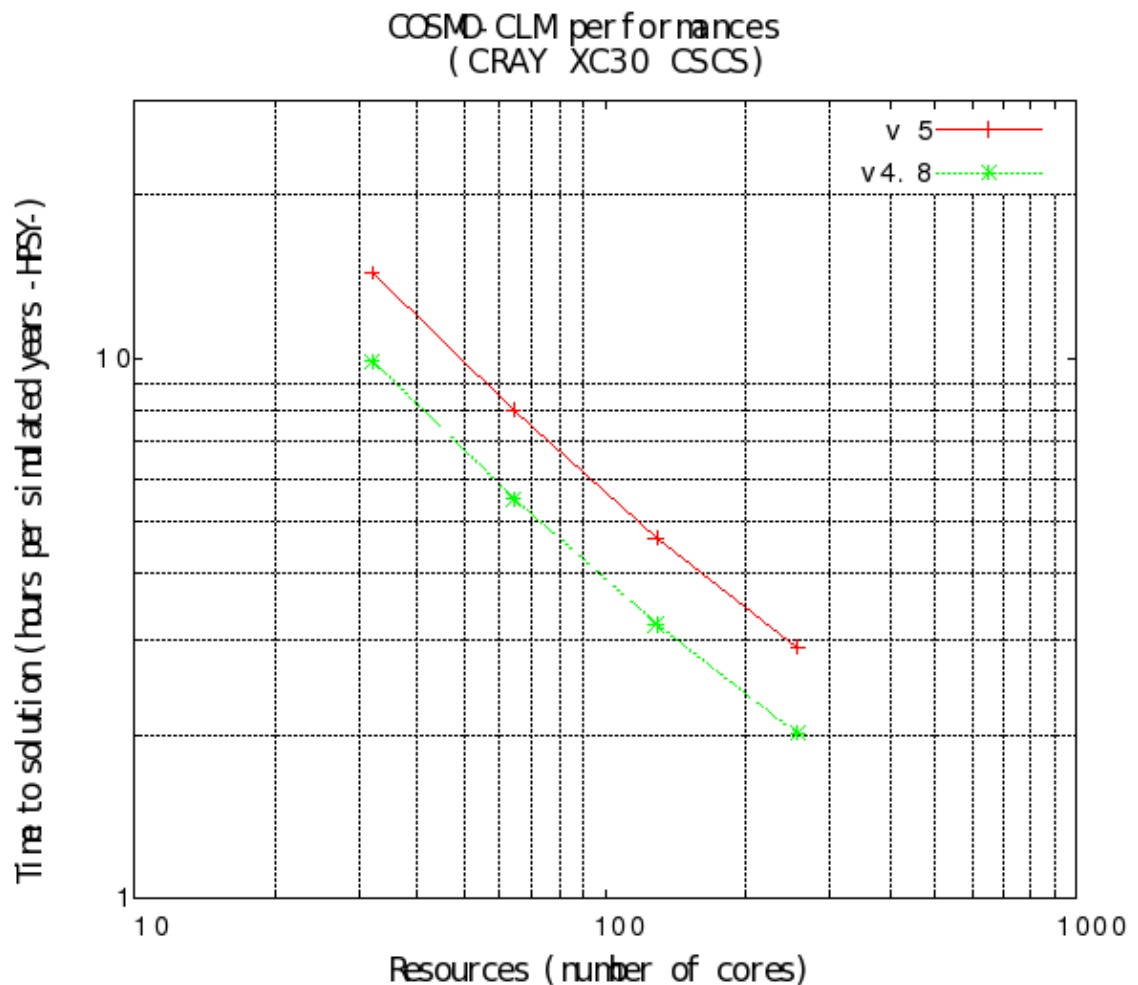


Figure 1: Time to solution of 5.0 and 4.8 COSMO-CLM versions in dependence on core number on Cray XC30 at CSCS, Lugano.

p.26, l.898-900: I propose to rephrase these two sentences for “It is not surprising that the couplings with soil-vegetation models shows only moderate extra costs as they replace the use of TERRA, the internal soil-vegetation model activated in stand-alone versions of COSMO-CLM.”

Answer: We changed the sentences. They are now in § 4.5, line 953.

p.28, l.949-955: This paragraph is not clear. Going from non-alternating to alternating reduces the time to solution by 35.1 %. Improving the performances of the derivative calculation reduces the time to solution by 9.2%. Going from 16 cores in SMT mode to 32

cores in ST mode results in a reduction of time to solution by 25.5 %. But then why is the “discrepancy” calculated by comparing this 25.5% to the 9.2% linked to the improvement of the derivative calculations? It should be calculated by comparing the 25.5% to the non-alternating to alternating gain of 35.1%, shouldn't it?

Answer: Thank you for asking for clarification of this puzzling result. We explain this complex result now in more detail. See §4.6, line 1017 ff

p.30, l.1040-1043: The 10% variation in the time to solution results should be introduced in the text and not only in the conclusion.

Answer: Thank you for the suggestion. We added this information at the end of §4.1

Minor remarks and technical corrections

I think it would be less confusing to use CCLM everywhere and not sometimes CCLM and sometimes COSMO-CLM

Answer: COSMO-CLM is the official name chosen by the CLM community, with CCLM as the official abbreviation when there is not enough space like in figures. We use now CCLM nearly everywhere. However, to avoid confusion between CLM and CCLM, the full name COSMO-CLM is used more than once.

p.1, l.8: The OASIS3-MCT interface is not really described in the paper. I suggest changing “present” for “use”.

Answer: Thank you for the comment. We realised that we introduced a confusion by using “interface” for model routines where coupling is performed instead for the OASIS3-MCT API (widely known as “PSMILE library”). We modified the text: “We present a unified interface, based on OASIS3-MCT coupling library”

p.3, l.58 & p.6, l.166: Valcke 2013 refers to a paper describing the “old” OASIS3 version and not the more recent OASIS3-MCT version. The reference Valcke et al., 2013 should be used instead.

Answer: We changed the reference.

p.3, l.67: I propose changing “is based” for “would be based”

Answer: We changed the text, l67.

p. 4, l.94: Please add “depends” after “but” in “but on the coupling method

Answer: Done

p.6, l.168: Please add “which” after “data” in “amount of data is a requirement”

Answer: Done

p.6, l.186-187: The sentence “The coupling of COSMO-CLM with the global ocean model NEMO is realized by means of two different regional versions of the NEMO model ...” sounds weird to me because of the opposition between “global” and “re- gional”. I suggest simply “COSMO-CLM is coupled to two different regional versions of the NEMO model ...”

Answer: Done, line 191.

p.10, l.337: The fact that each component needs to be a separate executable is not a constraint anymore with the last OASIS3-MCT_3.0 version; maybe this could be mentioned.

Answer: We added a remark on that feature in OASIS3, See line 340.

p.11, l.339 & l.366: Please change “whose” for “which”

Answer: Done, line 344 and 373

p.11, l.343: I suggest changing “is directly executed via the Message Passing Interface” for “is directly executed via the Model Coupling Toolkit (MCT, Jacob et al 2005) based on the Message Passing Interface (MPI)” and add the reference “Jacob, R., J. Larson, and E. Ong: MxN Communication and Parallel Interpolation in CCSM3 Using the Model Coupling Toolkit. Int. J. High Perf. Comp. App., 19(3), 293-307 2005 “

Answer: We thank the reviewer for this suggestion making this point more clear. We changed the text accordingly, line 349 ff.

P.11, l.357-358: I suggest changing “This component partitioning does not have to be the same” for “The component partitioning and grid do not have to be the same”

Answer: We thank the reviewer for this suggestion and changed the text accordingly in line 364.

p.11, l.361: I suggest adding “and accumulation” after “time averages” I propose “average or accumulation”

Answer: Done, line 368

p.11, l.373: I suggest changing “OASIS3-MCT includes the MPI library” for “OASIS3-MCT includes the MCT library based on MPI ” (but this is redundant with p.11, l.343 -see also my remark #9 above

Answer: We followed the reviewers suggestion and keep the redundancy for better readability, line 380.

p.13, l.428: Please add a) after 4.1

Answer: Done, line 435.

p.13, l. 442: Please change “interpolation” for “coupling” as it is not only the interpolation that is improved but the interpolation and the communication.

Answer: We added “and communication” for clarity, line 449.

p.20, l.687-691: I am not convinced these are effectively the two main goal of performance analysis. These sentences are unnecessary and contribute to the heaviness of the text (see also my first “Important remark” above.

Answer: Thank you for the comment. We removed the discussion of what is not done and changed the text accordingly. See line 718 ff.

p.21, l.722: Please change “compansated” for “compensated”

Answer: Done, line 761.

p.22, l.737-738, I suggest rephrasing the sentence “In a perfectly scaling parallel application the costs would remain constant if the resources are doubled, the parallel efficiency would be 100 %, the speed would be doubled and the speed-up would be 200 %.” for “If the resources of a perfectly scaling parallel application are doubled, the speed would be doubled and therefore the cost would remain constant, the parallel efficiency would be 100 %, and the speed-up would be 200 %.”

Answer: We thank the reviewer for this suggestion and changed the text accordingly, line 777.

p.23, l.791: Please change “CPUh” for “core hours” to be coherent with the rest of the text.

Answer: We thank the reviewer for this suggestion and changed the text accordingly, line 797.

Table 8 should be placed after Table 7 and not after all the Figures.

Answer: We thank the reviewer for this suggestion. Table 8 is now located after figure 6 showing the optimum configurations.

p.26, l906: Please change “atmosphere” for “coupled model”

Answer: We thank the reviewer for this suggestion and changed the text accordingly, line 991 ff.

p.30, l.1031: Please change “scaling;” by “scaling,”

Answer: We thank the reviewer for this suggestion and changed the text accordingly, line 1077.

Coupling of the regional climate model COSMO-CLM 4.8 using OASIS3-MCT with regional ocean, land surface or global atmosphere model: description and performance

Andreas Will¹, Naveed Akhtar², Jennifer Brauch³, Marcus Breil⁴, Edouard Davin⁵,
Ha T.M. Ho-Hagemann⁶, Eric Maisonnave⁷, Markus Thürkow⁸, and
Stefan Weiher¹

¹Institute for Environmental Sciences, BTU Cottbus-Senftenberg, Germany

²Institute for Atmospheric and Environmental Sciences, Goethe University, Frankfurt am Main,
Germany

³German Weather Service, Offenbach am Main, Germany

⁴Institute of Meteorology and Climate Research, KIT, Karlsruhe, Germany

⁵Institute for Atmospheric and Climate Science, ETH, Zurich, Switzerland

⁶Institute of Coastal Research, Helmholtz-Center Geesthacht, Germany

⁷Centre Européen de Recherche et de Formation Avancée en Calcul Scientifique,
CERFACS-CNRS, Toulouse, France

⁸Institute of Meteorology, FU Berlin, Germany

Correspondence to: Andreas Will, will@b-tu.de

Abstract. We present the prototype of a regional climate system model based on the COSMO-CLM regional climate model coupled via OASIS3-MCT with several model components, analyze the performance of the couplings, present a strategy to find an optimum configuration of computational resources with respect to computational costs and time to solution for a given domain, model physics and dynamics and present a separation of the extra cost of coupling in five major components.

The OASIS3-MCT library is used to couple COSMO-CLM with two land surface models (CLM and VEG3D), a regional ocean model for the Mediterranean Sea (NEMO-MED12), two ocean models for the North and Baltic Sea (NEMO-NORDIC and TRIMNP+CICE) and the atmosphere of an earth system model (MPI-ESM).

We present a unified OASIS3-MCT interface which handles all couplings in a similar way, minimizes the model source code modifications and defines the physics and numerics of the couplings. Furthermore, we discuss solutions for specific regional coupling problems like handling of different domains, multiple usage of MCT interpolation library and efficient exchange of 3D fields.

A series of real-case simulations over Europe has been conducted and the computational performance of the couplings has been analyzed. The usage of the LUCIA tool of the OASIS3-MCT coupler enabled separation of the unavoidable cost of coupled component model(s), direct cost of coupling, load imbalance, cost of different usage of processors by COSMO-CLM in coupled and stand alone mode and residual cost including i.a. COSMO-CLM additional computations. The re-

sulting limits for time to solution and cost are shown and the potential of further improvement of the computational efficiency is summarized.

It was found that the OASIS3-MCT coupler keeps the direct coupling cost of communication and horizontal interpolation below 5 % of the extra cost of coupling for all investigated couplings. For the first time this could be demonstrated for an exchange of approximately 450 2D fields per time step necessary for the atmosphere-atmosphere coupling between COSMO-CLM and MPI-ESM.

A procedure for finding an optimum configuration for each of the couplings was developed considering the time to solution and cost of the simulations. The optimum configurations are presented for sequential, concurrent and mixed (sequential+concurrent) coupling layouts. The procedure applied can be regarded as independent on the specific coupling layout and coupling details.

1 Introduction

Most of ~~the~~ current Regional Climate Models (RCMs) ~~suffer from a lack of parts of~~ ~~lack frameworks~~ ~~for~~ the interactivity between the atmosphere and the other components of the climate system. The interactivity is either altered by the use of a simplified component model (e.g. over land) or even partly suppressed when top and lateral and/or ocean surface boundary conditions of the atmospheric model are prescribed by reanalysis or large-scale Earth System Model (ESM) outputs.

The neglected meso-scale feedbacks and inconsistencies of the boundary conditions (Laprise et al., 2008; Becker et al., 2015) might ~~well be~~ ~~be well~~ accountable for a substantial part of large- and regional-scale biases found in RCM simulations at 10–50 km horizontal resolution (see e.g. Kotlarski et al. (2014) for Europe). This hypothesis gains further evidence from the results of convection-permitting simulations, in which these processes are not regarded either. These simulations provide more regional-scale information and improve e.g. the precipitation distribution in mountainous regions but they usually do not show a reduction of the large-scale biases (see e.g. Prein et al. (2013)).

The potential of ~~explicitly simulating~~ ~~explicit simulation of~~ the processes neglected or prescribed in these ~~land-atmosphere~~ ~~land-atmosphere~~ RCMs has been investigated using ESMs with variable horizontal resolution (Hertwig et al., 2015; Hagos et al., 2013), RCMs two-way coupled with the ~~atmosphere~~ ~~atmospheric component~~ of global ESMs (Lorenz and Jacob, 2005; Inatsu and Kimoto, 2009), two-way coupled with regional oceans (Döscher et al., 2002; Gualdi et al., 2013; Zou and Zhou, 2013; Bülow et al., 2014; Akhtar et al., 2014; Pham et al., 2014; Ho-Hagemann et al., 2013, 2015) and/or with more sophisticated land surface models (Wilhelm et al., 2014; Davin et al., 2011).

Besides various improvements, a significant increase of ~~the~~-climate change signal was found by Somot et al. (2008) in the ARPEGE model with ~~a~~-~~the~~ horizontal grid refined over Europe and two-way coupled with a regional ocean for the Mediterranean Sea. These results strongly suggest that building Regional Climate System Models (RCSMs) with ~~explicite modelling~~ ~~explicit modeling~~ of the interaction between ~~the~~-meso scales in ~~the~~ atmosphere, ocean and land-surface ~~and with the~~, ~~with~~

large scales in the atmosphere (and ocean) is necessary to consistently represent regional climate dynamics and gain further insights ~~in~~ into regional climate change.

The non-hydrostatic regional climate model COSMO-CLM (Rockel et al., 2008) belongs to ~~this~~ the class of land-atmosphere RCMs that do not allow a meso-scale interaction between ~~the~~ different components of the climate system. ~~The current paper aims at presenting~~ In this paper we present a first step ~~in a view to overcome these deficiencies: the COSMO-CLM individually of a~~ coupling approach which aims at overcoming the previously mentioned deficiencies - individual two-way ~~coupled~~ coupling of COSMO-CLM with other climate component models ~~via~~ using OASIS3-MCT (~~Valeke, 2013~~) (Valcke et al., 2013) over Europe. These climate component models are (i) the Community Land Model (CLM) version 4.0, the soil and vegetation model VEG3D for the land component, (ii) the NEMO model version 3.2 for the Mediterranean, the regional ocean model TRIMNP along with the sea ice model CICE and the NEMO model (version 3.3, including the LIM3 sea ice model) for the Baltic and the North Sea and ~~, finally,~~ (iii) the global Earth System Model MPI-ESM for the large-scale global atmosphere. ~~Further~~ Additional model components, which are not discussed in this article but ~~which~~ can be coupled with COSMO-CLM via OASIS3-MCT are the ocean model ROMS (Byrne et al., 2015) and the hydrological model ParFLOW (Gasper et al., 2014) together with CLM.

An alternative coupling strategy available for COSMO-CLM ~~is~~ would be based on an internal coupling of the models of interest with the master routine MESSy resulting in the compilation of one executable (Kerkweg and Joeckel, 2012). This coupling strategy is not investigated in this study.

The coupled climate models, either global (ESMs) or regional (RCSMs), are obviously computationally ~~very demanding,~~ demanding. This is not only due to the sum of the costs of the individual model components ~~but also due to,~~ but also additional costs of the coupler, additional computations needed for coupling, load imbalances and/or inappropriate numerical properties of the coupled model components. Maintaining a reasonable computational cost contributes to a large extent to ~~the~~ models' usability. ~~This is why the present article~~ For this reason the present paper also focuses on ~~this~~ aspect that the coupled systems computational efficiency which greatly relies on the parallelization of the OASIS3-MCT coupler.

~~The optimization~~ Optimization of the computational performance is ~~regarded~~ considered to be highly dependent on the model system and/or the computational machine used. However, several studies ~~indicate~~ show transferability of optimization strategies and universality of certain aspects of the performance. Worley et al. (2011) analyzed the performance of the Community Earth System Model (CESM) and found a good scalability of the concurrently running CLM and ~~of the~~ sequentially running CICE down to approximately 100 grid points per processor for two different resolutions and computing architectures. Furthermore, they found the CICE scalability to be limited by a domain decomposition, which follows that of the ocean model, ~~and thus to result in~~ resulting to a very low number of ice grid points in subdomains. Lin-Jiong et al. (2012) investigated ~~the a~~ a weak scaling

(discussed in section 4.3) of the FAMIL model (IAP, Beijing) and found a ~~similar performance as for performance similar to that of~~ the optimized configuration of the CESM (Worley et al., 2011). This result indicates that a careful investigation of the model performance leads to similar results for similar computational problems. An analysis of CESM at very high resolutions by Dennis et al. 95 (2012) showed that a cost reduction ~~of up to by~~ a factor of three ~~or less~~ can be achieved using an optimal layout of model components. Later ~~on~~ Alexeev et al. (2014) presented an algorithm for finding an optimum model coupling layout (concurrent, sequential) and processor distribution between the model components minimizing the load imbalance in CESM.

These results indicate that the optimized computational performance is weakly dependent on the 100 computing architecture or on the individual model components but ~~depends~~ on the coupling method. Furthermore, the application of an optimization procedure was found beneficial.

In this study we present a detailed analysis of coupled COSMO-CLM performances on the IBM POWER6 machine *Blizzard* located at DKRZ, Hamburg. We calculate the speed and costs of the individual model components and of the coupler itself and identify the ~~origins causes~~ of reduced speed 105 or increased costs for each coupling ~~configuration~~ and reasonable processor configurations. We suggest an optimum configuration for different couplings considering costs and speed of the simulation and discuss the current and potential performances of the coupled systems. ~~The particularities~~ Particularities of the performance of a coupled RCM are highlighted together with the potential of the ~~new~~ coupling software OASIS3-MCT. We suggest a procedure of optimization of an RCM, 110 which can be generalized. However, we will show that some relevant optimizations are possible only due to features available with the OASIS3-MCT coupler.

The paper is organized as follows: The coupled model components are described in section 2. Section 3 focuses on the OASIS3-MCT coupling method and its interfaces for the individual couplings. The coupling method description encompasses the ~~description of~~ OASIS3-MCT functionality, ~~the~~ 115 method of the coupling optimization and ~~the~~ particularities of coupling of a regional climate model system. The model interface description gives a summary of the physics and numerics of the individual couplings. In section 4 the computational efficiency of ~~the~~ individual couplings is presented and discussed. Finally, the conclusions and an outlook are given in section 5. For improved readability, Tables 1 and 2 provide an overview of the acronyms frequently used throughout the paper and of the 120 investigated couplings.

2 ~~Model~~ Description of model components ~~description~~

The further development of the COSMO model in Climate Mode (COSMO-CLM) presented here aims at overcoming the limitations of the regional soil-atmosphere climate model, as discussed in the introduction, by replacing prescribed vegetation, lower boundary condition over sea surfaces and

125 the lateral and top boundary conditions ~~by interactions with~~ with interactions between dynamical models.

The models selected for coupling with COSMO-CLM need to fulfill the requirements of the intended range of application which are (1) the simulation at varying scales from convection-resolving up-to-50 ~~km-coarse-grid-scales~~ km grid spacing, (2) local-scale up to continental-scale simulation domains and (3) full capability at least for European model domains. We decided to couple the NEMO ocean model for the Mediterranean Sea (NEMO-MED12) and the Baltic and Northern Seas (NEMO-NORDIC), alternatively the TRIMNP regional ocean model together with the sea ice model CICE for the Baltic and Northern Seas (TRIMNP+CICE), the Community Land Model (CLM) of soil and vegetation (replacing the multi-layer soil model TERRA), alternatively the VEG3D soil and vegetation model and the global Earth System Model MPI-ESM for two-way coupling with the regional atmosphere. Table 2 gives an overview of all coupled-model systems ~~investigeted, of~~ investigated, their components and ~~of the~~ institutions at which they are maintained. An overview of the coupled models selected for coupling with COSMO-CLM (CCLM) is given in table 3 together with ~~some key aspects of the configuration used in this study; the main model developer, configuration details~~ of high relevance for computational performance, the model complexity (see Balaji et al. (2017) and a reference in which a detailed model description can be found. The model domains are plotted in Figure 1. More information on the availability of the model components can be found in Appendix A.

In the following, the model components used are briefly described with respect to model history, space-time scales of applicability and ~~with respect to~~ model physics and dynamics relevant for the coupling.

2.1 COSMO-CLM

COSMO-CLM is the COSMO model in climate mode. ~~The~~ COSMO model is ~~the a~~ non-hydrostatic limited-area atmosphere-soil model originally developed by Deutscher Wetterdienst for operational numerical weather prediction (NWP). ~~Meanwhile, it can be~~ Additionally, it is used for climate, environmental (Vogel et al., 2009) and idealized studies (Baldauf et al., 2011).

The COSMO physics and dynamics are designed for operational applications at horizontal resolutions of 1 to 50 km for NWP and RCM applications. The basis of this capability is a stable and efficient solution of the non-hydrostatic system of equations for the moist, deep atmosphere on a spherical, rotated, terrain-following, staggered Arakawa C grid with a hybrid z-level coordinate. The model ~~dynamics is documented in Doms and Baldauf (2015) and the model physics in Doms et al. (2011)~~ physics and dynamics are discribed in Doms et al. (2011) amd Doms and Baldauf (2015) respectively. The features of the model are discussed in Baldauf et al. (2011).

The ~~climate mode (CLM) (Rockel et al., 2008) of the COSMO model is, strictly speaking,~~ COSMO model's climate mode (Rockel et al., 2008) is a technical extension for long-time simulations and all

related developments are unified with COSMO regularly. The important aspects of the climate mode are ~~the~~ time dependency of the vegetation parameters and of the prescribed SSTs and ~~the~~ usability of the output of several global and regional climate models as initial and boundary conditions. All other aspects related to ~~CLM like the~~ the climate mode e.g. the restart option for soil and atmosphere, the
165 NetCDF model in- and output, online computation of climate quantities, and the sea ice module or spectral nudging can be used in other modes of the COSMO model as well.

The model version `cosmo_4.8_clm19` is the recommended ~~model~~ version of the CLM-Community (Kotlarski et al., 2014) and it is used ~~as basis of the development of the couplings for the couplings but for CCLM+CLM and for stand-alone simulations. CCLM as part of the CCLM+CLM coupled~~
170 system is used in a slightly different version (`cosmo_5.0_clm1`). The way this affects the performance results is presented in section 4.4.

2.2 MPI-ESM

The global Earth System Model of the Max Planck Institute for Meteorology Hamburg (MPI-ESM; Stevens et al. (2013)) consists of subsystem models for ocean, atmo-, cryo-, pedo- and the
175 ~~biosphere~~bio-sphere. The hydrostatic general circulation model ECHAM6 uses the transform method for horizontal computations. The derivatives are computed in spectral space, while the transports and physics tendencies on a regular grid in physical space. A pressure-based sigma coordinate is used for vertical discretization. The ocean model MPIOM (Jungclaus et al., 2013) is a regular grid model with the option of local grid refinement. The terrestrial bio- and ~~pedosphere~~pedo-sphere component
180 model is JSBACH (Reick et al., 2013; Schneck et al., 2013). The marine biogeochemistry model used is HAMOCC5 (Ilyina et al., 2013). A key aspect is the implementation of the bio-geo-chemistry of the carbon cycle, which allows e. g. ~~investigating~~investigation of the dynamics of the greenhouse gas concentrations (Giorgetta et al., 2013). The subsystem models are coupled via the OASIS3-MCT coupler (~~Valeke, 2013~~)(Valcke et al., 2013) which was implemented recently by I. Fast of DKRZ in
185 the CMIP5 model version. This allows parallelized and efficient coupling of a huge amount of data, which is a requirement of atmosphere-atmosphere coupling.

The reference MPI-ESM configuration uses a spectral resolution of T63, which is equivalent to a spatial resolution of about 320 km for atmospheric dynamics and 200 km for model physics. Vertically the atmosphere is resolved by 47 hybrid sigma-pressure levels with the top level at 0.01 hPa.
190 The reference MPIOM configuration uses the GR15L40 resolution which corresponds to a bipolar grid with a horizontal resolution of approximately 165 km near the Equator and 40 vertical levels, most of them within the upper 400 m. The North and the South Pole are located over Greenland and Antarctica in order to avoid the “pole problem” and to achieve a higher resolution in the Atlantic region (Jungclaus et al., 2013).

195 2.3 NEMO

The Nucleus for European Modelling of the Ocean (NEMO) is based on the primitive equations. It can be adapted for regional and global applications. The sea ice (LIM3) or the marine biogeochemistry module with passive tracers (TOP) can be used optionally. NEMO uses staggered variable positions together with a geographic or Mercator horizontal grid and a terrain-following σ -coordinate (curvilinear grid) or a z-coordinate with full or partial bathymetry steps (orthogonal grid). A hybrid vertical coordinate (z-coordinate near the top and σ -coordinate near the bottom boundary) is possible as well (for details see Madec (2011)).

~~The coupling of COSMO-CLM with the global ocean model NEMO is realized by means of is~~
coupled to two different regional versions of the NEMO model ~~adapted to the~~, adapted to specific
205 conditions of the region of application. For the North and Baltic Seas, the sea ice module (LIM3) of NEMO is activated and the model is ~~running~~ applied with a free surface to enable the tidal forcing. Whereas in the Mediterranean Sea, the ocean model runs with a classical rigid-lid formulation in which the sea surface height is simulated via pressure differences. Both model setups are briefly introduced in the following two sub-sections.

210 2.3.1 Mediterranean Sea

Lebeaupin et al. (2011), Beuvier et al. (2012) and Akhtar et al. (2014) adapted the NEMO version 3.2 (Madec, 2008) to the regional ocean conditions of the Mediterranean Sea, ~~hereafter~~ hereafter called *NEMO-MED12*. It covers the whole Mediterranean Sea excluding the Black Sea. The NEMO-MED12 grid is a section of the standard irregular ORCA12 grid (Madec, 2008) with an eddy-resolving $1/12^\circ$ horizontal resolution, stretched in latitudinal direction, equivalent to 6–8 km horizontal resolution. In the vertical, 50 unevenly spaced levels are used with 23 levels in the top layer of 100 m depth. A time step of 12 min is used.

The initial conditions for potential temperature and salinity are taken from the Medatlas (MEDAR-Group, 2002). The fresh-water inflow from rivers is prescribed by a climatology taken from the
220 RivDis database (Vörösmarty et al., 1996) with seasonal variations calibrated for each river by Beuvier et al. (2010) based on Ludwig et al. (2009). In this context, the Black Sea is considered as a river for which climatological monthly values are calculated from a dataset of Stanev and Peneva (2002). The water exchange with the Atlantic Ocean is parameterized using a buffer zone west of the Strait of Gibraltar with a thermohaline relaxation to the World Ocean Atlas data of Levitus et al. (2005).

225 2.3.2 North and Baltic Seas

Hordoir et al. (2013), Dieterich et al. (2013) and Pham et al. (2014) adapted the NEMO version 3.3 to the regional ocean conditions of the North and Baltic Sea, ~~hereafter~~ hereafter called *NEMO-NORDIC*. Part of NEMO 3.3 is the sea ice model LIM3 including a representation of dynamic and

thermodynamic processes (for details see Vancoppenolle et al. (2009)). The NEMO-NORDIC domain covers the whole Baltic and North Sea with two open boundaries to the Atlantic Ocean: the southern, meridional boundary in the English Channel and the northern, zonal boundary between the Hebride Islands and Norway. The horizontal resolution is 2 nautical miles (about 3.7 km) with 56 stretched vertical levels. The time step used is 5 min. No fresh-water flux correction for the ocean surface is applied. NEMO-NORDIC uses a free top surface to include the tidal forcing in the dynamics. Thus, the tidal potential has to be prescribed at the open boundaries in the North Sea. Here, we use the output of the global tidal model of Egbert and Erofeeva (2002).

The lateral fresh-water inflow from rivers plays a crucial role for the salinity budget of the North and Baltic Seas. It is taken from the daily time series of river runoff from the E-HYPE model output operated at SMHI (Lindström et al., 2010). The World Ocean Atlas data (Levitus et al., 2005) are used for the initial and lateral boundary conditions of potential temperature and salinity.

2.4 TRIMNP and CICE

TRIMNP (Tidal, Residual, Intertidal Mudflat Model Nested Parallel Processing) is the regional ocean model of the University of Trento, Italy (Casulli and Cattani, 1994; Casulli and Stelling, 1998). The domain of TRIMNP covers the Baltic Sea, the North Sea and a part of the North East Atlantic Ocean with the north-west corner over Iceland and the south-west corner over Spain at the Bay of Biscay. TRIMNP is designed with a horizontal grid mesh size of 12.8 km and 50 vertical layers. The thickness of the top 20 layers is each 1 m and increases with depth up to 600 m for the remaining layers. The model time step is 240 s. Initial states and boundary conditions of water temperature, salinity, and velocity components for the ocean layers are determined using the monthly ORAS-4 reanalysis data of ECMWF (Balmaseda et al., 2013). The daily Advanced Very High Resolution Radiometer AVHRR2 data of the National Oceanic and Atmospheric Administration of USA are used for surface temperature and the World Ocean Atlas data (Levitus and Boyer, 1994) for surface salinity. No tide is taken into account in the current version of TRIMNP. The climatological means of fresh-water inflow of 33 rivers to the North Sea and the Baltic Sea are collected from Wikipedia.

The sea ice model CICE version 5.0 is developed at the Los Alamos National Laboratory, USA (<http://oceans11.lanl.gov/trac/CICE/wiki>), to represent dynamic and thermodynamic processes of sea ice in global climate models (for more details see Hunke et al. (2013)). In this study CICE is adapted to the region of the Baltic Sea and Kattegat, a part of the North Sea, on a 12.8 km grid with five ice categories. Initial conditions of CICE are determined using the AVHRR2 SST.

2.5 VEG3D

VEG3D is a multi-layer soil-vegetation-atmosphere transfer model (Schädler, 1990) designed for regional climate applications and maintained by the Institute of Meteorology and Climate Research at the Karlsruhe Institute of Technology. VEG3D considers radiation interactions with vegetation

and soil, calculates the turbulent heat fluxes between the soil, the vegetation and the atmosphere, as
265 well as the thermal transport and hydrological processes in soil, snow and canopy.

The radiation interaction, the moisture and turbulent fluxes between soil surface and the atmosphere are regulated by a massless vegetation layer located between the lowest atmospheric level and the soil surface, having its own canopy temperature, specific humidity and energy balance. The multi-layer soil model solves the heat conduction equation for temperature and the Richardson equation for soil water content. Thereby, vertically differing soil types can be considered within one soil
270 column, comprising 10 stretched layers with its bottom at a depth of 15.34 m. The heat conductivity depends on the soil type and the water content. In case of soil freezing the ice-phase is taken into account. The soil texture has 17 classes. Three classes are reserved for water, rock and ice. The remaining 14 classes are taken from the USDA Textural Soil Classification (Staff, 1999).

275 Ten different landuse classes are considered: water, bare soil, urban area and seven vegetation types. Vegetation parameters like the leaf area index or the plant cover follow a prescribed annual cycle.

Up to two additional snow layers on top are created, if the snow cover is higher than 0.01 m. The physical properties of the snow depend on its age, its metamorphosis, melting and freezing. A
280 snow layer on a vegetated grid cell changes the vegetation albedo, emissivity and turbulent transfer coefficients for heat as well.

An evaluation of VEG3D in comparison with TERRA in West Africa is presented by Köhler et al. (2012).

2.6 Community Land Model

285 The Community Land Model (CLM) is a state-of-the-art land surface model designed for climate applications. Biogeophysical processes represented by CLM include radiation interactions with ~~vegetation~~ [vegetation](#) and soil, the fluxes of momentum, sensible and latent heat from vegetation and soil and the heat transfer in soil and snow. Snow and canopy hydrology, stomatal physiology and photosynthesis are modeled as well.

290 Subgrid-scale surface heterogeneity is represented using a tile approach allowing five different land units (vegetated, urban, lake, glacier, wetland). The vegetated land unit is itself subdivided into 17 different plant-functional types (or more when the crop module is active). Temperature, energy and water fluxes are determined separately for the canopy layer and the soil. This allows a more realistic representation of canopy effects than by bulk schemes, which have a single surface temperature and energy balance. The soil column has 15 layers, the deepest layer reaching 42 meters depth.
295 Thermal calculations explicitly account for the effect of soil texture (vertically varying), soil liquid water, soil ice and freezing/melting. CLM includes a prognostic water table depth and groundwater reservoir allowing for a dynamic bottom boundary conditions for hydrological calculations rather than a free drainage condition. A snow model with up to five layers enables the representation of

300 snow accumulation and compaction, melt/freezing cycles in the snow pack and the effect of snow aging on surface albedo.

CLM also includes processes such as carbon and nitrogen dynamics, biogenic emissions, crop dynamics, transient land cover change and ecosystem dynamics. These processes are activated optionally and are not considered in the present study. A full description of the model equations and input datasets is provided in Oleson et al. (2010) (for CLM4.0) and Oleson et al. (2013) (for CLM4.5).
305 An offline evaluation of CLM4.0 surface fluxes and hydrology at the global scale is provided by Lawrence et al. (2011).

CLM is developed as part of the Community Earth System Model (CESM) (Collins et al., 2006; Dickinson et al., 2006) but it has been also coupled to other global (NorES) or regional (Steiner et al., 2005, 2009; Kumar et al., 2008) climate models. In particular, an earlier version of CLM (CLM3.5) has been coupled to COSMO (Davin et al., 2011; Davin and Seneviratne, 2012) using a "sub-routine" approach for the coupling. Here we use a more recent version of CLM (CLM4.0 as part of the CESM1_2.0 package) coupled to COSMO via OASIS3-MCT rather than through a sub-routine call. Note that CLM4.5 is also included in CESM1_2.0 and can be also coupled to
315 COSMO using the same framework.

3 Description and optimization of COSMO-CLM couplings via OASIS3-MCT

The computational performance, ~~the usability and the~~ maintainability of a complex model system ~~depends depend~~ on the coupling method used, ~~on~~ the ability of the coupler to ~~use~~ run efficiently in the computing architecture ~~efficiently and, last but not least, and~~ on the flexibility of
320 the coupler to deal with different requirements on the coupling depending on model physics and numerics.

In the following, the physics and numerics of the coupling of COSMO-CLM with the different model components via OASIS3-MCT are discussed and the different aspects of optimization of the computational performance of the individual couplings are highlighted. In section 3.1 the main properties of the OASIS3-MCT coupling method are described, the new OASIS3-MCT features are highlighted and the steps of optimization of the computational performance are described. In sections 3.2 to 3.5 the physics and numerics of the couplings are described. ~~There, In these sections~~ a list of the exchanged variables, the additional computations and the interpolation methods ~~can be found~~ are presented. The time step organization of each coupled model is given in the Appendix B.

3.1 OASIS3-MCT coupling method and performance optimization

Lateral-, top- and/or bottom-boundary conditions for regional geophysical models are traditionally read from files and updated regularly at runtime. We call this approach *offline (one-way) coupling*. For various reasons, one could decide to calculate these boundary conditions with another geophys-

ical model - at runtime - in an *online (one-way) coupling*. If this additional model in return receives
335 information from the first model modifying the boundary conditions provided by the first to the
second, an *online two-way coupling* is established. In any of these cases, model exchanges must be
synchronized. This could be done by (1) reading data from file, (2) calling one model as a subroutine
of the other or (3) by using a coupler which is a software that enables online data exchanges between
models.

340 Communicating information from model to model boundaries via reading from and writing to
a file is known to be quite simple to implement but computationally inefficient, ~~in particular in~~
particularly in the case of non-parallelized I/O and high frequencies of disc access. In contrast, call-
ing component models as COSMO-CLM subroutines exhibits much better performances because
the information is exchanged directly in memory. Nevertheless, the inclusion of an additional model
345 in a "subroutine style" requires comprehensive modifications of the source code. Furthermore, the
modifications need to be updated for every new source code version. Since the early ~~90ies~~90s, soft-
ware solutions have been developed, which allow coupling between geophysical models in a non-
intrusive, flexible and computationally efficient way.

One of the software solutions for coupling of geophysical models is the OASIS coupler, which is
350 widely used in the climate modeling community (see for example Valcke (2013) and Maisonnave
et al. (2013)). Its latest fully parallelized version, OASIS3-MCT version 2.0 (Valcke et al., 2013),
proved its efficiency for high-resolution quasi-global models on top-end supercomputers (Masson
et al., 2012).

In the OASIS coupling paradigm, each model is a *component* of a *coupled system*. Each compo-
355 nent is included as a separate executable ~~up to OASIS3-MCT version 2.0. Using the version 3.0~~
this is not a constraint anymore.

3.1.1 The OASIS3-MCT coupling method

~~A separate executable (coupler) was necessary to the former version of OASIS.~~ OASIS3-MCT
only consists of a FORTRAN Application Programming Interface (API), ~~whose~~which subrou-
360 tines have to be added in all coupled-system components. The part of the program in which the
OASIS3-MCT API routines are located is called *component interface*. There is ~~not anymore an no~~
independent OASIS executable anymore, as was the case with OASIS3. With OASIS3-MCT, ev-
ery communication between the model components is directly executed via the Model Coupling
Toolkit (MCT, in Jacob et al. (2005)) based on the Message Passing Interface (MPI)library. ~~This is~~
365 significantly improving. This significantly improves the performance over OASIS3, because the
bottleneck ~~formed by~~due to the sequential separate coupler is entirely removed as shown e. g. in
Gasper et al. (2014).

In the following, we point out the potential of the new OASIS3-MCT coupler and discuss the
peculiarities of its application for coupling in the COSMO model in CLimate Mode (COSMO-

370 CLM). If there is no difference between the OASIS versions, we use the acronym OASIS, otherwise
the OASIS version is specified.

At runtime, all components are launched together on a single MPI context. The parameters defin-
ing the properties of a coupled system are provided to OASIS via an ASCII file called *namcouple*.
By means of this file the components, coupling fields and coupling intervals are associated. Specific
375 calls of the *OASIS3-MCT Application Programming Interface (API)* in a *component interface* de-
scribed in sections 3.2 to 3.5 define a component's coupling characteristics, that is, (1) the name of
incoming and outgoing coupling fields, (2) the grids on which each of the coupling fields are dis-
cretized, (3) a mask (binary-sparse array) describing where coupling fields are described on the grids
and (4) the partitioning (MPI-parallel decomposition into subdomains) of the grids. ~~This component~~
380 ~~partitioning does~~ The component partitioning and grid do not have to be the same for each compo-
nent as OASIS3-MCT is able to scatter and gather the arrays of coupling fields if they are exchanged
with a component model that is decomposed differently. Similarly, OASIS is able to perform interpo-
lations between different grids. OASIS also is able to perform time ~~averages~~ average or accumulation
for exchanges at a coupling time step, e. g. if the components' time steps differ. In total, six to eight
385 API routines have to be called by each component model to start MPI communications, declare
the component's name, possibly get back MPI local communicator for internal communications,
declare the grid partitioning and variable names, finalize the component's coupling characteristics
declaration, send and receive the coupling fields and, finally, close the MPI context at the compo-
nent's runtime end. ~~This reduced~~ The number of routines, ~~whose~~ which arguments require easily
390 identifiable model quantities, is the most important feature of the OASIS3-MCT coupling library
that contributes to its non-intrusiveness. In addition, each component can be modified separately or
another component can be added later. This facilitates a shared maintenance between the users of the
coupled-model system: when a new development or a version upgrade is done in one component, the
modification scarcely affects the other components. This ensures the modularity and interoperability
395 of any OASIS-coupled system.

As previously mentioned, OASIS3-MCT includes the ~~MPI library~~ MCT library, based on MPI, for
direct parallel communications between components. To ensure that calculations are delayed only
by receiving of coupling fields or interpolation of these fields, MPI non-blocking sending is used by
OASIS3-MCT so that sending coupling fields is a quasi-instantaneous operation. The SCRIP library
400 (Jones, 1997) included in OASIS3-MCT provides a set of standard operations (for example bilinear
and bicubic interpolation, Gaussian-weighted N-nearest-neighbor averages) to calculate, for each
source grid point, an interpolation weight that is used to derive an interpolated value at each (non-
masked) target grid point. OASIS3-MCT can also (re-)use interpolation weights calculated offline.
Intensively tested for demanding configurations ~~(?)~~ (Craig et al., 2012), the MCT library performs
405 the definition of the parallel communication pattern needed to optimize exchanges of coupling fields
between each component's MPI subdomain. It is important to note that unlike the "subroutine cou-

pling" each component coupled via OASIS3-MCT can keep its parallel decomposition so that each of them can ~~, theoretically,~~ be used at its optimum scalability. In some cases, this optimum can be adjusted to ensure a good load balance between components. ~~These~~The two optimization aims that
410 strongly matter for computational performance are discussed in the next section.

3.1.2 The coupled-system synchronization and optimization

A coupled model component receiving information from one or several other components has to wait for the information ~~until~~before it can perform its own calculations. In case of a two-way coupling this component provides information needed by the other coupled-system component(s). As mentioned earlier, the information exchange is quasi-instantaneously performed, if the time needed to
415 perform interpolations can be neglected which is the case even for 3D-field couplings (as discussed in section ~~??~~4.6). Therefore, the total duration of a coupled-system simulation can be separated into two parts for each component: (1) a *waiting time* in which a component waits for boundary conditions and (2) a *computing time* in which a component's calculations are performed. The duration of
420 a stand-alone, that is, un-coupled component simulation approximates ~~this~~the coupled-component's computing time. In a coupled system this time can be shorter than in the uncoupled mode, since the reading of boundary conditions from file (in stand-alone mode) is partially or entirely replaced by the coupling. It is also important to note that components can perform their calculations *sequentially* or *concurrently*.

425 The ~~total-sequential~~ coupled-system's total sequential simulation time can be expected to be equal to the sum of the individual component's calculation times, potentially increased by the time needed to interpolate and communicate coupling fields between the components. The computational constraint induced by a sequential coupling algorithm depends on the computing architecture. If one process can be started on each core, the cores allocated for one model component are idle while others
430 are performing calculations and vice versa. In such a case the performance optimisation strategy needs to consider model component waiting time. If more than one process can be started on each core, each model component can use all cores sequentially and an allocation of the same number of cores to each model component can avoid any waiting time. This is discussed ~~further below~~ in more detail in the following paragraphs.

435 The constraints of sequential coupling are often alleviated if calculations of a coupled-system component can be performed with coupling fields of another component's previous coupling time step. This concurrent coupling strategy is possible if one of the two sets of exchanged quantities is slowly changing in comparison to the other set. For example, sea surface temperatures of an ocean model are slowly changing in comparison to fluxes coming from an atmosphere model. However, now the
440 time to solution of each model component can be substantially different and an optimisation strategy needs to minimise the waiting time.

Thus, the strategy of synchronization of the model components depends on the layout of the coupling

(sequential or concurrent) in order to reduce the waiting time as much as possible. It is important to note that huge differences in computational performance can be found for different coupling layouts
445 due to different scalability of the modular model components.

Since computational efficiency is one of the key aspects of any coupled system the various aspects affecting it are discussed. These are the performances of the model components, of the coupling library and of the coupled system. Hereby the design of the interface and the OASIS3-MCT coupling parameters, which ~~allow to optimize the efficiency~~enables optimization of the efficiency, are described.
450

The model component performance depends on the component's scalability. The optimum partitioning has to be set for each parallel component by means of a strong scaling analysis (discussed in section 4.1). This analysis, which results in finding the scalability limit (the maximum speed) or the scalability optimum (the acceptable level of parallel efficiency), can be difficult to obtain for
455 each component in a multi-component context. In this article, we propose to simply consider the previously defined concept of the computing time (excluding the waiting time from the total time to solution). In chapter 4 we will describe our strategy to separate the measurement of computing and waiting time-times for each component and how to ~~simply~~ deduce the optimum MPI partitioning from the scaling analysis.

The optimization of ~~the~~ OASIS3-MCT coupling library performance is relevant for the efficiency of the data exchange between components discretized on different grids. The parallelized interpolations are performed by the OASIS3-MCT library routines called by the source or by the target component. An interpolation will be faster if performed (1) by the model with the larger number of MPI processes available (up to the OASIS3-MCT interpolation scalability limit) and/or (2) by the
465 fastest model (until the OASIS3-MCT interpolation together with the fastest model's calculations last longer than the calculations of the slowest model).

A significant improvement of interpolation ~~performance~~and communication performances can be achieved by coupling of multiple variables that share the same coupling characteristics via a single communication, that is, by using the technique called *pseudo-3D coupling*. Via this option, a single
470 interpolation and a single send/receive instruction are executed for a whole group of coupling fields, for example, all levels and variables in an atmosphere-atmosphere coupling at one time instead of all coupling fields and levels separately. The option groups several small MPI messages into a big one and, thus, reduces communications. Furthermore, the amount of matrix multiplications is reduced because it is performed on big arrays. This functionality can easily be set via the ~~namecouple~~
475 'namcouple' parameter file (see section B.2.4 in Valcke et al. (2013)). The impact on the performance of COSMO-CLM atmosphere-atmosphere coupling is discussed in section ~~??~~4.6). See also Maisonnave et al. (2013).

The optimization of the ~~coupled-system performance~~performance of a coupled-system relies on the allocation of an optimum number of computing resources to each model. If the components' cal-

480 calculations are performed concurrently the waiting time needs to be minimized. This can be achieved
by balancing the load of the two (or more) components between the available computing resources:
the slower component is granted more resources leading to an increase in its parallelism and a de-
crease in its computing time. The opposite is done for the fastest component until an equilibrium is
reached. Chapter 4 gives examples of this operation and describes the strategy to find a compromise
485 between each component's optimum scalability and the load balance between all components.

On all high-performance operating systems it is possible to run one process of a parallel ap-
plication on one core in a so-called *single-threading* (ST) mode (fig. 2a). Should the core of the
operating system feature the so-called *simultaneous multi-threading* (SMT) mode, two (or more)
processes/threads of the same (in a *non-alternating processes distribution* (fig.2b)) or of different (in
490 an *alternating processes distribution* (fig.2c)) applications can be executed simultaneously on the
same core. Applying SMT mode is more efficient for well-scaling parallel applications leading to an
increase in speed in the order of magnitude of 10 % compared to the ST mode. Usually it is possible
to specify, which process is executed on which core (see fig. 2). ~~This allows, to use~~ In this cases
the SMT mode with alternating distribution of model component processes ~~, and to avoid can be~~
495 used, and the waiting time of sequentially coupled components can be avoided. Starting each model
component on each core is usually the optimum configuration, since the reduction of waiting time
of cores outperforms the increase of the time to solution by using ST mode instead of SMT mode (at
each time one process is executed on each core). In the case of concurrent couplings, however, it is
possible to use SMT mode with a non-alternating processes distribution.

500 The optimization procedure applied is described in more detail in section 4.3 for the couplings
considered. The results are discussed in section ~~??~~4.6.

3.1.3 Regional climate model coupling particularities

~~Additionally~~ In addition to the standard OASIS functionalities, some adaptation of the OASIS3-
MCT API routines were necessary to fit special requirements of the regional-to-regional and regional-
505 to-global couplings presented in this article.

A regional model covers only a portion of earth's sphere and requires boundary conditions at its
domain boundaries. This has two immediate consequences for coupling: first, two regional models
do not necessarily cover exactly the same part of earth's sphere. This implies that the geographic
boundaries of the model's computational domains and of coupled variables may not be the same in
510 the source and target ~~component~~ components of a coupled system. Second, a regional model can be
coupled with a global model or another limited-area model and some of the variables which need to
be exchanged are three-dimensional as in the case of atmosphere-to-atmosphere or ocean-to-ocean
coupling.

A major part of the OASIS community uses global models. Therefore, OASIS standard features
515 fit global model coupling requirements. Consequently, the coupling library must be adapted or used

in an unconventional way, described in the following, to be able to cope with the extra demands mentioned.

Limited-area field exchange has to deal with a mismatch of the domains of the coupled model components. Differences between the (land and ocean) models coupled to COSMO-CLM lead to two solutions for the mismatch of the model domains. For coupling with the Community Land Model (CLM) the CLM domain is extended in such a way that at least all land points of the COSMO-CLM domain are covered. Then, all CLM grid points located outside of the COSMO-CLM domain are masked. To achieve this, a uniform array on the COSMO-CLM grid is interpolated by OASIS3-MCT to the CLM grid using the same interpolation method as for the coupling fields. On the CLM grid the uniform array contains the projection weights of the COSMO-CLM on the CLM grid points. This field is used to construct a new CLM domain containing all grid points necessary for interpolation. However, this solution is not applicable to all coupled-system components. In ocean models, a domain modification would complicate the definition of ocean boundary conditions or even lead to numerical instabilities at the new boundaries. Thus, the original ocean domain, that must be smaller than the COSMO-CLM domain, is interpolated to the COSMO-CLM grid. At runtime, all COSMO-CLM ocean grid points located inside the interpolated area are filled with values interpolated from the ocean model and all COSMO-CLM ocean grid points located outside the interpolated area are filled with external forcing data.

Multiple usage of the MCT library occurred in the CCLM+CLM coupled system implementation and made making some modifications of the OASIS3-MCT version 2.0 necessary. Since the MCT library has no re-entrancy properties, a duplication of the MCT library and a renaming of the OASIS3-MCT calling instruction were necessary. This modification ensures the capability of coupling any other CESM component via OASIS3-MCT. The additional usage of the MCT library occurred in the CESM framework of CLM version 4.0. More precisely, the DATM model interface in the CESM module is using the CPL7 coupler including the MCT library for data exchange.

Interpolation of 3D fields is necessary in an atmosphere-to-atmosphere coupling. The OASIS3-MCT library is used to provide 3D boundary conditions to the regional model and a 3D feedback to the global coarse-grid model. OASIS is not able to interpolate the 3D fields vertically, mainly because of the complexity of vertical interpolations in geophysical models (different orographies, level numbers and formulations of the vertical grid). However, it is possible to decompose the operation into two steps: (1) horizontal interpolation with OASIS3-MCT and (2) model-specific vertical interpolation performed in the source or target component's interface. The first operation does not require any adaption of the OASIS3-MCT library and can be solved in the most efficient manner by the pseudo-3D coupling option described in section 3.1.2. The second operation requires a case-dependent algorithm addressing aspects such as inter- and extrapolation extra-polation of the boundary layer over different orographies, change of the coordinate variable, conservation properties as well as interpolation efficiency and accuracy.

An exchange of 3D fields, which occurs in the CCLM+MPI-ESM coupling, requires a more intensive usage of the OASIS3-MCT library functionalities than observed so far in the climate modeling community. The 3D regional-to-global coupling is even more computationally demanding than its global-to-regional opposite. Now, all grid points of the COSMO-CLM domain have to be interpolated instead of just the grid points of a global domain that are covered by the regional domain. The amount of data exchanged is rarely reached by any other coupled system of the community due to (1) the high number of exchanged 2D fields, (2) the high number of exchanged grid points (full COSMO-CLM domain) and (3) the high exchange frequency at every ECHAM time step. In addition, as will be explained in section 3.2, the coupling between COSMO-CLM and MPI-ESM needs to be sequential and, thus, the exchange speed has a direct impact on the simulation's total time to solution.

Interpolation methods used in OASIS3-MCT are the SCRIP standard interpolations: bilinear, bicubic, first- and second-order conservative. However, the interpolation accuracy might be not not be sufficient and/or the method is inappropriate for certain applications. This is for example the case with the atmosphere-to-atmosphere coupling CCLM+MPI-ESM. The linear methods turned out to be of low accuracy and the second-order conservative method requires the availability of the spatial derivatives on the source grid. Up to now, the latter cannot be calculated efficiently in ECHAM (see section 3.2 for details). Other higher-order interpolation methods can be applied by providing weights of the source grid points at the target grid points. This method was successfully applied in the CCLM+MPI-ESM coupling by application of a bicubic interpolation using a 16-point stencil. In section 3.2 to 3.5 the interpolation methods recommended for the individual couplings are given.

3.2 CCLM+MPI-ESM

In the CCLM+MPI-ESM two-way coupled system the 3D atmospheric fields are exchanged between the atmospheres of COSMO-CLM and MPI-ESM running sequentially. In MPI-ESM the COSMO-CLM tendencies can be regarded as a parameterization of meso-scale processes in a limited domain of the global atmosphere. In COSMO-CLM the MPI-ESM boundary conditions are used as in standard one-way nesting. Both atmosphere models run sequentially.

COSMO-CLM recalculates the ECHAM time step in dependence on the lateral- and top-boundary conditions provided by ECHAM. In ECHAM the solution is updated in a limited area of the globe using the solution provided by COSMO-CLM. For computational-efficiency reasons the data exchange in ECHAM is done in grid point space. This avoids costly transformations between grid point and spectral space. Since the simulation results of COSMO-CLM need to become effective in ECHAM dynamics, the two-way coupling is implemented in ECHAM after the transformation from spectral to grid point space and before the computation of advection (see Fig. 8 and DKRZ (1993) for details).

ECHAM provides the boundary conditions for COSMO-CLM at time level $t = t_n$ of the three time levels $t_n - (\Delta t)_E$, t_n and $t_n + (\Delta t)_E$ of ECHAM's leap frog time integration scheme. However, the second part of the Assilin time filtering in ECHAM for this time level has to be executed after the advection calculation in `dyn` (see Fig. 8) in which the tendency due to two-way coupling needs to be included. Thus, the fields sent to COSMO-CLM as boundary conditions do not undergo the second part of the Assilin time filtering. The COSMO-CLM is integrated over j time steps between the ECHAM time level t_{n-1} and t_n . However, the coupling time may also be a multiple of an ECHAM time step.

A complete list of variables exchanged between ECHAM and COSMO-CLM is given in Table 4). The data sent by ECHAM are the 3D variables of COSMO-CLM temperature, u- and v-components of the wind velocity, specific humidity, cloud liquid and ice water content and the two-dimensional fields surface pressure, surface temperature and surface snow amount. At initial time the surface geopotential is sent to COSMO-CLM for calculation of the orography differences between the model grids. After horizontal interpolation to the COSMO-CLM grid via the bilinear SCRIP interpolation¹ the 3D variables are vertically interpolated to the COSMO-CLM grid keeping the height of the 300 hPa level constant and using the hydrostatic approximation. Afterwards, the horizontal wind vector velocity components of ECHAM are rotated from the geographical (lon, lat) ECHAM to the rotated (rlon, rlat) COSMO-CLM coordinate system. Here `send fld` ends and the interpolated data are used to initialize the boundlines at next COSMO-CLM time levels $t_m = t_{n-1} + k \cdot (\Delta t)_C \leq t_n$, with $k \leq j = (\Delta t)_E / (\Delta t)_C$. However, the final time of COSMO-CLM integration $t_{m+j} = t_m + j \cdot (\Delta t)_C = t_n$ is equal to the time t_n of the ECHAM data received.

After integrating between $t_n - i \cdot (\Delta t)_E$ and t_n the 3D fields of temperature, u- and v velocity components, specific humidity and cloud liquid and ice water content of COSMO-CLM are vertically interpolated to the ECHAM vertical grid following the same procedure as in the COSMO-CLM ~~receive interface~~ receive interface and keeping the height of the 300 hPa level of the COSMO-CLM pressure constant. The wind velocity vector components are rotated back to the geographical directions of the ECHAM grid. The 3D fields and the hydrostatically approximated surface pressure are sent to ECHAM, horizontally interpolated to the ECHAM grid by OASIS3-MCT² and received in ECHAM grid space. In ECHAM the COSMO-CLM solution is relaxed at the lateral and top boundaries of the COSMO-CLM domain by means of a cosine weight function over a range of five to ten ECHAM grid boxes using a weight between zero at the outer boundary and one in the central part of the COSMO-CLM domain. Additional fields are calculated and relaxed in the COSMO-

¹This interpolation is used for the performance tests only. For physical coupling the conservative interpolation second order (CO2) is used, which requires the additional computation of derivatives. Alternatively, a bicubic interpolation can be used that has the same accuracy as CO2.

²The bilinear interpolation is used. The usage of a second-order conservative interpolation requires horizontal derivatives of the variables exchanged. This is not implemented in this version of the COSMO-CLM send interface.

620 CLM domain for a consistent update of the ECHAM prognostic variables. These are the horizontal derivatives of temperature, surface pressure, u and v wind velocity, divergence and vorticity.

The two-way coupled system CCLM+MPI-ESM with prescribed COSMO-CLM solution within the COSMO-CLM domain (weight=1) provides a stable solution over climatological time scales. A strong initialization perturbation is avoided by slowly increasing the maximum coupling weight to 1
625 with time, following the function $weight = weight_{max} \cdot (\sin((t/t_{end}) \cdot \pi/2))$, with t_{end} equal to 1 month.

3.3 CCLM+NEMO-MED12(Jennifer)

COSMO-CLM and the NEMO ocean model are coupled concurrently for the Mediterranean Sea (NEMO-MED12) and for the North and Baltic Sea (NEMO-NORDIC). Table 5 gives an overview of
630 the variables exchanged. Bicubic interpolation between the horizontal grids is used for all variables.

At the beginning of the NEMO time integration (see Fig. 7) the COSMO-CLM receives the sea surface temperature (SST) and - only in the case of coupling with the North and Baltic Sea - also the sea ice fraction from the ocean model. At the end of each NEMO time step COSMO-CLM sends average water, heat and momentum fluxes to OASIS3-MCT. In the NEMO-NORDIC setup
635 COSMO-CLM additionally sends the averaged sea level pressure (SLP) needed in NEMO to link the exchange of water between North and Baltic Sea directly to the atmospheric pressure. The sea ice fraction affects the radiative and turbulent fluxes due to different albedo and roughness length of ice. In both coupling setups SST is the lower boundary condition for COSMO-CLM and it is used to calculate the heat budget in the lowest atmospheric layer. The averaged wind stress is a direct
640 momentum flux for NEMO to calculate the water motion. Solar and non-solar radiation are needed by NEMO to calculate the heat fluxes. $E - P$ ("Evaporation minus Precipitation") is the net gain ($E - P > 0$) or loss ($E - P < 0$) of fresh water at the water surface. This water flux adjusts the salinity of the uppermost ocean layer.

In all COSMO-CLM grid cells where there is no active ocean model underneath, the lower bound-
645 ary condition (SST) is taken from ERA-Interim re-analyses. The sea ice fraction in the Atlantic Ocean is derived from the ERA-Interim SST where $SST < -1.7^\circ C$ which is a salinity-dependent freezing ~~temperatur~~temperature.

On the NEMO side, the coupling interface is included similar to COSMO-CLM, as can be seen in Fig. 9. There is a setup of the coupling interface at the beginning of the NEMO simulation. At
650 the beginning of the time loop NEMO receives the upper boundary conditions from OASIS3-MCT and before the time loop ends, it sends the coupling fields (average SST and sea ice fraction for NEMO-NORDIC) to OASIS3-MCT.

3.4 CCLM+TRIMNP+CICE

In the CCLM+TRIMNP+CICE coupled system (denoted as COSTRICE; Ho-Hagemann et al. (2013)),
655 all fields are exchanged every hour between the three models COSMO-CLM, TRIMNP and CICE
running concurrently. An overview of variables exchanged among the three models is given in Table
5. The “surface temperature over sea/ocean” is sent to CCLM instead of “SST” to avoid a potential
inconsistency in case of sea ice existence. As shown in Fig. 7, COSMO-CLM receives the skin
temperature (T_{skin}) at the beginning of each COSMO-CLM time step over the coupling areas, the
660 North and Baltic Seas. The skin temperature T_{skin} is a weighted average of sea ice and sea surface
temperature. It is not a linear combination of skin temperatures over water and over ice weighted
by the sea ice fraction. Instead, the skin temperature over ice T_{Ice} and the sea ice fraction A_{Ice} of
CICE are sent to TRIMNP where they are used to compute the heat flux HFL , that is, the net out-
going long-wave radiation. HFL is used to compute the skin temperature of each grid cell via the
665 Stefan-Boltzmann Law.

At the end of the time step, after the physics and dynamics computations and output writing,
COSMO-CLM sends the variables listed in Table 5 to TRIMNP and CICE for calculation of wind
stress, fresh water, momentum and heat flux. TRIMNP can either directly use the sensible and latent
heat fluxes from COSMO-CLM (considered as flux coupling method; see e.g. Döscher et al. (2002))
670 or compute the turbulent fluxes using the temperature and humidity density differences between
air and sea as well as the wind speed (considered as the coupling method via state variables; see
e.g. Rummukainen et al. (2001)). The method used is specified in the subroutine `heat_flux` of
TRIMNP.

~~The sea ice model CICE requires from TRIMNP, additionally~~ In addition to the fields received
675 from COSMO-CLM, the sea ice model CICE requires from TRIMNP the SST, salinity, water veloc-
ity components, ocean surface slope, and freezing/melting potential energy. CICE sends to TRIMNP
the water and ice temperature, sea ice fraction, fresh-water flux, ice-to-ocean heat flux, short-wave
flux through ice to ocean and ice stress components. The horizontal interpolation method applied in
CCLM+TRIMNP+CICE is the SCRIP nearest-neighbour inverse-distance-weighting fourth-order
680 interpolation (DISTWGT).

Note that the coupling method differs between CCLM+TRIMNP+CICE and CCLM+NEMO-NORDIC
(see section 3.3). In the latter, SSTs and sea ice fraction from NEMO are sent to CCLM so that
the sea ice fraction from NEMO affects the radiative and turbulent fluxes of CCLM due to different
albedo and roughness length of ice. But in CCLM+TRIMNP+CICE, only SSTs are passed to CCLM.
685 Although these SSTs implicitly contain information of sea ice fraction, which is sent from CICE to
TRIMNP, the albedo of sea ice in CCLM is not taken from CICE but calculated in the atmospheric
model independently. The reason for this inconsistent calculation of albedo between these two
coupled systems originates from a fact that a tile-approach has not been applied for the CCLM
version used in the present study. Here, partial covers within a grid box are not accounted for, hence,

690 partial fluxes, i.e. the partial sea ice cover, snow on sea ice and water on sea ice are not considered.
In a water grid box of this CCLM version, the albedo parameterisation switches from ocean to sea
ice if the surface temperature is below a freezing temperature threshold of $-1.7^{\circ}C$. Coupled to
NEMO-NORDIC, CCLM obtains the sea ice fraction, but the albedo and roughness length of a grid
box in CCLM are calculated as a weighted average of water and sea ice portions which is a parameter
695 aggregation approach.

Moreover, even if the sea ice fraction from CICE would be sent to CCLM, such as done for
NEMO-NORDIC, the latent and sensible heat fluxes in CCLM would still be different to those
in CICE due to different turbulence schemes of the two models CCLM and CICE. This different
calculation of heat fluxes in the two models leads to another inconsistency in the current setup which
700 only can be removed if all model components of the coupled system use the same radiation and
non-radiation energy fluxes. These fluxes should preferably be calculated in one of the models at the
highest resolution, for example in the CICE model for fluxes over sea ice. Such a strategy shall be
applied in future studies, but is beyond the scope with the CCLM version used in this study.

3.5 CCLM+VEG3D and CCLM+CLM

705 The two-way coupling between COSMO-CLM and the land surface models VEG3D or CLM is sim-
ilar to the other in several respects. First, the call to the LSM (OASIS send and receive; see Fig. 7)
is placed at the same location in the code as the call to COSMO-CLM's native land surface scheme,
TERRA_ML, which is switched off when either VEG3D or CLM is used. This ensures that the se-
quence of calls in COSMO-CLM remains the same regardless of whether TERRA_ML, VEG3D
710 or CLM is used. In the default configuration used here COSMO-CLM and CLM (or VEG3D)
are executed sequentially, thus ~~imitating-mimicking~~ the "subroutine"-type of coupling used with
TERRA_ML. Note that it is also possible to run COSMO-CLM and the LSM concurrently but this
is not discussed here. Details of the time step organization of VEG3D and CLM are described in the
appendix and shown in Fig. 12 and 13 .

715 VEG3D runs at the same time step and on the same horizontal rotated grid (0.44° here) as
COSMO-CLM with ~~thus~~ no need for any horizontal interpolations. CLM uses a regular lat-lon
grid and the coupling fields are interpolated using bilinear interpolation (atm to LSM) and distance-
weighted interpolation (LSM to atm). The time step of CLM is synchronized with the COSMO-CLM
radiative transfer scheme time step (one hour in this application) with the idea that the frequency
720 of the radiation update determines the radiative forcing at the surface.

The LSMs need to receive the following atmospheric forcing fields (see also Table 6): the total
amount of precipitation, the short- and long-wave downward radiation, the surface pressure, the wind
speed, the temperature and the specific humidity of the lowest atmospheric model layer.

CLM additionally receives the atmospheric forcing height³ for calculation of ~~the~~ turbulence in the atmospheric boundary layer. VEG3D ~~needs additionally~~ additionally needs information about the time-dependent composition of the vegetation to describe its influence on radiation interactions and turbulent fluxes correctly. This includes the leaf area index, the plant cover and a vegetation function which describes the annual cycle of vegetation parameters based on a simple cosine function depending on latitude and day. They are exchanged at the beginning of each simulated day.

One specificity of the coupling concerns the turbulent fluxes of latent and sensible heat. In its turbulence scheme, COSMO-CLM does not directly use surface fluxes. It uses surface states (surface temperature and humidity) together with turbulent diffusion coefficients of heat, moisture and momentum. Therefore, the diffusion coefficients need to be calculated from the surface fluxes received by COSMO-CLM. This is done by deriving, in a first step, the coefficient for heat (assumed to be the same as the one for moisture in COSMO-CLM) based on the sensible heat flux. In a second step an effective surface humidity is calculated using the latent heat flux and the derived diffusion coefficient for heat.

4 Computational efficiency

Optimising the Computational efficiency is an important property of numerical model's usability and applicability and has many aspects. A particular coupled model systems can be very inefficient even if each component model has a high computational efficiency in stand-alone mode and in other couplings. Thus, optimizing the computational performance of a coupled model system can save a substantial amount of resources in terms of simulation time ~~or costs. Sometimes, it is even a prerequisite for the applicability of a model system at higher resolutions or on climatological~~ time scales. There are two main goals of a performance analysis: (1) ~~To identify code patterns of inefficient behaviour in parallel applications for a given resources configuration by using sophisticated tools such as e. g. SCALASCA (Geimer et al., 2010) and VampirTrace (Müller et al., 2008).~~ (2) ~~To analyze and cost.~~ We focus here on aspects of computational efficiency related directly to coupling of different component models overall tested in other applications and use real case model configuration.

We use a three step approach. First, the scalability of ~~a coupled model system and its components in order to obtain~~ different coupled model systems and of its components is investigated. Second, an optimum configuration of resources ~~.The second is the subject of this chapter is~~ derived and third, different components of extra cost of coupling at optimum configuration are quantified. For this purpose the *Load-balancing Utility and Coupling Implementation Appraisal* (LUCIA), developed at CERFACS, Toulouse, France (Maisonnavé and Caubel, 2014) is used, which is available together with the OASIS3-MCT coupler.

³This field is needed for initialization only. In this test series it is exchanged at every coupling time.

More precisely, we investigate the scalability of each coupled system's components in terms of simulation speed, computational ~~costs~~-cost and parallel efficiency, the time needed for horizontal interpolations by OASIS3-MCT and the load balance in the case of concurrently running components. Based on these results, an optimum configuration for all couplings is suggested. Finally, the ~~costs of the optimum~~ cost of all component models at optimum configurations are compared with an optimum stand-alone the cost of COSMO-CLM configuration and the potential for further optimization is discussed stand-alone at configuration used in coupled system and at optimum configuration ($CCLM_{sa,OC}$) of the stand-alone simulation.

4.1 Simulations ~~Simulation~~ setup and methodology

A parallel program's runtime $T(n, R)$ mainly depends on two variables: the problem size n and the number of cores R , that is, the resources. In scaling theory, a *weak scaling* is performed with the notion to solve an increasing problem size in the same time, while as in a *strong scaling* a fixed problem size is solved more quickly with an increasing amount of resources. Due to ~~resources~~-resource limits on the common high-performance computer we chose to conduct a strong-scaling analysis with a common model setup allowing for an easier comparability of the results. By means of the scalability study we identified an optimum configuration for each coupling which served as basis to address two central questions: (1) How much does it cost to add one (or more) component(s) to COSMO-CLM? (2) How big are the ~~costs of~~ cost of different components and of OASIS3-MCT to transform the information between the components' grids? The first question can only be answered by a comparison to a reference which is, in this study, a CCLM stand-alone COSMO-CLM simulation. The second question can directly be answered by the measurements of LUCIA. We used this part of the OASIS3-MCT library-tool to measure the computing and waiting time of each component in a coupled model system (see section 3.1.2) as well as the time needed for interpolation of fields before and after sending or receiving.

A ~~common model setup for the CORDEX-EU domain~~ recommended configuration was chosen for the reference model COSMO-CLM COSMO-CLM at 0.44 horizontal resolution. The other components' setups are those used by the developers of the particular coupling (see section 2)-for more details) for climate modelling applications in the CORDEX-EU domain. This means, that I/O, model physics and dynamics is chosen in the same way as for climate applications in order to obtain a realistic estimate of the performance of the couplings. The simulated period is one month, the horizontal grid has 132 by 129 grid points and 0.44° (ca. 50 km) horizontal grid spacing. In the vertical, 45 levels are used for the CCLM+MPI-ESM and CCLM+VEG3D couplings as well as for the stand-alone COSMO-CLM CCLM_{sa} simulations. All other couplings use 40 levels. The impact of this difference on the numerical performance is ~~compensated~~-compensated by a simple post-processing scaling of the measured COSMO-CLM-CCLM computing time $T_{CCLM,45}$ of the COSMO-CLM-CCLM components that employ 45 levels assuming a linear scaling of the

COSMO-CLM-CCLM computing time with the number of levels as $T_{CCLM} = 0.8 \cdot T_{CCLM,45} \cdot \frac{40}{45} + 0.2 \cdot T_{CCLM,45}$.⁴ The usage of a real-case configuration allows to provide realistic computing times.

The computing architecture used is *Blizzard* at *Deutsches Klimarechenzentrum* (DKRZ) in Hamburg, Germany. It is an IBM Power6 machine with nodes consisting of 16 dual-core CPUs (16 processors, 32 cores). A simultaneous multi-threading (SMT; see section 3.1.2) allows to launch two processes on each core. A maximum of 64 threads that can be launched on one node.

The measures used in this paper to present and discuss the computational performance are well known in scalability analyses: (1) *time to solution* in Hours Per Simulated Year (HPSY), (2) *costs* in Core Hours Per Simulated Year (CHPSY) and (3) *parallel efficiency* (PE) (see Table 7 for details).

Usually, $HPSY_1$ is the time to solution of a model component executed serially, that is, using one process ($R = 1$) and $HPSY_2$ is the time to solution if executed using $R_2 > R_1$ parallel processes. Some model components, like ECHAM, cannot be executed serially. This is why the reference number of threads is $R_1 \geq 2$ for all coupled-system components.

~~In~~ If the resources of a perfectly scaling parallel application are doubled, the speed would be doubled and therefore the cost would remain constant, the parallel efficiency would be 100 %, ~~the speed would be doubled~~ and the speed-up would be 200 %. A parallel efficiency of 50 % is reached if the ~~costs~~ $CHPSY_2$ are twice as big as those of the reference configuration $CHPSY_1$.

4.2 Strategy for finding an optimum configuration

~~The optimization strategy that we pursue is rather empirical than strictly mathematical, which is why we understand "optimum" more as "near-optimum". Nonetheless, our results show that these empirical methods are sufficient for the complexity of the couplings investigated here and lead to satisfying results. Besides costs and Inconsistencies of the time to solution, we suggest a limit for parallel efficiency of 50% of approximately 10 % until which increasing costs can be regarded as still acceptable. Usually, this is limiting the time to solution which can be achieved and depends on the cost efficiency of the reference configuration. In this study for all couplings the one-node configuration is regarded to have 100 % parallel efficiency. This leads to the constraint $R_{CCLM} = R_{CCIM+CLM} = R_{CCLM+VEG3D}$ for the number R of cores investigated, and a clear strategy for finding the maximum number of nodes for which $PE \geq 50\%$ were found between measurements obtained from simulations conducted at two different physical times. This gives a measure of the dependency of the time to solution on the status of the machine used, particularly originating from the I/O. Nevertheless, the time to solution and cost are given with higher accuracy to highlight the consistency of the numbers.~~

⁴The estimation that 80 % of COSMO-CLM's computations depend on the number of model levels is based on COSMO-CLM's internal time measurements. $T_{CCLM,45}$ is the time measured by LUCIA.

⁴The estimation that 80 % of COSMO-CLM's computations depend on the number of model levels is based on COSMO-CLM's internal time measurements. $T_{CCLM,45}$ is the time measured by LUCIA.

The strategies for identifying an optimum configuration are different for sequential and concurrent couplings due to the possible waiting time which needs to be considered with concurrent couplings.

830 For sequentially running components (CCLM+CLM and CCLM+MPI-ESM) we used the SMT mode and an alternating distribution of processes to make sure that all cores were busy at all times. Hereby possible component internal load imbalances due to e.g. parts of the code not executed in parallel are neglected. A detailed analysis of CCLM+MPI-ESM performance on one node ($n = 1$) showed a significant reduction of time to solution and costs, if alternating instead of non-alternating distribution of processes in SMT mode (see section ?? for details) is used. The optimum configuration
835 is found by starting the measuring of the computing time on one node for all components, doubling the resources and measuring the computing time again and again as long as each component's gain in speed, compared to its speed on one node, outweighs the increase in costs. If costs are, however, not an issue it is suggested to stop increasing resources before a parallel efficiency of 50% of each component model is reached.

840 For concurrent couplings (CCLM+NEMO-MED12 and CCLM+TRIMNP+CICE) the SMT mode with non-alternating process distribution is used aiming to speed up all components in comparison to the ST mode. The constraint for the distribution of cores is $\sum_{m=1}^M R_m = \#nodes - 32$. A summary of the configuration of each coupled system is given in Table 8.

The optimization process of a concurrently coupled model system additionally needs to consider
845 minimising the load imbalance between all components. This means that the computing times of all components need to be similar in order to reduce the costs due to idle cores. Practically speaking, one starts with a first-guess distribution of processes between all components on one node, measure each component's computing and waiting time and adjust the processes distribution between the model components if the waiting time of at least one component is larger than 5% of the total runtime.
850 If, finally, the waiting times of all components are small, the following chain of action is repeated several times: doubling resources for each component, measuring computing times, adjusting and re-distributing the processes if necessary. If costs are a limiting factor this is repeated until the costs reach a pre-defined limit. If costs are not a limiting factor, the procedure should be repeated until the model with the highest time to solution reaches the proposed parallel efficiency limit of 50%.

855 4.2 Scalability results

Figure 3 shows the results of the performance measurement *time to solution* for all model components individually in coupled mode and for ~~stand-alone COSMO-CLM~~ CCLM_{sa} (in ST and SMT mode). As reference, the slopes of a model at no speed-up and at perfect speed-up are shown. Three groups can be identified. CLM and VEG3D have the shortest times to solution and, thus,
860 they are the fastest components. The three ~~ocean components and the COSMO-CLM components~~ models of ocean coupling with CCLM and the CCLM models in coupled as well as in stand-alone mode need about 2–10 HPSY. The overall slowest ~~components~~ component models are CICE and

ECHAM which need about 20 HPSY ~~independently on the amount of resources used at reference~~ configuration. Within the range of resources investigated CICE, ECHAM and VEG3D exhibit almost
865 no speed-up ~~-in coupled mode (i.e. including additional computations)~~. On the contrary, MPIOM,
NEMO-MED12 and CLM have a very good scalability up to the tested limit of 128 cores.

Figure 4 shows the second relevant performance measure, the absolute ~~costs~~ cost of computation
in CPUs-core hours per simulated year for the same couplings together with the perfect and no
speed-up slopes. The afore mentioned three groups slightly change their composition. VEG3D and
870 CLM are not only the fastest but also the cheapest components, the latter becoming even cheaper
with increasing resources. A little bit more expensive but mostly in the same order of magnitude as
the land surface components are the ocean components MPIOM and TRIMNP followed by CICE,
NEMO-MED12 and all the different ~~COSMO-CLM components coupled~~ CCLM. The NEMO model
is approximately two times more expensive than TRIMNP. ~~Surprisingly, The configuration of the~~
875 ~~CICE model is as expensive as the regional climate model COSMO-CLM. The most expensive~~
~~coupled component is ECHAM with almost doubled costs as resources are doubled. This and the~~
~~high coupling costs of COSMO-CLM coupled to MPI-ESM will be analyzed in section ?? and~~
~~??~~ CCLM. The cost of CCLM differ by a factor of two between the stand-alone and the different
coupled versions. The most expensive one is coupled to ECHAM, which is also the most expensive
880 component model.

In order to analyze the performance of the couplings in more detail we took measurements
of stand-alone COSMO-CLM in single-threading (ST) and multi-threading (SMT) mode. The di-
rect comparison provides the information of how much COSMO-CLM's speed ~~benefits and cost~~
benefit from switching from ST to SMT mode. As shown in Fig. 3 at 16 cores the COSMO-
885 CLM in SMT mode is 27 % faster. When allocating 128 cores both modes arrive at about the
same speed ~~and costs~~. ~~The parallel efficiency shown in Fig. 5 allows to understand this behavior.~~
~~COSMO-CLM in ST and SMT mode exhibits a very similar PE. This can be explained by increasing~~
cost of MPI communications with decreasing number of grid points/thread. Since the number of
threads in SMT mode is twice for the same ~~number of processes and an increased loss of PE~~
890 ~~between 160 core number and 80 thus the number of~~ grid points per process. This can be explained
by a weak scalability of unavoidable communication of data between the threads computing the
values in subdomains. The values at three grid points close to the subdomain boundary need to be
communicated to the thread computing the values in the neighboring grid points. In conclusion, it is
recommended to keep the number of horizontal grid points per process higher than $100 = 10 \times 10$.
895 thread is half, the scalability limit of approximately 1.5 points exchanged per computational grid
point is reached at approximately 100 points/thread (if 3 boundlines are exchanged) resulting in
a scalability limit at approximately 80 cores in SMT mode and 160 cores in ST mode (see also
CCLM+NEMO-MED12 coupling in section 4.4).

The difference in time to solution (Fig. 3) and costs (Fig. 4) between coupled and stand-alone
900 COSMO-CLM is a direct measure of the additional

4.3 Strategy for finding an optimum configuration

The optimization strategy that we pursue is rather empirical than strictly mathematical, which is
why we understand "optimum" more as "near-optimum". Due to the heterogeneity of our coupled
systems, a single algorithm cannot be proposed (as in Balaprakash et al. (2014)). Nonetheless, our
905 results show that these empirical methods are sufficient, regarding the complexity of the couplings
investigated here, and lead to satisfying results.

Obviously, "optimum" has to be a compromise between cost and time to solution. In order to find
a unique configuration we suggest the optimum to have a parallel efficiency higher than 50 % of the
cost of the reference configuration, until which increasing cost can be regarded as still acceptable. In
910 the case of scalability of all components and no substantial cost of necessary additional calculations,
this guarantees that the coupled-system's time to solution is only slightly bigger than that of the
component with the highest cost.

However, such "optimum" configuration depends on the reference configuration. In this study for all
couplings the one-node configuration is regarded to have 100 % parallel efficiency.

915 An additional constraint is sometimes given by the CPU accounting policy of the computing
centre, if consumption is measured "per node" and not "per core". This leads to a restriction of
the "optimum" configuration (r_1, r_2, \dots, r_n) of cores r_i for each model component of the coupled
system to those, for which the total number of cores $R = \sum_i r_i$ is a multiplex of the number of cores
 r_n per node: $R = \#nodes \cdot r_n$.

920 An exception is the case of very low scalability of a component model which has a time to solution
and costs due to the COSMO-CLM component interface. Hereby, similar to the time to solution of
the coupled model system. In this case an increase of the number of cores and the threading mode
(ST or SMT) are kept constant. COSMO-CLM components of concurrent couplings are compared to
stand-alone COSMO-CLM in SMT mode. COSMO-CLM components of sequential couplings are
925 compared to stand-alone COSMO-CLM in ST mode. The latter has the same amount of processes
per node and only one process per core. For coupling COSMO-CLM to ocean models results in an
increase of cost and in no decrease of time to solution. In such a case the optimum configuration is
the one with lower cost, even if the limit of 50 % parallel efficiency is fulfilled for the configuration
with higher cost.

930 The strategies of identifying an optimum configuration are different for sequential and concurrent
couplings due to the possible waiting time, which needs to be considered with concurrent couplings.

For sequential couplings (CCLM+CLM, CCLM+VEG3D and CCLM+MPI-ESM) the SMT mode
and an alternating distribution of processes (ADP) is used to keep all cores busy at all times. The

935 possible component-internal load imbalances, which occurs when parts of the code are not executed
in parallel, are neglected. The effect of ADP has been investigated for CCLM+MPI-ESM coupling
on one node ($n = 1$) in more detail and the results are presented in section 4.6.

The optimum configuration is found by starting the measuring of the computing time on one node
for all components, doubling the resources and measuring the computing time again and again as
940 long as all components' parallel efficiencies remain above 50 %. One could decide to stop at a higher
parallel efficiency if cost are a limiting factor.

~~For concurrent couplings (CCLM+NEMO-MED12 and TRIMNP+CCLM+TRIMNP+CICE, these~~
~~additional times to solution and costs are 1–5 % at 16 cores and 5–13 % at 32 cores. The comparison~~
~~of coupled and stand-alone COSMO-CLM in ST mode at 32 cores exhibits 11 % additional time~~
945 ~~to solution and costs for COSMO-CLM coupled to VEG3D) the SMT mode with non-alternating~~
~~processes distribution is used aiming to speed up all components in comparison to the ST mode and~~
~~76 % for COSMO-CLM coupled to MPI-ESM. At 128 cores, the differences increase to 21 and~~
~~93 reduce the inter-node communication.~~

The optimization process of a concurrently coupled model system additionally needs to consider
950 minimizing the load imbalance between all components. For a given total number of cores (cost)
used the time to solution is minimized, if all components have the same time to solution (no load
imbalance) and thus no cores are idle during the simulation. Practically speaking, one starts with a
first-guess distribution of processes between all components on one node, measures each component's
computing and waiting time and adjusts the processes distribution between the model components if
955 the waiting time of at least one component is larger than 5 % respectively. It is worth noting here that
~~COSMO-CLM coupled to CLM should exhibit about the same coupling costs as COSMO-CLM~~
~~coupled to VEG3D since both coupling interfaces lead to similar times to solution % of the total~~
~~runtime. If, finally, the waiting times of all components are small, the following chain of action~~
~~is repeated several times: doubling resources for each component, measuring computing times,~~
960 ~~adjusting and re-distributing the processes if necessary. If cost are a limiting factor this is repeated~~
~~until the cost reach a pre-defined limit. However, as mentioned in section 2.6 CLM is coupled to~~
~~eosmo_5.0_clm1 model version which is a more recent version than eosmo_4.8_clm19 used~~
~~for all other couplings presented here. Therefore, the true additional costs can be slightly different.~~

The parallel efficiency shown in Fig. 5 gives a better understanding of the development of costs
965 and speed. For CLM it exhibits a so-called *super-linear speed-up* which has not been investigated
in detail. The components CICE, ECHAM and VEG3D exhibit a very fast loss of PE close to
the no-speed-up limit indicating nearly no scalability. TRIMNP loses PE fast in comparison to
NEMO-MED12 indicating "no speed-up" of some parts of the model. The ocean models MPIOM
and NEMO-MED12 are still far away from the PE limit
970 If cost are not a limiting factor, the procedure
should be repeated until the model with the highest time to solution reaches the proposed parallel-efficiency
limit of 50 %.

4.4 The optimum configurations

Based on the results of the scalability study, we recommend an optimum configuration for stand-alone COSMO-CLM. We applied the strategy for finding an optimum configuration described in section 4.3 to the CCLM couplings with a regional ocean (TRIMNP+CICE or NEMO-MED12), an alternative land surface scheme (CLM or VEG3D) or the atmosphere of a global earth system model (MPI-ESM). The optimum configurations found for $CCLM_{sa}$ and all coupled systems which are summarized are shown in Fig. 6 and in more detail in Table 8. Considering time to solution and costs, we find that the optimum processes configuration for stand-alone COSMO-CLM is 64 cores using SMT mode resulting in 3.6 HPSY and costs of 230.4 CHPSY. This configuration will be used as common reference for all couplings to quantify the additional time and costs of adding one or more components to COSMO-CLM. The parallel efficiency used as criterion of finding the optimum configuration is shown in Fig. 5.

The optimum configurations of the couplings with CLM and The minimum number of cores, which should be used is 32 (one node). For sequential coupling an alternating distribution of processes is used and thus one CCLM and one coupled component model (VEG3D) are identical: the coupled system is using SMT mode and 128 cores for each component model. In both couplings, the time to solution of the coupled land surface component is small in comparison to COSMO-CLM. CLM needs only 22% of CLM process are started on each core. For CCLM+VEG3D's time to solution. The different COSMO-CLM version used in the coupling CCLM and CCLM+CLM has a longer time to solution and costs and a higher parallel efficiency. That's why the gain in speed still dominates the increase in costs. CLM the CCLM is more expensive and thus the scalability limit of CCLM determines the optimum configuration. In this case the fair reference for CCLM is CCLM stand-alone ($CCLM_{sa}$) on 32 cores in single threading (ST) mode. As shown in Fig. 5 the parallel efficiency of 50% for COSMO stand-alone in ST mode is reached at 128 cores compared to the measurements at 32 cores. In the CCLM+VEG3D coupling the weak scaling behavior of VEG3D can be neglected because COSMO-CLM dominates the coupled system's costs. At or 4 nodes and thus the 128 cores, COSMO-CLM used in the coupling CCLM core configuration is selected as optimum.

For concurrent coupling the SMT mode with non-alternating distribution of processes is used, which is more efficient than the alternating SMT and the ST modes. The cores are shared between CCLM and the coupled component models (NEMO-MED12 and TRIMNP+VEG3D) reaches a point at which the increase in costs slightly dominates the gain in speed. From this perspective, running on 96 cores would be preferable. We nonetheless chose 128 cores for a better comparison to CCLM+CLM. Both coupled system's time to solution is only marginally bigger than that of stand-alone COSMO-CLM: 4.0 CICE). For these couplings CCLM is the most expensive component as well and thus the reference for CCLM is $CCLM_{sa}$ on 16 cores (0.5 node) in SMT mode. As shown in Fig. 5 the parallel efficiency of 50 HPSY for CCLM % for COSMO stand-alone in SMT mode using

16 cores as reference is reached at approximately 100 cores. For CCLM+CLM and 3.7 HPSY for CCLM+VEG3D. The corresponding costs are about double the costs of the stand-alone reference: 512.0 and 473.6 CHPSY, respectively. The costs of the OASIS3-MCT interpolations are 3.0% of the total coupled system's CHPSY in the CCLM+CLM coupling which is still acceptable. There are no interpolations performed for CCLM+VEG3D.

NEMO-MED12 scales very well in the analyzed resources range making COSMO-CLM the limiting component of the CCLM+ coupling a two nodes configuration with 78 cores for CCLM and 50 cores for NEMO-MED12 coupled system. Because the load imbalance was unacceptably high at a resources distribution of 64 by 64 cores, it was decided to run NEMO-MED12 with 14 cores less and giving these to COSMO-CLM was resulting in an overall decrease in load imbalance to an acceptable 3.931% of the total costs. Surprisingly, increasing cost. Increasing the number of cores beyond 80 for COSMO-CLM did not change much the time to solution, because COSMO-CLM already approaches the parallel-efficiency limit by using 78 cores. This prevented finding the optimum configuration using three nodes. The corresponding NEMO-MED12 measurements at 50 cores are a bit out of scaling as well. This is probably caused by the I/O which increased for unknown reasons on the machine used between the time of conduction of the first series of simulations and of the optimized simulations. A further increase in resources is not recommended because COSMO-CLM already approached the parallel-efficiency limit by using 78 cores. The coupled systems's optimum For CCLM+TRIMNP+CICE no scalability is found for CICE. As shown in Fig. 5 a parallel efficiency smaller than 50% is found for CICE at approximately 15 cores. As shown in Fig. 3 the time to solution and costs are 4.0 for all core numbers investigated is higher for CICE than for CCLM in SMT mode. Thus, a load imbalance smaller than 5 HPSY and 512.0 CHPSY, respectively. The costs for OASIS3-MCT interpolations are negligible with 0.03% of the total costs can hardly be found using one node. The optimum configuration found is thus a one-node configuration using the CCLM reference configuration (16 cores).

Due to CICE's low speed-up and The CCLM+MPI-ESM coupling is a combination of sequential coupling between CCLM and ECHAM and concurrent coupling between ECHAM and the ocean model MPIOM. As shown in Fig. 4 MPIOM is much cheaper than ECHAM and thus, the coupling is dominated by the sequential coupling between CCLM and ECHAM. As shown in Fig. 3 ECHAM is the most expensive component and it exhibits no decrease of time to solution by increasing the number of cores from 28 to 56, i.e. it exhibits a very low scalability. Thus, as described in the strategy for finding the fact that the time to solution of CICE is generally one order of magnitude higher than that of TRIMNP and COSMO-CLM, there is no common speed of all three components. Clearly, CICE is the limiting component in this coupled system so that more than 32 cores altogether can not be used efficiently. Considering CICE's parallel efficiency, more than 10 cores are not feasible dividing up the rest into 16 for COSMO-CLM and 6 for TRIMNP in the optimum configuration. The total, even if a parallel efficiency higher than 50% for up to 64 cores (see Fig. 5) is found,

the optimum configuration is the 32 core (one node) configuration, since no significant reduction of the time to solution is 18.0 HPSY and the total costs amount to 576.0 CHPSY of which 20.9% are wasted in load imbalance can be achieved by further increasing the number of cores.

In the CCLM+MPI-ESM coupling, ECHAM is the limiting component model making it not feasible for the coupled system to run on more than 32 cores. This configuration leads to a total time of solution of 34.8 An analysis of additional cost of coupling requires a definition of a reference. We use the cost of CCLM stand-alone at optimum configuration ($CCLM_{sa,OC}$). We found the SMT mode with non-alternating distribution of processes and 64 cores to be the optimum configuration for CCLM resulting in a time to solution of 3.6 HPSY and total costs of 1113.6 cost of 230.4 CHPSY of which 3.6% are due to the load imbalance between MPIOM and ECHAM. The costs of OASIS3-MCT horizontal interpolations are considerably small with 0.7% of the total costs. As shown in section 4.2, SMT mode with non-alternating processes distribution is the most efficient and the scalability limit is reached at approximately 80 cores in SMT mode due to limited number of grid points used. The double of 64 cores is beyond the scalability limit of this particular model grid.

4.5 Extra time and costs

Figure 6 exhibits significant differences between shows the times to solution (vertical axis) and costs (box area) of the model components component models of the coupled systems at optimum configurations of the together with the load imbalance. It exhibits significant differences between the coupled model systems, $CCLM_{OC}$ and $CCLM_{sa,OC}$. The direct coupling cost of the OASIS3-MCT coupler are not shown. This is due to the fact that they are negligible in comparison with the cost of the model components. This is not necessarily the case, in particular when a huge amount of fields is exchanged. The relevant steps to reduce these direct coupling cost are described in section 4.6.

Table 8 gives a summary of an analysis of each optimum configuration (line 3.1 and 3.2) using the opportunities provided by LUCIA and by additional internal measurements of timing. It focuses on the cost analysis of the COSMO-CLM stand-alone time to solution and costs. These results are given quantitatively in the columns of Table 8. Its first section summarizes the configuration of each coupling. The second section gives the absolute and relative time to solution of the coupled systems together with the relative difference between the cost of time to solution CS for the coupled system and COSMO-CLM stand-alone (and $CCLM_{sa}$), given as $CS - CCLM_{sa}$. In the following section the absolute and relative costs are given followed by relative extra costs of OASIS3-MCT horizontal interpolation and of the load imbalance. Finally, the relative differences of (line 3.3) and provides its separation into 5 components:

1. *costs coupled component(s)*: are given between the coupled system and COSMO-CLM stand-alone ($CS - CCLM_{sa}$), between the coupled and stand-alone COSMO-CLM ($CCLM - CCLM_{sa}$) and

~~between the coupled and stand-alone COSMO-CLM using the same resources as COSMO-CLM in the coupled mode ($CCLM - CCLM_{sa,sc}$). The relative extra time and costs are given in % of the reference $CCLM_{sa}$ time to solution and costs, respectively. cost of additional component(s), coupled to CCLM~~

1085

2. ~~*OASIS hor. interp.*: cost of OASIS horizontal interpolations between the grids and communication between the component models~~

3. ~~*load imbalance*: cost of waiting time of the component model with the shorter time to solution in case of concurrent coupling~~

1090

4. ~~$CCLM_{sa,sc} - CCLM_{sa}$: cost difference due to usage of another CCLM process mapping (alternating/non alternating SMT or ST mode and a different number of cores).~~

5. ~~$CCLM - CCLM_{sa,sc}$: extra cost of CCLM in coupled mode. It contains additional computations in the coupling interface, differences due to different model versions (as in CCLM+CLM), differences in performance of CCLM by using the core and memory by several component models and uncertainties of measurement due to variability in performance of the computing system.~~

1095

The ~~CCLM~~ optimum configurations of sequential couplings CCLM+CLM and CCLM+VEG3D coupling can be identified as the ~~coupling configurations~~ with the smallest extra time (11.1 % and 2.8 %) and extra ~~costs~~ (cost (122.2 % and 105.6 %)). ~~The coupling CCLM~~ respectively (see line 3.3 in Table 8). They use 128 cores for each component model in SMT mode with alternating processes distribution (line 1.5 in Table 8). A substantial part (56.2 %) of the extra cost in CCLM+CLM ~~is just slightly more expensive with 11.1~~ and CCLM+VEG3D can be explained by a different mapping of CCLM (line 3.3.4 in Table 8). The 128 CCLM processes of our reference optimum configuration are mapped on 64 cores ($CCLM_{sa,OC}$ mapping). The 128 COSMO-CLM processes in optimum configuration of the coupled mode are mapped on 128 cores ($CCLM_{OC}$ mapping) but, in each core, memory, bandwidth and disk access are shared with a land-surface model process. These higher cost can be regarded as the price for keeping the time to solution only marginally bigger than that of $CCLM_{sa,OC}$ (see line 2.1 in table 8) and avoiding of 50 % ~~additional time and 122.2~~ idle time in sequential mode. The replacement of the inexpensive CCLM model component TERRA (1 % of $CCLM_{sa}$ cost) by an external land surface component model is the second important part of extra cost with 4.3 % for CLM and 19.3 % ~~additional costs~~. However, the couplings with soil-vegetation models do not need to have extra costs. In this case the coupled model is replacing TERRA, which is the internal soil-vegetation model of COSMO-CLM. All other couplings need to simulate additionally the regional ocean or global earth system dynamics for VEG3D (line 3.3.1 in Table 8). The 5 times higher cost of VEG3D in comparison with CCLM is due to low scalability of VEG3D (see Fig. 3). The OASIS horizontal interpolations (line 3.3.2 in Table 8) produce 6.3 %

1100

1105

1110

1115

extra cost in CCLM+CLM. No extra cost occurs due to horizontal interpolation in CCLM+VEG3D coupling, since the same grid is used in CCLM and VEG3D, and due to load imbalance, which is obsolete in sequential coupling. The remaining extra cost are assumed to be the cost difference between the coupled CCLM and $CCLM_{sa,OC}$. They are found to be 55.4 % and 29.7 % for CLM and VEG3D coupling respectively. A substantial part of the relatively high extra cost of CCLM in coupled mode of CCLM+CLM might be explained by higher cost of `cosmo_5.0_clm1`, used in CCLM+CLM, in comparison with `cosmo_4.8_clm19`, used in all other couplings (see line 1.7 in Table 8). $CCLM_{sa}$ performance measurements with both versions (but on a different machine than *Blizzard*) reveal a `cosmo_5.0_clm1` time to solution 45 % smaller than for `cosmo_4.8_clm19`.

The coupling with the concurrent coupling of CCLM with NEMO for Mediterranean Sea (CCLM+NEMO-MED12) is as expensive as CCLM+CLM. The coupling with and exhibits at the systems' optimum configuration 4.0 HPSY time to solution and 512.0 CHPSY cost (line 3.1 and 3.2 in Table 8). The extra cost of 122 % are dominated by the cost of the coupled component, which are 79.9 % of the $CCLM_{sa,OC}$ cost. The second important cost of 16.3 % can be explained by the higher number of cores used by $CCLM_{OC}$ than $CCLM_{sa,OC}$ at optimum configurations (line 1.5 and 3.3.4 in Table 8). The load imbalance of 6.9 % of $CCLM_{sa,OC}$ is below the intended limit of 5 % of the cost of the coupled system. The extra cost of $CCLM_{OC}$ of 19 % are smaller than for the land surface scheme couplings.

The optimum configuration of the coupling with TRIMNP+CICE for the North and Baltic Sea (CCLM+TRIMNP+CICE) takes has a time to solution of 18 HPSY and cost of 576 CHPSY. This is 3.5 times longer due to a than $CCLM_{sa,OC}$ due to lack of scalability of the sea ice model CICE and costs 1.5 times more than the optimum stand-alone COSMO-CLM. The most expensive coupling presented here is the coupling with the global atmosphere (CCLM+MPI-ESM). It takes 7.5 times longer due to lack of scalability of the additional computations in MPI-ESM and costs almost four times more. Section ??, in which the CCLM+MPI-ESM extra time expensive than $CCLM_{sa,OC}$ (line 2.3 and costs are discussed, provides a comparison with MPI-ESM stand-alone as well.

The comparison of costs of the coupled and stand-alone COSMO-CLM (Table 8 line 14) shows a major dependency on the number of allocated cores. Despite the longer runtime, COSMO-CLM coupled to TRIMNP+CICE is by 273.3 of Table 8). The dominating component of the extra cost are the cost of the coupled models. The ocean model TRIMNP cost 27.2 % and the ice model CICE 77.9 % of $CCLM_{sa,OC}$ cost. The second important component of extra cost is the load imbalance. Due to CICE's low speed-up and the fact that the time to solution of CICE is generally significantly higher than that of TRIMNP and CCLM, there is no common speed of all three components. The load imbalance at optimum configuration is 71.5 % of $CCLM_{sa,OC}$ cost. However, a further decrease of CCLM and TRIMNP cores reduces the load imbalance but not the cost of coupling, since the time to solution of CICE is decreasing very slowly with the number of processors. The CCLM mapping used in the coupled system is 30 % cheaper than the optimum stand-alone COSMO-CLM only because

of 16 cores used instead of 64. The additional costs of COSMO-CLM using 78 cores and coupled to NEMO-MED12 are 35.4% of $CCLM_{sa,OC}$. This is reducing the extra cost without increasing the time to solution. The OASIS3-MCT interpolation cost of 0.8% of COSMO-CLM using 128 cores and coupled to VEG3D and CLM are 87.2% of $CCLM_{sa,OC}$ cost are negligible. The extra cost of CCLM in coupled mode are found to be 2.6% and 119.2%, respectively. An exception are the additional costs of 83.1% for COSMO-CLM using 32 cores and coupled to MPI-ESM% of $CCLM_{sa,OC}$ cost only.

To quantify the additional costs by the COSMO-CLM coupling interface, all coupled COSMO-CLM components are compared to the stand-alone COSMO-CLM reference using the same configuration (thread mode and number of cores; see Table 8, line 15). The COSMO-CLM interface with the smallest additional costs of 4.9% is the concurrent coupling (see definition in Balaji et al. (2017)) and most expensive coupling presented here is the sequential coupling of CCLM atmosphere with the atmosphere of the global earth system model MPI-ESM. The latter is a concurrent coupling via OASIS3-MCT between the global atmosphere model ECHAM and the global ocean model MPIOM. At optimum configuration the time to solution of CCLM+ECHAM+MPIOM is 34.8 HPSY and the cost are 1113.6 CHPSY (line 2.1 and 3.3.1 in Table 8). It takes 7.67 times longer than $CCLM_{sa,OC}$ due to lack of scalability of ECHAM in coupled mode. A model-internal timing measurement revealed no scalability and high cost of a necessary additional computation of horizontal derivatives executed in ECHAM coupling interface using a spline method. Connected herewith, the cost of ECHAM, which are 261% of $CCLM_{sa,OC}$ is the one of COSMO-CLM coupled to NEMO-MED12, followed by 17.2% of $CCLM_{sa,OC}$ when coupled to TRIMNP+CICE, 20.4% of $CCLM_{sa,OC}$ cost. The second coupled component model MPIOM cost 20.1% when coupled to VEG3D. The additional costs of COSMO-CLM coupled to CLM are 40.9%. The load imbalance using 4 cores for MPIOM and 28 for ECHAM is 17.2%. However, they are not the true additional costs due to different COSMO-CLM versions used in stand-alone and in the coupled-system simulations. The coupling interface of COSMO-CLM a further reduction of the number of MPIOM cores (and increase of the number of ECHAM cores) can reduce the load imbalance but not the time to solution and cost of MPI-ESM. The cost of CCLM stand-alone using the same mapping ($CCLM_{sa,sc}$) as for CCLM coupled to MPI-ESM exhibits the biggest additional costs with 76.4% of $CCLM_{sa,OC}$ (see section ?? for details).

Figure 6 shows no direct coupling costs of the OASIS3-MCT coupler. This is due to the fact that they are negligible in comparison with the costs of the model components. This is not necessarily the case, in particular when a huge amount of fields is exchanged. The relevant steps to reduce the direct coupling costs are described in section ?? higher than the cost of $CCLM_{sa,OC}$ (line 3.3.4 in Table 8). Interestingly, the cost of OASIS horizontal interpolations is 3.3% only. This achievement is discussed in more detail in the next section. Finally, the extra cost of CCLM in coupled mode of CCLM+ECHAM+MPIOM are 77.4%. They are the highest of all couplings.

Additional internal measurements allowed to identify additional computations in CCLM coupling interface to be responsible for a substantial part of these cost. The vertical spline interpolation of the 3D fields exchanged between the models was found to consume 51.8 % of $CCLM_{sa,OC}$ cost, which are 2/3 of the extra cost of $CCLM_{OC}$.

1195 ~~The extra costs~~ Interestingly, a direct comparison of complexity and grid point number G (see definition in Balaji et al. (2017)) given in Table 3 with extra cost of coupling given in Table 8 for CCLM as $CCLM - CCLM_{sa,sc}$ are resulting from additional computations necessary for coupling. They are described in section ?? exhibits, that the couplings with short time to solution and lowest extra cost are those of low complexity. On the other hand, the most expensive coupling with longest
1200 time to solution is that of highest complexity and with largest number of gridpoints.

4.5.1 Direct coupling costs

4.6 Coupling cost reduction

The CCLM+MPI-ESM coupling is one of the most intensive couplings that has up to now been realized with OASIS3(-MCT) in terms of number of coupling fields and coupling time steps: 450
1205 2D fields are exchanged every ECHAM coupling time step, that is, every ten simulated minutes (see section 3.2). Most of these 2D fields are levels of 3D atmospheric fields. We show in this section that a conscious choice of coupling software and computing platform features can have a significant impact on simulation speed and costs time to solution and cost.

To make the CCLM+MPI-ESM coupling more efficient, all levels of a 3D variable are sent and
1210 received in one a single MPI message using the concept of pseudo-3D coupling, as described in section 3.1.2, thus reducing the number of sent and received fields (see Table 4). The change from 2D to pseudo-3D coupling lead to a decrease of the cost of the coupled system running on 32 cores by 3.7 % of the coupled system, which corresponds to 35,725 % of $CCLM_{sa}$. Since this measured computing time does not include OASIS3-MCT interpolations, the decrease can be attributed to a
1215 reduction in MPI communications. The costs $CCLM_{sa,OC}$ cost. At the same time the cost of the OASIS3-MCT interpolations are reduced to 24.0 by 76 %, which corresponds to an overall additional reduction of 1.4 cost by 12 % of the costs of the coupled system or 13.5 $CCLM_{sa,OC}$ cost. The total reduction of cost by exchanging one 3D field are 34 % of $CCLM_{sa} CCLM_{sa,OC}$ cost.

The second optimization step is a change of hardware usage mapping of running processes on
1220 cores. Instead of non-alternating, an alternating processes distribution of cores is used. On one node, this reduced the coupled system's distribution of processes of sequentially running component models is used such that on each core one process of each component model is started. This reduced the time to solution and cost of the coupled system running on 32 cores and using pseudo-3D coupling by 35.8 %, which is 226 % of $CCLM_{sa,OC}$. The expected reduction of time to solution
1225 and costs by 35.5 is 25.5 %. It is a combined effect of increasing the time to solution by changing

the mapping from 16 cores in SMT mode to 32 cores in ST mode (here $CCLM_{sa}$ measurements are used) and of reducing it by making 50% ~~An even higher decrease of the idle time of the cores in sequential coupling available for computations.~~ A separate investigation of CCLM, ECHAM and MPIOM time to solution and cost revealed strong deviations from the expectation for the individual components. A higher relative decrease of 46.4% was found for MPI-ESM-ECHAM due to a dramatic reduction of the time to solution of the inefficient calculation of the derivatives (needed for coupling with COSMO-CLM only) by one process. The COSMO-CLM's time to solution in coupled mode was reduced by 9.2% ~~This gain is smaller than what could have been expected from the stand-alone COSMO-CLM measurements. Going from 16 cores in SMT mode to 32 cores in ST mode is resulting in a reduction of time to solution by 25.5 only. Additional internal measurements of CCLM revealed, that the discrepancy of 16.3%. The discrepancy of 16.3% = (25.5 - 9.2)% originates from the % originates from~~ reduced scalability of some subroutines of COSMO-CLM in coupled mode, which is probably related to sharing of ~~storage space memory~~ between COSMO-CLM and ECHAM if running on the same core in coupled mode. In particular the COSMO-CLM interface and the physics computations show almost no speed-up.

~~As demonstrated, the implementation of the The combined effect of usage of 3D-field exchange and of an alternating processes distribution lead to an overall reduction of the total time to solution and costs cost of the coupled system CCLM+MPI-ESM by approximately 4039%. This corresponds to approximately 387, which corresponds to 261 % of the $CCLM_{sa}$ costs.~~

1245 4.6.1 Additional costs and time to solution

~~Several of the couplings investigated exhibit unnecessarily high costs of individual components and/or a lack of scalability. This can originate from additional computations, from a different behaviour of the model components if coupled and/or from specific properties of the machine used.~~

~~The scalability results of all coupled components exhibit a weak scaling of parts of VEG3D, TRIMNP, CICE and ECHAM. In the CCLM+VEG3D coupling, this circumstance is negligible because the main costs lie with COSMO-CLM. However, all other component models make an efficient coupling at higher speed rather difficult (see Fig. 6).~~

~~An analysis of the origin of increased time to solution and/or costs of the component models in coupled mode requires the availability of a model-internal analysis of timing. This information is available for the CCLM+MPI-ESM coupling.~~

~~Figures ?? and ?? show the time to solution and costs of the model system components, of the CCLM+MPI-ESM coupled system and of the "improved" coupled system and its components. The latter are calculated by neglecting two of the additional computations, which, first, have been found to be responsible for the major part of the additional time to solution and, second, can be replaced by significantly more efficient alternative methods.~~

The first computation neglected is the calculation of horizontal derivatives executed in the ECHAM component interface (see 3.2). It increases the costs from 170 HPSY (ECHAM (improved)) to 620 HPSY (ECHAM; see Fig. ??) if 32 cores are used for CCLM+MPI-ESM. This has two reasons: First, a costly third-order spline method is used. This can be replaced by a fourth-order explicit interpolation. Second, the calculation can be executed only on one core due to a lack of a halo in ECHAM needed for the exchange of neighboring grid point values among cores with a common boundary. This leads to a substantial load imbalance (not seen by LUCIA) and a fast loss of parallel efficiency with increasing number of cores. To overcome this problem, there are two possibilities: Either halos are introduced in ECHAM, which is planned for the upcoming ECHAM model version or the derivatives are calculated in COSMO-CLM and sent to ECHAM additionally to the absolute fields. The second option is the preferred one. ECHAM (improved) is the fastest and second-cheapest (after MPIOM) of the coupled models.

The second additional computation neglected is the vertical interpolation of the exchanged model variables in COSMO-CLM. It increases the costs from 310 HPSY (CCLM (improved)) to 430 HPSY (CCLM; see Fig. ??). The interpolation method used is a spline interpolation, which is a rather costly interpolation and which can be replaced by a second-to-fourth order explicit interpolation.

A neglect of the two inefficient additional computations decreases the costs from 1050 (CCLM+MPI-ESM) to 480 (CCLM+MPI-ESM (improved)) CHPSY if 32 cores are used and from 3100 to 850 CHPSY if 128 cores are used. It reduces the time to solution from 34.8 HPSY to 17 HPSY if 32 cores are used and from 26 to 6.8 HPSY if 128 cores are used (see Fig. ??). Using 32 cores the costs of CCLM+MPI-ESM (improved) are 108 % higher and the time to solution is 372 % longer. Using 128 cores, the costs are 234 % higher and the time to solution is 88 % longer than for $CCLM_{sa,sc}$. Thus, CCLM+MPI-ESM (improved) can have a time to solution, which is comparable to $CCLM_{sa}$ and other couplings at 30 % higher costs. However, this improvement of the computational performance remains for future work.

% of the $CCLM_{sa,OC}$ cost.

5 Conclusions

We present the couplings between the regional land-atmosphere climate model COSMO-CLM and two land surface schemes (VEG3D, CLM), two ocean models (NEMO, TRIMNP+CICE) for the Mediterranean Sea and for the North and Baltic Sea and the global atmosphere of MPI-ESM earth system model using the fully parallelized coupler OASIS3-MCT. A unified OASIS3-MCT interface (UOI) was developed and successfully applied for all couplings. All couplings are organized in a least intrusive way such that the modifications of all model components are mainly limited to the call of two subroutines receiving and sending the exchanged fields (as shown in Fig. 7 to 13). The

1295 next step is ~~the~~ development of the UOI for multiple couplings which allows regional climate system modelling over Europe.

A series of simulations has been conducted ~~aiming with an aim~~ to analyse the computational performance of the couplings. The CORDEX-EU grid configuration of COSMO-CLM on a common computing system (*Blizzard* at DKRZ) has been used in order to keep the results for time to solution, 1300 ~~eosts-cost~~ and parallel efficiency comparable.

~~The results confirm the finding that the parallel efficiency is decreasing substantially if the number of grid points per core is well below 100. For the configuration used (120x110 grid points) this limits the number of nodes, which can be used efficiently, to approximately four (128 cores or 256 threads).~~

1305 ~~The~~ LUCIA tool of OASIS3-MCT has been used to measure the computing time used by each model component and the coupler for communication and horizontal interpolation in dependence on the computing resources used. This allows ~~to estimate an estimation of~~ the computing time for intermediate computing resources and thus ~~to determine determination of~~ an optimum configuration based on a limited number of measurements. Furthermore, the scaling of each ~~model component~~ 1310 ~~component model~~ of the coupled system can be analysed and compared with that of the model in stand-alone mode. Thus, the ~~additional costs of the coupling extra cost of coupling is measured~~ and the origins of the relevant ~~additional costs are measured extra cost can be analysed~~.

The scaling of COSMO-CLM was found to be very similar in stand-alone and in coupled mode. The weaker scaling, which ~~oeeured-occurred~~ in some configurations, was found to originate from 1315 additional computations ~~which do not scale but are~~ necessary for coupling ~~which are not scaling~~. In some cases the model physics or the I/O routines exhibited a weaker scaling; ~~most probably due to~~ limited memory.

~~For the~~ ~~The results confirm that parallel efficiency is decreasing substantially if the number of grid points per core is below 80. For the configuration used (132x129 grid points), this limits the number of cores, which can be used efficiently to 80 in SMT mode and 160 in ST mode.~~

1320 ~~For the~~ first time a sequential coupling of approximately 450 2D fields using the parallelized coupler OASIS3-MCT was investigated. It was shown that the direct ~~eosts-cost~~ of coupling by OASIS3-MCT (interpolation and communication) are negligible in comparison with the ~~eosts-cost~~ of the coupled atmosphere-atmosphere model system. We showed that the exchange of one (pseudo-)3D 1325 field instead of many 2D fields reduces the ~~eosts-cost~~ of communication drastically. Furthermore, the idling of cores due to sequential coupling could be avoided by a dedicated launching of one process of each of the two sequentially running models on each core making use of the multi-threading mode available on ~~Blizzard~~ ~~the machine Blizzard used and on several other machines~~.

~~Inconsistencies of the time to solution of approximately 10% were found between measurements obtained from simulations conducted at different physical times. This gives a measure of the dependency of the time to solution on the status of the machine used, originating in particular from the I/O.~~

A strategy for finding ~~of~~ an optimum configuration was developed. Optimum configurations were identified for all investigated couplings considering all three aspects of climate modeling performance: time to solution, ~~costs~~ cost and parallel efficiency. The optimum configuration of ~~coupled systems, that involve a coupled system, that involves~~ a component not scaling well with ~~the~~ available resources, is suggested to ~~have as small costs as acceptable from the point of view of the~~ be used at minimum cost, if time to solution cannot be decreased significantly. This is the case for ~~the~~ CCLM+MPI-ESM and ~~the~~ CCLM+TRIMNP+CICE ~~coupling~~ couplings. An exception is the CCLM+VEG3D coupling. VEG3D was found to have a weak scaling but a small ~~work-load~~ work-load in comparison to COSMO-CLM. Thus, it has ~~nearly no minimal~~ impact on the performance of the coupled system.

The analysis of ~~the optimum configurations led to the identification of a weak scalability of the MPI-ESM, CICE and VEG3D model components and high costs of additional computations in COSMO-CLM when coupled with MPI-ESM or CLM (see line 15, extra cost of coupling at~~ optimum configuration using LUCIA and CCLM stand-alone performance measurements allowed to distinguish five components (line 3.3.1-3.3.5 in table 8). ~~A detailed analysis of the origin of weak scalability and:~~ cost of coupled components, OASIS horizontal interpolation and communication (direct coupling cost), load imbalance (if concurrently coupled), additional/or increased costs was based on the time measurements of the subroutines of the model components which was only available for CCLM+MPI-ESM. The quantification of the additional costs at different configurations allowed to analyse the potential for improved performance and to develop a strategy by replacing the spline derivatives calculations and interpolation by explicit methods and by a parallel calculation of the derivatives. A direct comparison of the land model couplings exhibits a doubling of costs minor cost of different mapping of CCLM and extra cost of CCLM in coupled mode. The letter contain in particular the cost of additional computations of coupling and extraordinary model behavior in coupled mode. This allowed to identify the bottlenecks of each coupling and to gain understanding, which are avoidable and/or dependent.

The optimum configuration of land surface scheme couplings exhibit same speed and doubling of cost in comparison with COSMO-CLM stand-alone and higher costs for CCLM. It was found to be close to its absolute optimum, since 60 % to 75 % of the extra cost of coupling are unavoidable. These are the extra cost of (1) keeping the speed of the coupled system high, resulting in an unavoidable increase of cost with core number, (2) the need of using the less efficient single threading mode to avoid 50 % of idle time of cores in sequential coupling and (3) the cost of the coupled component. The main part of high extra cost of CCLM in coupled mode (+CLM than for CCLM 55.4 %) could be attributed to higher cost of the model version used in CCLM+VEG3D due to higher costs of additional computations in COSMO-CLM. The direct comparison of the ocean couplings shows a doubling of the costs for NEMO and a factor of 2.5 for the CLM coupling.

The optimum configuration of the regional ocean coupling for the Mediterranean CCLM+NEMO-MED12 exhibits same speed and doubling of cost as well. In this case the cost of the ocean model are much higher and the extra cost of mapping are much smaller, which is due to usage of concurrent coupling.

The optimum configuration of the regional ocean coupling for the North and Baltic Sea CCLM+TRIMNP+CICE coupling exhibits much higher time to solution (+ 350%) and cost (+150%) due to lack of scaling of the CICE component model. High extra cost of load imbalance (71 %) are related to the lack of scaling of CICE as well.

A direct comparison between NEMO and TRIMNP+CICE is not possible because the costs of NEMO-NORDIC have not been measured on the same machine and for the same configuration. The lower parallel efficiency and costs of TRIMNP in comparison with NEMO-MED12 might result from the smaller number of grid points in the can be more than explained by the difference in the number of gridpoints and time steps. The surface of North and Baltic Sea than in the Mediterranean Sea is approximately half of the Mediterranean surface. Furthermore, approximately a double horizontal resolution is used in the NEMO-MED12 coupling resulting in a factor of 16.

The application of the optimum configuration of the coupling between the regional and global atmosphere CCLM+MPI-ESM exhibits the longest extra time to solution (766 %) and highest extra cost (383 %). They were resulting from extraordinary high cost and no scalability of ECHAM (261 %) and high extra cost of CCLM in coupled mode (77 %). A more detailed analysis of the origins of these extra cost was possible due to availability of additional internal time measurements of the component models. This revealed that additional computations necessary for coupling are responsible for the extra costs. The lack of scaling of ECHAM was due to non-parallelised computation of derivatives in the ECHAM coupling interface. The high extra cost of CCLM in coupled mode are due to necessary additional vertical interpolation in the CCLM coupling interface.

The procedure of finding an optimum configuration presented here is was found applicable to each coupling layout investigated and thus it could be applicable to other coupled model systems as well.

The Analysis of extra cost of coupling was found to be a useful step of development of a Regional Climate System Model, which is coupling several model components. It provides useful information on the bottle-necks of each coupling and allows to estimate the Bottle-necks of coupling have been identified in the CCLM+TRIMNP+CCLM and the CCLM+MPI-ESM couplings. The results for time to solution, costs and parallel efficiency of different couplings can serve as a starting point for finding an optimum coupling layout and configuration for multiple couplings. It is applicable to each coupling layout and thus it could be very helpful for an efficient usage of other coupled model systems as well.

Appendix A: Source code availability

1405 COSMO-CLM is an atmosphere model coupled to the soil-vegetation model TERRA. Other regional processes in the climate system like ocean and ice sheet dynamics, plant responses, aerosol-cloud interaction, and the feedback to the GCM driving the RCM are made available by coupling COSMO-CLM via OASIS3-MCT with other models.

1410 The COSMO-CLM model source code is freely available for scientific usage by members of the CLM-Community (www.clm-community.eu). The CLM-Community is a network of scientists who accept the CLM-Community agreement. For details on how to become a member, please check the CLM webpage.

The current recommended version of COSMO-CLM is COSMO_131108_5.0_clm9⁵. It comes together with a recommendation for the configurations for the European domain.

1415 The development of fully coupled COSMO-CLM is an ongoing research project within the CLM-Community. The unified coupling interface via OASIS3-MCT is available by contacting one of the authors and will be part of a future official COSMO-CLM version. All other components, including OASIS interface, are available by contacting the authors. The OASIS3-MCT coupling library can be downloaded at <https://verc.enes.org/oasis/>.

1420 The two way coupled system CCLM+MPIESM was developed at BTU Cottbus and FU Berlin. Please contact Andreas Will (will@b-tu.de) for more information about the source codes.

The Community Land Model (CLM) is freely available as part of the Community Earth System Model(CESM) package and can be obtained through a SVN server after registration. Registration and access: <http://www.cesm.ucar.edu/models/cesm1.2>.

1425 For information about a possible usage of VEG3D, please contact Marcus Breil at KIT (marcus.breil@kit.edu).

The Nucleus for European Modelling of the Ocean (NEMO) is a community model. It can be adapted for regional and global applications. To access NEMO, please visit the webpage <http://www.nemo-ocean.eu/> and register there with signing the CeCILL licence agreement. Please contact Jennifer Brauch (jennifer.brauch@dwd.de) to get more information about the employed NEMO configurations.

1430 For information about the modified version of TRIMNP, please contact Ha Hagemann at HZG (ha.hagemann@hzg.de). The sea ice model CICE version 5.0 is developed at the Los Alamos National Laboratory, USA (<http://oceans11.lanl.gov/trac/CICE/wiki>). Please contact Ha Hagemann at HZG for more details to set up CICE for the North Sea and Baltic Sea.

⁵Status of October 2016

1435 **Appendix B: Model time step organisation**

In the following, the time step organisation within the coupled models is described. This aims at providing a basis of understanding of the coupling between the models.

B1 COSMO-CLM

Figure 7 gives an overview of the model initialization procedure, of the *Runge-Kutta* time step loop and of final calculations. The subroutines that contain all modifications of the model necessary for coupling are highlighted in red.

At the beginning ($t = t_m$) of the COSMO-CLM time step $(\Delta t)_c$ in `initialize_loop` the lateral, top and the ocean surface boundary conditions are updated. In `organize_data` the future boundary conditions at $t_f \geq t_m + \Delta t_c$ on the COSMO grid are read from a file (if necessary). As next `send_fld` and `receive_fld` routines are executed sending the COSMO-CLM fields to or receiving them from OASIS3-MCT in coupled simulations (if necessary). The details including the positioning of the `send_fld` routines will be explained in section 3.2 to 3.5.

At the end of the `initialize_loop` routine the model variables available at previous $t_p \leq t_m$ and next time $t_m < t_f$ of boundary update are interpolated linearly in time (if necessary) and used to initialize the boundlines of the COSMO-CLM model grid at the next model time level $t_m + (\Delta t)_c$ for the variables u and v wind, temperature and pressure deviation from a reference atmosphere profile, specific humidity, cloud liquid and ice water content, surface temperature over water surfaces and - in the boundlines only - surface specific humidity, snow surface temperature and surface snow amount.

In `organize_physics` all tendencies due to physical parameterizations between the current t_m and the next time level $t_m + (\Delta t)_c$ are computed in dependence on the model variables at time t_m . Thus, they are not part of the Runge-Kutta time stepping. In `organize_dynamics` the terms of the Euler equation are computed.

The solution at the next time level $t_m + (\Delta t)_c$ is relaxed to the solution prescribed at the boundaries using an exponential function for the lateral boundary relaxation and a cosine function for the top boundary Rayleigh damping (Doms and Baldauf, 2015). At the lower boundary a slip boundary condition is used together with a boundary layer parameterisation scheme (Doms et al., 2011).

B2 MPI-ESM

Figure 8 gives an overview of the ECHAM leapfrog time step (see DKRZ (1993) for details). Here the fields at time level t_{n+1} are computed by updating the time level t_{n-1} using tendencies computed at time level t_n .

After model initialization in `initialize` and `init_memory` and reading of initial conditions in `iorestart` or `iointial` the time step begins in `stepon` by reading the boundary conditions

for the coupled models in `bc_list_read` if necessary, in this case for the ocean model MPIOM.

1470 In `couple_get_o2a` the fields sent by MPIOM to ECHAM (SSTs, SICs) for time level t_n are received if necessary.

The time loop (`stepon`) has three main parts. It begins with the computations in spectral space, followed by grid space and spectral-space computations. In `scan1` the spatial derivatives (`sym2`, `ewd`, `fft1`) are computed for time level t_n in Fourier space followed by the transformation into
1475 grid-space variables on the lon/lat grid. Now, the computations needed for two-way coupling with COSMO-CLM (`twc`) are done for time level t_n variables followed by advection (`dyn`, `ldo_advectionadvection`) at t_n , the second part of the time filtering of the variables at time t_n (`tf2`), the calculation of the advection tendencies and update of fields for t_{n+1} (`ldo_advection`). Now, the first part of the time filtering of the time level t_{n+1} (`tf1`) is done followed by the computation of physical tendencies at t_n (`physc`). The remaining spectral-space computations in `scan1` begin with the reverse
1480 fourier transformation (`fftd`).

B3 NEMO-MED12

In Fig. 9 the flow diagram of NEMO 3.3 is shown. At the beginning the mpp communication is initialized by `cpl_prism_init`. This is followed by the general initialisation of the NEMO model.

1485 All OASIS3-MCT fields are defined inside the time loop, when `sbc` (surface boundary conditions) is called the first time. In `sbc_cpl_init` the variables which are sent and received are defined over ocean and sea ice if applicable. At the end of `sbc_cpl_init` the grid is initialized, on which the fields are exchanged. In `cpl_prism_rcv` NEMO receives from OASIS3-MCT the fields necessary as initial and upper boundary conditions. NEMO-MED12 and NEMO-Nordic follow the time
1490 lag procedure of OASIS3-MCT appropriate for concurrent coupling. NEMO receives the restart files provided by OASIS3-MCT containing the COSMO-CLM fields at restart time. At all following coupling times the fields received are not the COSMO-CLM fields at the coupling time but at a previous time, which is the coupling time minus a specified time lag. If a sea ice model is used, the fluxes from COSMO-CLM to NEMO have to be modified over surfaces containing sea ice. Hereafter, NEMO
1495 is integrated forward in time. At the end of the time loop in `sbc_cpl_snd` the surface boundary conditions are sent to COSMO-CLM. After the time loop integration the mpp communication is finished in `cpl_prism_finalize`.

B4 TRIMNP+CICE

Figures 10 and 11 show the flow diagrams of TRIMNP and CICE in which red parts are modifications of the models and blue parts are additional computations necessary for coupling. First,
1500 initialization is done by calling `init_mpp` and `cice_init` in TRIMNP and CICE, respectively. In `cice_init`, the model configuration and the initial values of variables are set up for CICE while for TRIMNP `setup_cluster` is used for the same purpose. In both models the receiving

(ocn_receive_fld, ice_receive_fld) and sending (ocn_send_fld, ice_send_~
1505 _fld) subroutines are used in the first time step ($t = 0$) prior to the time loop to provide the initial forcing. The time loop of TRIMNP covers a grid loop in which several grids on higher resolutions are potentially *one-way* nested for specific sub-regions with rather complex bathymetry, e. g. Kattegat of the North Sea. Note that for the coupling, only the first/main grid is applied. The grid loop begins with rcv_parent_data that sends data from the coarser grid to the nested grid. Then,
1510 do_update updates the forcing data passed from COSMO-CLM and CICE as well as the lateral boundary data are read from files. After updating, the physics and dynamics computations are mainly done in heat_flux, turbo_adv, turbo_gotm, do_constituent, do_explicit and do_implicit. At the end of the grid loop, the main grid sends data to the finer grid by calling snd_parent_data if necessary. At the end of each time step, output and restart data are written
1515 to files. Eventually, stop_mpp is called at the end of the main program to de-allocate the memory of all variables and finalize the program.

The time loop of CICE has two main parts. In the first part ice_step, physical, dynamical and thermo-dynamical processes of the time step $t = t_n$ are mainly computed in step_therm1, step_therm2, step_radiation, biogeochemistry and step_dynamics, followed by
1520 write_restart and final_restart for writing the output and restart files. Then, the time step is increased to a new time step $t = t_{n+1}$, followed by an update of forcing data from COSMO-CLM and TRIMNP via ice_receive_fld if necessary and a sending of fields to COSMO-CLM and TRIMNP via ice_send_fld. At the end of the time loop, all file units are released in release_all_fileunits and oas_ice_finalize concludes the main program.

1525 **B5 VEG3D**

Figure 12 shows the flow diagram of VEG3D for the coupled system. In a first step the subroutine oas_veg3d_init is called in order to initialize the MPI communication for the coupling. Afterwards, the model setup is specified by reading the VEG3D namelist and by loading external landuse and soil datasets. The definition of the grid and the coupling fields is done in oas_veg3d_define.
1530 The main program includes two time loops. In the first time loop vegetation parameters are calculated for every simulated day. In the second loop (over the model time steps) the coupling fields from COSMO-CLM are received via OASIS3-MCT in receive_fld_2cos at every coupling time step. Using these updated fields the energy balance of the canopy for the current time level t_n is solved iteratively and based on this the latent and sensible heat fluxes are calculated. The heat
1535 conduction and the Richardson equation for the time level t_{n+1} are solved by a semi-implicit Crank-Nicholson method. After these calculations the simulated coupling fields from VEG3D are sent to COSMO-CLM in send_fld_2cos. At the end, output and restart files are written for selected time steps. The oas_veg3d_finalize subroutine stops the coupling via OASIS3-MCT.

B6 CLM

1540 CLM is embedded within the CESM modelling system and its multiple components. In the case of
land-only simulations, the active components are the driver/internal coupler (CPL7), CLM and a data
atmosphere component. The later is substituted to the atmospheric component used in coupled mode
and provides the atmospheric forcing usually read from a file. In the framework of the OASIS3-MCT
coupling, however, the file reading is deactivated and replaced by the coupling fields received from
1545 OASIS3-MCT (`receive_field_2cos`). The send operation (`send_field_2cos`) is also po-
sitioned in the data atmosphere component in order to enforce the same sequence of calls as in
CESM. The definition of coupling fields and grids for the OASIS3-MCT coupling is also done in
the data atmosphere component during initialization before the time loop. Additionally, the initial-
ization (`oas_clm_init`) and finalization (`oas_clm_finalize`) of the MPI communicator for
1550 the OASIS3-MCT coupling is positioned in the CESM driver, respectively before and after the time
loop. The sequence of hydrological and biogeophysical calculations during the time loop are given
in black and the calls to optional modules are marked in grey.

Acknowledgements. The development of COSMO-CLM couplings would have not been possible without the
continuous work done by OASIS, COSMO and CLM-Community colleagues and provision of computing time
1555 and support by computing centers. In particular we would like to thank Ulrich Schaettler (DWD) and Hans-
Jürgen Panitz (KIT Karlsruhe) for source code maintenance of COSMO and COSMO-CLM. The OASIS sup-
port leading to our results received funding from the European Union Seventh Framework program under the
IS-ENES2 project (grant agreement no. 312979). The overall support and provision of computing time by
DKRZ Hamburg and the hosting of a developers workshop by CSCS Lugano are highly acknowledged.

1560 Finally, we would like to highlight the contributions to the work presented here by further colleagues. First
of all, Irina Fast provided the solution for dedicated distribution of model tasks on cores and the MPI-ESM
version using the OASIS3-MCT coupler. Andreas Dobler (FU Berlin) made the pioneering work in coupling
of COSMO-CLM using OASIS3. Sophie Valcke (CERFACS) provided the OASIS3-MCT support necessary to
solve the problems of coupling with a regional model. Last but not least, Matthieu Leclair (ETH Zürich) helped
1565 to improve the manuscript a lot.

References

- Akhtar, N., Brauch, J., Dobler, A., Béranger, K., and Ahrens, B.: Medicanes in an ocean–atmosphere coupled regional climate model, *Nat. Hazards Earth Syst. Sci.*, 14, 2189–2201, doi:10.5194/nhess-14-2189-2014, 2014.
- 1570 Alexeev, Y., Mickelson, S., Leyffer, S., Jacob, R., and Craig, A.: The Heuristic Static Load-Balancing Algorithm Applied to the Community Earth System Model, in: 28th IEEE International Parallel and Distributed Processing Symposium, no. 28 in Parallel & Distributed Processing Symposium Workshops, pp. 1581–1590, IEEE, doi:10.1109/IPDPSW.2014.177, 2014.
- Balaji, V., Maisonnave, E., Zadeh, N., Lawrence, B. N., Biercamp, J., Fladrich, U., Aloisio, G., Benson, R., Caubel, A., Durachta, J., Foujols, M.-A., Lister, G., Mocavero, S., Underwood, S., and Wright, G.: CPMIP: measurements of real computational performance of Earth system models in CMIP6, *Geoscientific Model Development*, 10, 19–34, doi:10.5194/gmd-10-19-2017, <http://www.geosci-model-dev.net/10/19/2017/>, 2017.
- 1575 Balaprakash, P., Alexeev, Y., Mickelson, S. A., Leyffer, S., Jacob, R., and Craig, A.: Machine-learning-based load balancing for Community Ice CodE component in CESM, in: International Conference on High Performance Computing for Computational Science, pp. 79–91, Springer, 2014.
- Baldauf, M., Seifert, A., Foerstner, J., Majewski, D., Raschendorfer, M., and Reinhardt, T.: Operational convective-scale numerical weather prediction with the COSMO model: description and sensitivities, *Mon. Weather Rev.*, 139, 3887–3905, 2011.
- 1585 Balmaseda, M. A., Mogensen, K., and Weaver, A. T.: Evaluation of the ECMWF ocean reanalysis system ORAS4, *Quart. J. Roy. Met. Soc.*, 139, 1132–1161, doi:10.1002/qj.2063, 2013.
- Becker, N., Ulbrich, U., and Klein, R.: Systematic large-scale secondary circulations in a regional climate model, *Geophys. Res. Lett.*, 42, 1944–8007, doi:10.1002/2015GL063955, <http://dx.doi.org/10.1002/2015GL063955>, 2015.
- 1590 Beuvier, J., Sevault, F., Herrmann, M., Kontoyiannis, H., Ludwig, W., Rixen, M., Stanev, E., Béranger, K., and Somot, S.: Modelling the Mediterranean sea interannual variability during 1961–2000: focus on the Eastern Mediterranean Transient (EMT), *J. Geophys. Res.*, 115, C08 517, doi:10.1029/2009JC005850, 2010.
- Beuvier, J., Lebeaupin-Brossier, C., Beranger, K., Arsouze, T., Bourdalle-Badie, R., Deltel, C., Drilllet, Y., Drobinski, P., Ferry, N., Lyard, F., Sevault, F., and Somot, S.: MED12, Oceanic Component for the Modeling of the Regional Mediterranean Earth System, *Mercator Ocean Quarterly Newsletter*, 46, 60–66, 2012.
- 1595 Bülow, K., Dietrich, C., Elizalde, A., Gröger, M., Heinrich, H., Hüttl-Kabos, S., Klein, B., Mayer, B., Meier, H. M., Mikolajewicz, U., Narayan, N., Pohlmann, T., Rosenhagen, G., Schimanke, S., Sein, D., and Su, J.: Comparison of three regional coupled ocean atmosphere models for the North Sea under today’s and future climate conditions, *KLIWAS Schriftenreihe KLIWAS-27/2014*, Koblenz, Bundesanstalt für Gewässerkunde, doi:10.5675/Kliwas_27/2014, 2014.
- 1600 Byrne, D., Papritz, L., Frenger, I., Munnich, M., and Gruber, N.: Atmospheric Response to Mesoscale Sea Surface Temperature Anomalies: Assessment of Mechanisms and Coupling Strength in a High-Resolution Coupled Model over the South Atlantic, *J. Atmos. Sci.*, 72, 1872–1890, doi:10.1175/JAS-D-14-0195.1, 2015.
- Casulli, V. and Cattani, E.: Stability, Accuracy and Efficiency of a Semi-Implicit Method for Three-Dimensional Shallow Water Flow, *Computers Math. Applic.*, 27, 99–112, 1994.

- Casulli, V. and Stelling, G. S.: Numerical Simulation of 3D Quasi-Hydrostatic, Free-Surface Flows, *J. Hydr. Engrg.*, 124, 678–686, 1998.
- Collins, W. D., Bitz, C. M., Blackmon, M. L., Bonan, G. B., Bretherton, C. S., Carton, J. A., Chang, P., Doney, S. C., Hack, J. J., Henderson, T. B., Kiehl, J. T., Large, W. G., McKenna, D. S., Santer, B. D., and Smith, R. D.: The Community Climate System Model version 3 (CCSM3), *J. Clim.*, 19, 2122–2143, 2006.
- 1610 Craig, A., Vertenstein, M., and Jacob, R.: A new flexible coupler for earth system modeling developed for CCSM4 and CESM1., *International Journal of High Performance Computing Applications*, 26, 31–42, doi:0.1177/1094342011428141, 2012.
- Davin, E. L. and Seneviratne, S. I.: Role of land surface processes and diffuse/direct radiation partitioning in simulating the European climate, *BIOGEOSCIENCES*, 9, 1695–1707, doi:10.5194/bg-9-1695-2012, 2012.
- 1615 Davin, E. L., Stoeckli, R., Jaeger, E. B., Levis, S., and Seneviratne, S. I.: COSMO-CLM2: a new version of the COSMO-CLM model coupled to the Community Land Model, *Clim. Dyn.*, 37, 1889–1907, doi:10.1007/s00382-011-1019-z, 2011.
- Dennis, J. M., Vertenstein, M., Worley, P. H., Mirin, A. A., Craig, A. P., Jacob, R., and Mickelson, S.: Computational performance of ultra-high-resolution capability in the Community Earth System Model, *Int. J. High Perf. Comp. Appl.*, 26, 5–16, doi:10.1177/1094342012436965, 2012.
- 1620 Dickinson, R., Oleson, K., Bonan, G., Hoffman, F., Thornton, P., Vertenstein, M., Yang, Z., and Zeng, X.: The Community Land Model and its climate statistics as a component of the Community Climate System Model, *J. Clim.*, 19, 2302–2324, 2006.
- 1625 Dieterich, C., Schimanke, S., Wang, S., Väli, G., Liu, Y., Hordoir, R., Axell, L., and Meier, H.: Evaluation of the SMHI coupled atmosphere-ice-ocean model RCA4-NEMO, Tech. Rep. 47, Sveriges Meteorologiska och Hydrologiska Institut (SMHI), Sweden, 2013.
- DKRZ: The ECHAM3 Atmospheric General Circulation Model, Report no. 6, 2nd revision, Deutsches Klimarechenzentrum, Hamburg, 1993.
- 1630 Doms, G. and Baldauf, M.: A Description of the nonhydrostatic regional model LM, Part I: Dynamics and Numerics - COSMO V5.1, Tech. rep., Deutscher Wetterdienst, P.O. Box 100465, 63004 Offenbach, Germany, 2015.
- Doms, G., Förstner, J., Heise, E., Herzog, H.-J., Mironov, D., Raschendorfer, M., Reinhardt, T., Ritter, B., Schrodin, R., Schulz, J.-P., and Vogel, G.: A Description of the nonhydrostatic regional model LM, Part II: Physical Parameterization - LM_F90 4.20, Tech. rep., Deutscher Wetterdienst, P.O. Box 100465, 63004 Offenbach, Germany, 2011.
- 1635 Döscher, R., Will'en, U., Jones, C., Rutgersson, A., Meier, H., et al.: The development of the regional coupled ocean-atmosphere model RCAO, *Boreal Environmental Research*, 7, 183–192, 2002.
- Egbert, G. D. and Erofeeva, S. Y.: Efficient Inverse Modeling of Barotropic Ocean Tides, *J. Atmos. Oceanic Technol.*, 19, 183–204, 2002.
- 1640 Gasper, F., Goergen, K., Shrestha, P., Sulis, M., Rihani, J., Geimer, M., and Kollet, S.: Implementation and scaling of the fully coupled Terrestrial Systems Modeling Platform (TerrSysMP v1.0) in a massively parallel supercomputing environment – a case study on JUQUEEN (IBM Blue Gene/Q), *Geosci. Model Dev.*, 7, 2531–2543, doi:10.5194/gmd-7-2531-2014, 2014.

- 1645 Geimer, M., Wolf, F., Wylie, B., Ábrahám, E., Becker, D., and Mohr, B.: The Scalasca performance toolset architecture. *Concur. Comp. Pract. Exper.*, 22, 702–719, 2010.
- Giorgetta, M. A., Jungclaus, J., Reick, C. H., Legutke, S., Bader, J., Boettinger, M., Brovkin, V., Crueger, T., Esch, M., Fieg, K., Glushak, K., Gayler, V., Haak, H., Hollweg, H.-D., Ilyina, T., Kinne, S., Kornblueh, L., Matei, D., Mauritsen, T., Mikolajewicz, U., Mueller, W., Notz, D., Pithan, F., Raddatz, T., Rast, S., Redler, R.,
- 1650 Roeckner, E., Schmidt, H., Schnur, R., Segschneider, J., Six, K. D., Stockhause, M., Timmreck, C., Wegner, J., Widmann, H., Wieners, K.-H., Claussen, M., Marotzke, J., and Stevens, B.: Climate and carbon cycle changes from 1850 to 2100 in MPI-ESM simulations for the Coupled Model Intercomparison Project phase 5, *J. Adv. Model. Earth Syst.*, 5, 572–597, doi:10.1002/jame.20038, 2013.
- Gualdi, S., Somot, S., Li, L., Artale, V., Adani, M., Bellucci, A., Braun, A., Calmanti, S., Carillo, A.,
- 1655 Dell’Aquila, A., Déqué, M., Dubois, C., Elizalde, A. Harzallah, A., Jacob, D., L’Hévéder, B., May, W., Ododo, P., Ruti, P., Sanna, A., Sannino, G., Scoccimarro, E. andSevault, F., and Navarra, A.: THE CIRCE simulations: Regional climate change projections with realistic representation of the mediterranean sea, *Bull. Amer. Meteorol. Soc.*, 94, 65–81, doi:10.1175/BAMS-D-11-00136.1, 2013.
- Hagos, S., Leung, R., and Rauscher, Sara A. Ringler, T.: Error Characteristics of Two Grid Refinement Approaches in Aquaplanet Simulations: MPAS-A and WRF, *Mon. Weather Rev.*, 141, 3022–30, doi:10.1175/MWR-D-12-00338.1, 2013.
- 1660 Hertwig, E., Storch, J. v., Handorf, D., Dethloff, K., Fast, I., and Krismer, T.: Effect of horizontal resolution on ECHAM6 AMIP performance, *Climate Dynamics*, 45, 185–211, doi:10.1007/s00382-014-2396-x, 2015.
- Ho-Hagemann, H. T. M., Rockel, B., Kapitza, H., Geyer, B., and Meyer, E.: COSTRICE - an atmosphere-ocean-sea ice model coupled system using OASIS3, HZG Report 2013-5, Tech. rep., Helmholtz-Zentrum Geesthacht, Geesthacht, Germany, 2013.
- 1665 Ho-Hagemann, H. T. M., Hagemann, S., and Rockel, B.: On the role of soil moisture in the generation of heavy rainfall during the Oder flood event in July 1997, *Tellus A*, 67, 1–17, doi:10.3402/tellusa.v67.28661, 2015.
- Hordoir, R., Dieterich, C., Basu, C., Dietze, H., and Meier, H. E. M.: Freshwater outflow of the Baltic Sea and transport in the Norwegian current: A statistical correlation analysis based on a numerical experiment, *Continental Shelf Research*, 64, 1–9, doi:10.1016/j.csr.2013.05.006, 2013.
- 1670 Hunke, E. C., Lipscomb, W. H., Turner, A. K., Jeffery, N., and Elliott, S.: CICE: The Los Alamos Sea Ice Model. Documentation and Software User’s Manual. Version 5.0, Tech. Rep. LA-CC-06-012, T-3 Fluid Dynamics Group, Los Alamos National Laboratory, 2013.
- 1675 Ilyina, T., Six, K. D., Segschneider, J., Maier-Reimer, E., Li, H., and Nunez-Riboni, I.: Global ocean biogeochemistry model HAMOCC: Model architecture and performance as component of the MPI-Earth System Model in different CMIP5 experimental realizations, *Journal of Advances in Modeling Earth Systems*, 5, 287–315, doi:doi:10.1029/2012MS000178, 2013.
- Inatsu, M. and Kimoto, M.: A scale interaction study on East Asian cyclogenesis using a general circulation model with an interactively nested regional model, *Mon. Weather Rev.*, 137, 2851–2868, doi:10.1175/2009MWR2825.1, 2009.
- 1680 Jacob, R., Larson, J., and Ong, E.: M × N communication and parallel interpolation in Community Climate System Model Version 3 using the model coupling toolkit, *International Journal of High Performance Computing Applications*, 19, 293–307, 2005.

- 1685 Jones, P.: A user's guide for SCRIP: A spherical coordinate remapping and interpolation package, Tech. rep.,
Los Alamos National Laboratory, 1997.
- Jungclaus, J. H., Fischer, N., Haak, H., Lohmann, K., Marotzke, J., Matei, D., Mikolajewicz, U., Notz, D., and
von Storch, J.-S.: Characteristics of the ocean simulations in MPIOM, the ocean component of the MPI Earth
System Model, *Journal of Advances in Modeling Earth Systems*, 5, 422–446, doi:doi:10.1002/jame.20023,
1690 2013.
- Kerkweg, A. and Joeckel, P.: The 1-way on-line coupled atmospheric chemistry model system MECO(n) -
Part 1: Description of the limited-area atmospheric chemistry model COSMO/MESSy, *GEOSCIENTIFIC
MODEL DEVELOPMENT*, 5, 87–110, doi:10.5194/gmd-5-87-2012, 2012.
- Köhler, M., Schädler, G., Gantner, L., Kalthoff, N., Königer, F., and Kottmeier, C.: Validation of two SVAT
1695 models for different periods during the West African monsoon, *Meteorol. Z.*, 21, 509–524, 2012.
- Kotlarski, S., Keuler, K., Christensen, O. B., Colette, A., Deque, M., Gobiet, A., Goergen, K., Jacob, D., Luethi,
D., van Meijgaard, E., Nikulin, G., Schaer, C., Teichmann, C., Vautard, R., Warrach-Sagi, K., and Wulfmeyer,
V.: Regional climate modeling on European scales: a joint standard evaluation of the EURO-CORDEX RCM
ensemble, *GEOSCIENTIFIC MODEL DEVELOPMENT*, 7, 1297–1333, doi:10.5194/gmd-7-1297-2014,
1700 2014.
- Kumar, S. V., Peters-Lidard, C. D., Eastman, J. L., and Tao, W.-K.: An integrated high-resolution
hydrometeorological modeling testbed using LIS and WRF, *Environ. Model. Softw.*, 23, 169–181,
doi:10.1016/j.envsoft.2007.05.012, 2008.
- Laprise, R., de Elia, R., Caya, D., Biner, S., Lucas-Picher, P., Diaconescu, E., Leduc, M., Alexandru, A., Sepa-
1705 rovic, L., and Climate, C. N. R.: Challenging some tenets of Regional Climate Modelling, *METEOROLOGY
AND ATMOSPHERIC PHYSICS*, 100, 3–22, doi:10.1007/s00703-008-0292-9, 2008.
- Lawrence, D. M., Oleson, K. W., Flanner, M. G., Thornton, P. E., Swenson, S. C., Lawrence, P. J., Zeng, X.,
Yang, Z.-L., Levis, S., Sakaguchi, K., Bonan, G. B., and Slater, A. G.: Parameterization Improvements and
Functional and Structural Advances in Version 4 of the Community Land Model, *J. Adv. Model. Earth Syst.*,
1710 3, doi:10.1029/2011MS000045, 2011.
- Lebeaupin, C., Béranger, K., Deltel, C., and Drobinski, P.: The Mediterranean response to different space-time
resolution atmospheric forcings using perpetual mode sensitivity simulations, *Ocean Modelling*, 36, 1–25,
doi:10.1016/j.ocemod.2010.10.008, 2011.
- Levitus, S. and Boyer, T. P.: World Ocean Atlas, vol. 4: Temperature, number 4, NOAA/OAR/ESRL PSD,
1715 Boulder, Colorado, USA, 1994.
- Levitus, S., Antonov, J. I., and Boyer, T. P.: Warming of the world ocean, *Geophys. Res. Lett.*, 32, L02 604,
doi:10.1029/2004GL021582, 2005.
- Lin-Jiong, Z., Yi-Min, L., Qing, B., Hai-Yang, Y., and Guo-Xiong, W.: Computational Performance of the
High-Resolution Atmospheric Model FAMIL, *Atmos. Oce. Sci. Lett.*, 5, 355–359, 2012.
- 1720 Lindström, G., Pers, C. P., Rosberg, R., Strömquist, J., and Arheimer, B.: Development and test of the HYPE
(Hydrological Predictions for the Environment) model – A water quality model for different spatial scales,
Hydrology Research, 41 (3–4), 295–319, 2010.
- Lorenz, P. and Jacob, D.: Influence of regional scale information on the global circulation: A two-way nesting
climate simulation, *Geophysical Research Letters*, 32, L18 706, doi:10.1029/2005GL023351, 2005.

- 1725 Ludwig, W., Dumont, E., Meybeck, M., and Heussner, S.: River discharges of water and nutrients to the Mediterranean and Black Sea: Major drivers for ecosystem changes during past and future decades?, *Progress in Oceanography*, 80, 199–217, doi:10.1016/j.pocean.2009.02.001, 2009.
- Madec, G.: NEMO ocean engine, Tech. Rep. 27, Note du Pole de modélisation, Institut Pierre-Simon Laplace (IPSL), France, 2008.
- 1730 Madec, G.: NEMO ocean engine (version 3.3), Tech. Rep. 27, Note du Pole de modélisation, Institut Pierre-Simon Laplace (IPSL), France, 2011.
- Maisonnavé, E. and Caubel, A.: LUCIA, load balancing tool for OASIS coupled systems, TR-CMGC 14-63, CERFACS, 2014.
- Maisonnavé, E., Valcke, S., and Foujols, M.-A.: OASIS Dedicated User Support 2009-2012, Synthesis, Tech. rep., TR/CMGC/13/19, SUC au CERFACS, URA CERFACS/CNRS No1875, Toulouse, France, 2013.
- 1735 Masson, S., Hourdin, C., Benshila, R., Maisonnavé, E., Meurdesoif, Y., Mazauric, C., Samson, G., Colas, F., Madec, G., Bourdallé-Badie, R., Valcke, S., and Coquart, L.: Tropical Channel NEMO-OASIS-WRF Coupled simulations at very high resolution, in: 13th WRF Users' Workshop – 25-29 June 2012, Boulder, CO, USA, 2012.
- 1740 MEDAR-Group: Mediterranean and Black Sea database of temperature, salinity and biochemical parameters and climatological atlas, 4 CD-ROM and www.ifremer.fr/sismer/program/medar/, European Commission Marine Science and Technology Programme (MAST), 2002.
- Müller, M. S., Knüpfer, A., Jurenz, M., Lieber, M., Brunst, H., Mix, H., and Nagel, W. E.: Developing Scalable Applications with Vampir, VampirServer and VampirTrace, in: *Parallel Computing: Architecture, Algorithms and Applications*, pp. 637–644, IOS Press, 2008.
- 1745 Oleson, K., Lawrence, D., Bonan, G., Flanner, M., Kluzek, E., Lawrence, P., Levis, S., Swenson, S., Thornton, P., Dai, A., Decker, M., Dickinson, R., Feddema, J., Heald, C., Hoffman, F., Lamarque, J.-F., Mahowald, N., Niu, G.-Y., Qian, T., Randerson, J., Running, S., Sakaguchi, K., Slater, A., Stockli, R., Wang, A., Yang, Z.-L., Zeng, X., and Zeng, X.: Technical description of version 4.0 of the Community Land Model (CLM), NCAR Tech. Note NCAR/TN-478+STR, Nat. Cent. for Atmos. Res., Boulder, CO, 2010.
- 1750 Oleson, K., Lawrence, D., Bonan, G., Drewniak, B., Huang, M., Koven, C., Levis, S., Li, F., Riley, W., Subin, Z., Swenson, S., Thornton, P., Bozbiyik, A., Fisher, R., Kluzek, E., Lamarque, J.-F., Lawrence, P., Leung, L., Lipscomb, W., Muszala, S., Ricciuto, D., Sacks, W., Sun, Y., Tang, J., and Yang, Z.-L.: Technical description of version 4.5 of the Community Land Model (CLM), NCAR Tech. Note NCAR/TN-503+STR, Natl. Cent. for Atmos. Res., Boulder, CO, doi:10.5065/D6RR1W7M, 2013.
- 1755 Pham, T., Brauch, J., Dieterich, D., Früh, B., and Ahrens, B.: New coupled atmosphere-ocean-ice system COSMO-CLM/NEMO: On the air temperature sensitivity on the North and Baltic Seas, *Oceanologia*, 56, 167–189, doi:10.5697/oc.56-2.167, 2014.
- Prein, A. F., Gobiet, A., Suklitsch, M., Truhetz, H., Awan, N. K., Keuler, K., and Georgievski, G.: Added value of convection permitting seasonal simulations, *Clim. Dyn.*, 41, 2655–2677, doi:10.1007/s00382-013-1744-6, 2013.
- 1760 Reick, C., Raddatz, T., Brovkin, V., and Gayler, V.: Representation of natural and anthropogenic land cover change in MPI-ESM, *Journal of Advances in Modeling Earth Systems*, 5, 459–482, doi:doi:10.1002/jame.20022, 2013.

- 1765 Rockel, B., Will, A., and Hense, A.: The Regional Climate Model CLM, *Meteorol. Z.*, 17, 347–348, 2008.
- Rummukainen, M., Raesänen, J., Bringfelt, B., Ullerstig, A., Omstedt, A., Willen, U., Hansson, U., and Jones, C.: A regional climate model for northern Europe: model description and results from the downscaling of two GCM control simulations, *Clim. Dyn.*, 17, 339–359, 2001.
- Schädler, G.: Numerische Simulationen zur Wechselwirkung zwischen Landoberfläche und atmosphärischer Grenzschicht, Ph.D. thesis, Karlsruher Institut für Technologie, Institut für Meteorologie und Klimaforschung, 1990.
- 1770 Schneck, R., Reick, C., and Raddatz, T.: Land contributions to natural CO₂ variability on time scales of centuries, *Journal of Advances in Modeling Earth Systems*, 5, 354–365, doi:doi:10.1002/jame.20029, 2013.
- Somot, S., Sevault, F., Déqué, M., and Crépon, M.: 21st century climate change scenario for the Mediterranean using a coupled Atmosphere-Ocean Regional Climate Model, *Global and Planetary Change*, 63, 112–126, doi:10.1016/j.gloplacha.2007.10.003, 2008.
- 1775 Staff, S. S.: Soil taxonomy: A basic system of soil classification for making and interpreting soil surveys. 2nd edition, Tech. rep., Natural Resources Conservation Service. U.S. Department of Agriculture Handbook 436, 1999.
- 1780 Stanev, E. and Peneva, E.: Regional sea level response to global forcing. Black Sea examples, *J. Global and Planet. Change*, 32, 33–47, 2002.
- Steiner, A., Pal, J., Giorgi, F., Dickinson, R., and Chameides, W.: The coupling of the Common Land Model (CLM0) to a regional climate model (RegCM), *Theor. Appl. Climatol.*, 82, 225–243, doi:10.1007/s00704-005-0132-5, 2005.
- 1785 Steiner, A. L., Pal, J. S., Rauscher, S. A., Bell, J. L., Diffenbaugh, N. S., Boone, A., Sloan, L. C., and Giorgi, F.: Land surface coupling in regional climate simulations of the West African monsoon, *Clim. Dyn.*, 33, 869–892, doi:10.1007/s00382-009-0543-6, 2009.
- Stevens, B., Giorgetta, M. A., Esch, M., Mauritsen, T., Crueger, T., Rast, S., Salzmann, M., Schmidt, H., Bader, J., Block, K., Brokopf, R., Fast, I., Kinne, S., Kornbluh, L., Lohmann, U., Pincus, R., Reichler, T., and 1790 Roeckner, E.: Atmospheric component of the MPI-M Earth System Model: ECHAM6, *Journal of Advances in Modeling Earth Systems*, 5, 146–172, doi:doi:10.1002/jame.20015, 2013.
- Valcke, S.: The OASIS3 coupler: A European climate modelling community software, *Geoscientific Model Development*, 6, 373–388, doi:doi:10.5194/gmd-6-373-2013, 2013.
- Valcke, S., Craig, T., and Coquart, L.: OASIS3-MCT User Guide, OASIS3-MCT 2.0, Tech. rep., 1795 TR/CMGC/13/17, CERFACS/CNRS SUC URA No 1875, Toulouse, France, 2013.
- Vancoppenolle, M., Fichfet, T., Goosse, H., Bouillon, S., Madec, G., and Maqueda, M.: Simulating the mass balance and salinity of arctic and antarctic sea ice, *Ocean Modelling*, 27, 33–53, 2009.
- Vogel, B., Vogel, H., Bäumer, D., Bangert, M., Lundgren, K., Rinke, R., and Stanelle, T.: The comprehensive model system COSMO-ART - Radiative impact of aerosol on the state of the atmosphere on the regional 1800 scale, *ACP*, 9, 8661–8680, doi:10.5194/acp-9-8661-2009, 2009.
- Vörösmarty, C. J., Fekete, B. M., and Tucker, B. A.: Global River Discharge Database, Version 1.0 (RivDIS V1.0), Volumes 0 through 6, A contribution to IHP-V Theme 1, Technical Documents in Hydrology Series, xxx, UNESCO, Paris, 1996.

- 1805 Wilhelm, C., Rechid, D., and Jacob, D.: Interactive coupling of regional atmosphere with biosphere in the
new generation regional climate system model REMO-iMOVE, *Geoscientific Model Development*, 7, 1093–
1114, doi:doi:10.5194/gmd-7-1093-2014, 2014.
- 1810 Worley, P. H., Mirin, A. A., Craig, A. P., Taylor, M. A., Dennis, J. M., and Vertenstein, M.: Performance
of the Community Earth System Model, in: *SC '11: Proceedings of 2011 International Conference for
High Performance Computing, Networking, Storage and Analysis*, IEEE, ACM, New York, NY, USA,
doi:10.1145/2063384.2063457, 2011.
- Zou, L. and Zhou, T.: Can a Regional Ocean Atmosphere Coupled Model Improve the Simlation of the In-
terannual Variability of the Western North Pacific Summer Monsoon?, *Journal of Climate*, 26, 2353–2367,
doi:10.1175/JCLI-D-11-00722.1, 2013.

Table 1: **List of acronyms** used throughout the paper

Acronym	Meaning
COSMO	Limited-area model of the Consortium for Small-scale Modelling
COSMO-CLM	COSMO model in CLimate Mode
CCLM	Short for COSMO-CLM used in figures, tables, formulas and coupled system acronyms
<i>CCLM_{OC}</i>	CCLM in coupled mode using the mapping of optimum processor configuration
<i>CCLM_{sa}</i>	CCLM stand-alone, not in coupled mode
<i>CCLM_{sa,sc}</i>	<i>CCLM_{sa}</i> using the same mapping as in coupled mode
<i>CCLM_{sa,OC}</i>	<i>CCLM_{sa}</i> using the mapping of optimum processor configuration
CLM	Community Land Model of NCAR
VEG3D	Soil and vegetation model of KIT
NEMO	Community model 'Nucleus for European Modelling of the Ocean'
TRIMNP	Tidal, Residual, Intertidal mudflat Model Nested parallel Processing regional ocean model
CICE	Sea ice model of LANL
MPI-ESM	Global Earth System Model of MPIfM Hamburg
ECHAM	Atmosphere model (ECMWF dynamics and MPIfM Hamburg physics) of MPI-ESM
MPIOM	MPIfM Hamburg Ocean Model of MPI-ESM
OASIS3-MCT	Coupling software for Earth System Models of CERFACS
CESM	Community Earth System Model
Institutions	
MPIfM	Max-Planck-Institut für Meteorologie Hamburg, Germany
LANL	Los Alamos National Laboratory, USA
CERFACS	Centre Europeen de Recherche et de Formation Avancee en Calcul Scientifique, Toulouse, France
CLM-Community	Climate Limited-area Modelling (CLM-)Community
ECMWF	European Center for Medium Range Weather Forecast, Reading, Great Britain
NCAR	National Center for Atmospheric Research, Boulder, USA
CNRS	Centre National de Recherche Scientifique, Paris, France
ETH	Eidgenössische Technische Hochschule, Zürich, Switzerland
KIT	Karlsruher Institut für Technologie, Germany
GUF	Goethe-Universität Frankfurt am Main, Germany
HZG	Helmholtz-Zentrum Geesthacht, Germany
BTU	Brandenburgische Technische Universität Cottbus-Senftenberg, Cottbus, Germany
FUB	Freie Universität Berlin, Germany
Model domains	
CORDEX-EU	CORDEX domain for regional climate simulations over Europe

Table 2: **Coupled model systems**, their components and the institution at which they are used. For the meaning of acronyms see Table 1.

Coupled model system	Institution	First coupled component	Second coupled component
CCLM+CLM	ETH	CLM	–
CCLM+VEG3D	KIT	VEG3D	–
CCLM+NEMO-MED12	GUF	NEMO-MED12	–
CCLM+TRIMNP+CICE	HZG	TRIMNP	CICE
CCLM+MPI-ESM	BTU and FUB	ECHAM	MPIOM

Table 3: **Properties of the coupled model components.** For the meaning of acronyms see Table 1. The configuration used is a coarse-grid regional climate simulation configuration used for sensitivity studies, tests and continental-scale climate simulations. Model complexity is measured as the number of prognostic variables. For a comprehensive definition, see (Balaji et al., 2017)

model	CCLM	CLM	VEG3D	MPI-ESM
Full name	COSMO model in climate mode	Community Land Model	Vegetation model	Max Planck Institute Earth System Model
Institution	CLM-Community	NCAR and other institutions	KIT	MPIFM Hamburg
Coupling area	CORDEX-EU	CORDEX-EU land	CORDEX-EU land	CORDEX-EU
Horizontal res. (km)	50	50	50	330
Nr. of levels	40/45	15	10	47
Time step (s)	300	300	300	600
Grid points (10^3)	766	142	95	3118
Complexity	35	<1	<1	58
Reference	(Baldauf et al., 2011)	(Oleson et al., 2010)	(Schädler, 1990)	(Stevens et al., 2013)
model	NEMO-MED12	NEMO-NORDIC	TRIMNP	CICE
Full name	Nucleus for European Modelling of the Ocean - Mediterranean Sea	Nucleus for European Modelling of the Ocean - North and Baltic Sea	Tidal, Residual, Intertidal mudflat	Sea Ice Model
Institution	CNRS	CNRS	Model Nested parallel Processing Univ. Trento, HZG	LANL
Coupling area	Mediterranean Sea (without Black Sea)	North and Baltic Sea	North and Baltic Sea	Baltic Sea and Kattegat
Horizontal res. (km)	6-8	3.7	12.8	12.8
Nr. of levels	50	56	50	5
Time step (s)	720	300	240	240
Grid points (10^3)	2767	4187	877	28
Complexity	8	8	11	<1
Reference	Madec (2008); Lebeaupin et al. (2011); Akhtar et al. (2014)	Hordoir et al. (2013), Dieterich et al. (2013); Pham et al. (2014)	Casulli and Cattani (1994), Casulli and Stelling (1998); Ho-Hagemann et al. (2013)	Hunke et al. (2013); Ho-Hagemann et al. (2013)

Table 4: **Variables exchanged between CCLM and the global model MPI-ESM.** The CF standard-names convention is used. Units are given as defined in CCLM. \otimes : information is sent by CCLM; \odot : information is received by CCLM. $3D$ indicates that a 3-dim. field is sent/received.

Variable (unit)	CCLM+MPI-ESM
Temperature (K)	$\odot \otimes 3D$
U-component of wind ($m s^{-1}$)	$\odot \otimes 3D$
V-component of wind ($m s^{-1}$)	$\odot \otimes 3D$
Specific humidity ($kg kg^{-1}$)	$\odot \otimes 3D$
Specific cloud liquid water content ($kg kg^{-1}$)	$\odot \otimes 3D$
Specific cloud ice content ($kg kg^{-1}$)	$\odot \otimes 3D$
Surface pressure (Pa)	$\odot \otimes$
Sea surface temperature SST (K)	\odot
Surface snow amount (m)	\odot
Surface geopotential ($m s^{-2}$)	\odot

$$SST = (sea_ice_area_fraction \cdot T_{sea\ ice}) + (SST \cdot (1 - sea_ice_area_fraction))$$

Table 5: As Table 4 but **variables exchanged between CCLM and the ocean models NEMO, TRIMNP and CICE.**

Variable (unit)	CCLM+ NEMO- MED12	CCLM+ NEMO- NORDIC	CCLM+ TRIMNP+ CICE
Surface temperature over sea/ocean (K)	⊙	⊙	⊙
2 m temperature (K)	–	–	⊗
Potential temperature NSL (K)	–	–	⊗
Temperature NSL (K)	–	–	⊗
Sea ice area fraction (1)	–	⊙	–
Surface pressure (Pa)	–	⊗	–
Mean sea level pressure (Pa)	–	–	⊗
Surface downward east- and northward stress (Pa)	⊗	⊗	–
Surface net downward shortwave flux ($W m^{-2}$)	⊗	⊗	⊗
Surface net downward longwave flux ($W m^{-2}$)	–	–	⊗
Non-solar radiation NSR ($W m^{-2}$)	⊗	⊗	–
Surface downward latent heat flux ($W m^{-2}$)	–	–	⊗
Surface downward heat flux HFL ($W m^{-2}$)	–	–	⊗
Evaporation-Precipitation $E - P$ ($kg m^{-2}$)	⊗	⊗	–
Total precipitation flux TPF ($kg m^{-2} s^{-1}$)	–	–	⊗
Rain flux RF ($kg m^{-2} s^{-1}$)	–	–	⊗
Snow flux SF ($kg m^{-2} s^{-1}$)	–	–	⊗
U- and V-component of 10 m wind ($m s^{-1}$)	–	–	⊗
2 m relative humidity (%)	–	–	⊗
Specific humidity NSL ($kg kg^{-1}$)	–	–	⊗
Total cloud cover (1)	–	–	⊗
Half height of lowest CCLM level (m)	–	–	⊗
Air density NSL ($kg m^{-3}$)	–	–	⊗

NSL = the lowest (near-surface) level of the 3-dimensional variable

NSR = surface net downward longwave flux + surface downward latent and sensible heat flux

HFL = surface net downward shortwave flux + surface downward longwave flux + surface downward latent and sensible heat flux

TPF = RF + SF = convective and large-scale rainfall flux + convective and large-scale snowfall flux

E-P = -(surface downward sensible heat flux / LHV) - TPF; LHV: Latent heat of vaporization = 2.501E6 J/kg

Table 6: As Table 4 but **variables exchanged between CCLM and the land surface models VEG3D and CLM.**

Variable (unit)	CCLM+VEG3D	CCLM+CLM
Leaf area index (1)	⊗	–
Plant cover (1)	⊗	–
Vegetation function (1)	⊗	–
Surface albedo (1)	⊙	⊙
Height of lowest level (m)	–	⊗
Surface pressure (Pa)	⊗	–
Pressure NSL (Pa)	⊗	⊗
Snow flux SF ($kg\ m^{-2}\ s^{-1}$)	⊗	⊗
Rain flux RF ($kg\ m^{-2}\ s^{-1}$)	⊗	⊗
Temperature NSL (K)	⊗	⊗
Grid-mean surface temperature (K)	⊙	⊙
Soil surface temperature (K)	⊙	–
Snow surface temperature (K)	⊙	–
Surface snow amount (m)	⊙	–
Density of snow ($kg\ m^{-3}$)	⊙	–
Thickness of snow (m)	⊙	–
Canopy water amount (m)	⊙	–
Specific humidity NSL ($kg\ kg^{-1}$)	⊗	⊗
Surface specific humidity ($kg\ kg^{-1}$)	⊙	–
Subsurface runoff ($kg\ m^{-2}$)	⊙	–
Surface runoff ($kg\ m^{-2}$)	⊙	–
Wind speed $ \vec{v} $ NSL ($m\ s^{-1}$)	⊗	–
U- and V-component of wind NSL ($m\ s^{-1}$)	–	⊗
Surface downward sensible heat flux ($W\ m^{-2}$)	⊙	⊙
Surface downward latent heat flux ($W\ m^{-2}$)	–	⊙
Surface direct and diffuse downwelling shortwave flux in air ($W\ m^{-2}$)	⊗	⊗
Surface net downward longwave flux ($W\ m^{-2}$)	⊗	⊗
Surface flux of water vapour ($s^{-1}\ m^{-2}$)	⊙	–
Surface downward east- and northward flux (U-/V-momentum flux, Pa)	–	⊙

NSL = the lowest (near-surface) level of the 3-dimensional variable

RF = convective and large-scale rainfall flux; SF = convective and large-scale snowfall flux

SWD_S = surface diffuse and direct downwelling shortwave flux in air

Table 7: **Measures of computational performance** used for computational performance analysis.

Measure (unit)	Acronym	Description
simulated years (1)	sy	Number of simulated physical years
number of cores (1)	n	Number of computational cores used in a simulation per model component
number of threads (1)	R	Number of parallel processes or threads configured in a simulation per model component. On <i>Blizzard</i> at DKRZ one or two threads can be started on one core.
time to solution ($HPSY$)	T	Simulation time of a model component measured by LUCIA per simulated year
speed ($HPSY^{-1}$)	s	$= T^{-1}$ is the number of simulated years per simulated hour by a model component
costs ($CHPSY$)	–	$= T \cdot n$ is the core hours used by a model component running on n cores per simulated year
speed-up (%)	SU	$= \frac{HPSY_1(R_1)}{HPSY_2(R_2)} \cdot 100$ is the ratio of time to solution of a model component configured for reference and actual number of threads
parallel efficiency (%)	PE	$= \frac{CHPSY_1}{CHPSY_2} \cdot 100$ is the ratio of core hours per simulated year for reference ($CHPSY_1$) and actual ($CHPSY_2$) number of cores

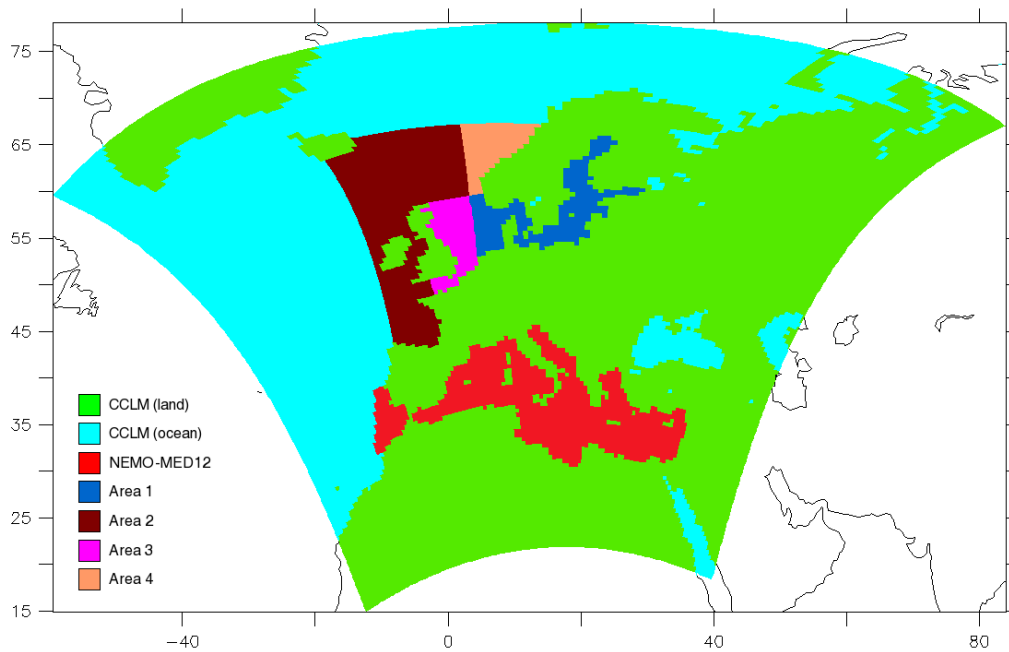


Figure 1: **Map of coupled system components.** All components are bounded by the COSMO-CLM extension (CORDEX-EU), except ECHAM and MPI-OM (global domain). CLM and VEG3D cover the same area than land points of COSMO-CLM. TRIMNP, CICE and NEMO-NORDIC are sharing the area 1. CICE also covers the area 4, NEMO-NORDIC the area 3, TRIMNP the areas 2, 3 and 4.

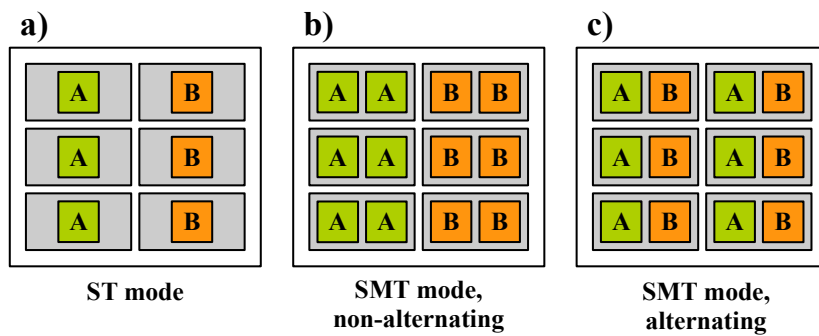


Figure 2: **Schematic processes distribution on a hypothetical computing node** with six cores (gray-shaded areas) in a) ST mode, b) SMT mode with non-alternating processes distribution and c) SMT mode with alternating processes distribution. "A" and "B" are processes belonging to two different parallel applications sharing the same node. In b) and c) two processes of the same (b) or different (c) application share one core using the simultaneous multi-threading (SMT) technique while in a) only one process per core is launched in the single-threading (ST) mode.

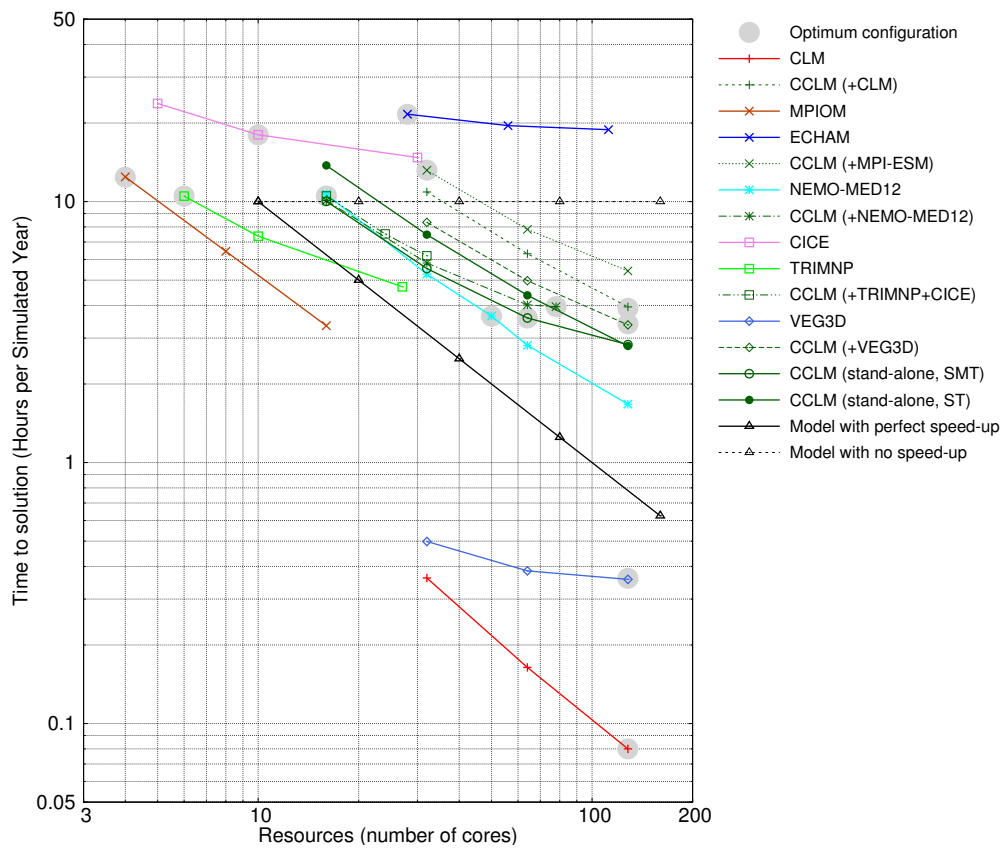


Figure 3: **Time to solution of model components** of the coupled systems (indicated for CCLM in brackets) and for CCLM stand-alone ($CCLM_{sa}$) in hours per simulated year (HPSY) in dependence on the computational resources (number of cores) in single threading (ST) and in multi threading (SMT) mode. The times for model components ECHAM and MPIOM of MPI-ESM are given separately. The optimum configuration of each component is highlighted by a gray dot. The hypothetical result for a model with perfect and no speed-up is given as well.

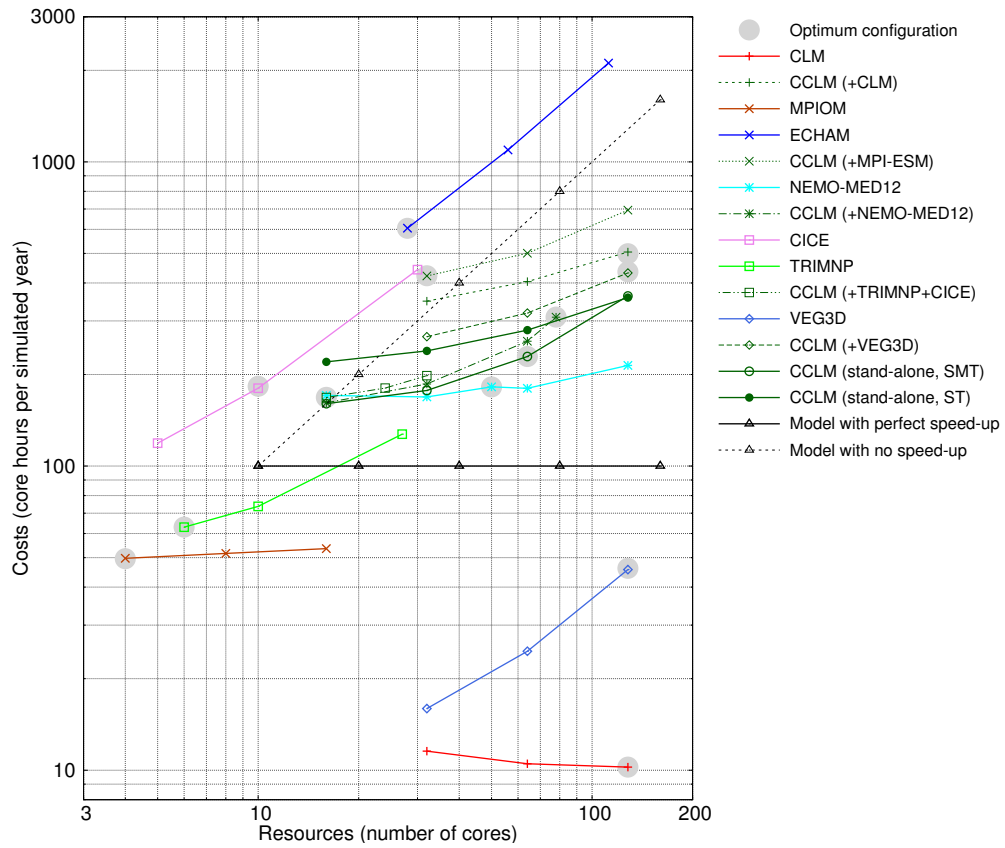


Figure 4: As Fig. 3 but for the **costs of the model components** in core hours per simulated year.

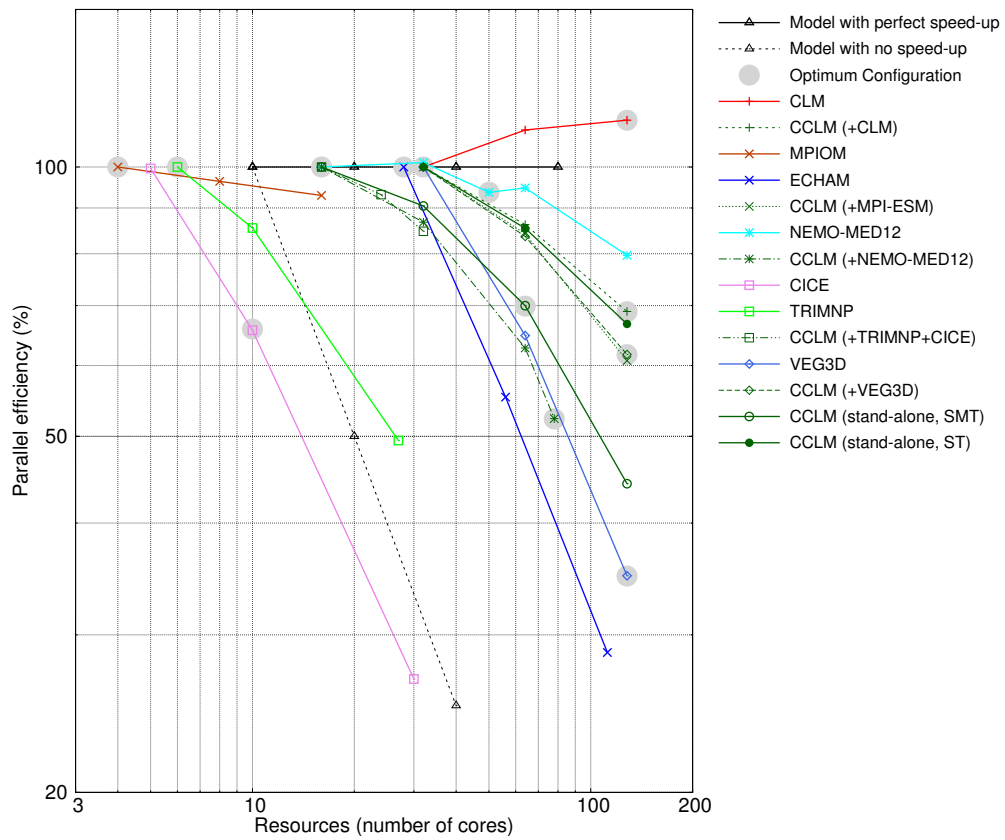


Figure 5: As Fig. 3 but for the **parallel efficiency of the model components** in % of the reference configuration.

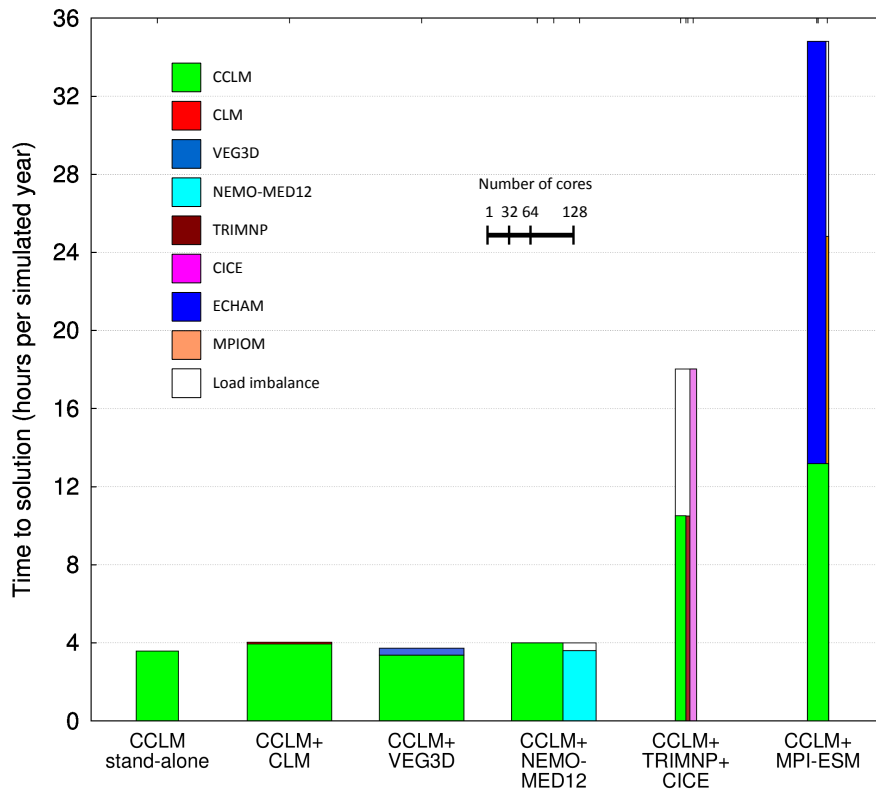


Figure 6: **Time to solution and costs of model components at optimum configuration** of couplings investigated and of stand-alone CCLM. The boxes' widths correspond to the number of cores used per component. The area of each box is equal to the costs (the amount of core hours per simulated year) consumed by each component calculations, including coupling interpolations. The white areas indicate the load imbalance between concurrently running components. See Table 8 for details.

Table 8: **Analysis of optimum configurations of the coupled systems (CS)** given in the table header (compare to Fig. 6). *seq* refers to sequential and *con* to concurrent couplings. *Thread mode* is either the ST or the SMT mode (see Fig. 2). *APD* indicates whether an alternating processes distribution was used or not. *levels in CCLM* gives the simulated number of levels and *CCLM version* is the COSMO-CLM model version used for coupling. Relative *Time to solution (%)* and *Cost (%)* are calculated with respect to the reference, which is the CCLM stand-alone configuration $CCLM_{sa}$ using 64 cores and non-alternating SMT mode. The time to solution includes the time needed for OASIS interpolations. All relative quantities in lines 2.2-2.3 and 3.2-3.3.5 are given in percent of $CCLM_{sa}$ time to solution (line 8) and cost (all others). $CS - CCLM_{sa}$ gives the differences between CS and the optimum $CCLM_{sa}$ configuration. This difference is separated in 5 components of cost: *coupled component* component models coupled with CCLM. *OASIS hor. interp.* all horizontal interpolations computed by OASIS. *load imbalance* load imbalance between the concurrently running models. $CCLM_{sa,sc} - CCLM_{sa}$ difference between stand-alone CCLM process mappings used in the particular coupling and for optimum configuration. $CCLM - CCLM_{sa,sc}$ difference between coupled and stand-alone CCLM using process mapping of the coupling

	CCLM stand- alone	CCLM+ CLM	CCLM+ VEG3D	CCLM+ NEMO- MED12	CCLM+ TRIMNP +CICE	CCLM+ ECHAM+ MPIOM
1.1 Type of coupling	–	seq	seq	con	con	seq + con
1.2 Thread mode	SMT	SMT	SMT	SMT	SMT	SMT
1.3 APD used	–	yes	yes	no	no	yes
1.4 # nodes	2	4	4	4	1	1
1.5 # cores per component	64	128, 128	128, 128	78, 50	16, 6, 10	32, 28, 4
1.6 levels in CCLM	45	40	45	40	40	45
1.7 CCLM version	4.8	5.0	4.8	4.8	4.8	4.8
2.1 Time to solution (<i>HPSY</i>)	3.6	4.0	3.7	4.0	18.0	34.8
2.2 Time to solution (%)	100.0	111.1	102.8	111.1	450.0	866.7
2.3 $CS - CCLM_{sa}(\%)$	–	11.1	2.8	11.1	350.0	766.7
3.1 CS Cost (<i>CHPSY</i>)	230.4	512.0	473.6	512.0	576.0	1113.6
3.2 CS Cost (%)	100.0	222.2	205.6	222.2	250.0	483.3
3.3 $CS - CCLM_{sa}(\%)$	–	122.2	105.6	122.2	150.0	383.3
3.3.1 coupled component (%)	–	4.3	19.7	79.9	27.2+77.9	261+20.1
3.3.2 OASIS hor. interp. (%)	–	6.3	0.0	0.05	0.76	3.3
3.3.3 load imbalance (%)	–	–	–	6.9	71.5	17.2
3.3.4 $CCLM_{sa,sc} - CCLM_{sa}(\%)$	–	56,2	56,2	16.3	-30.0	4.3
3.3.5 $CCLM - CCLM_{sa,sc}(\%)$	–	55,4	29,7	19.0	2.6	77.4

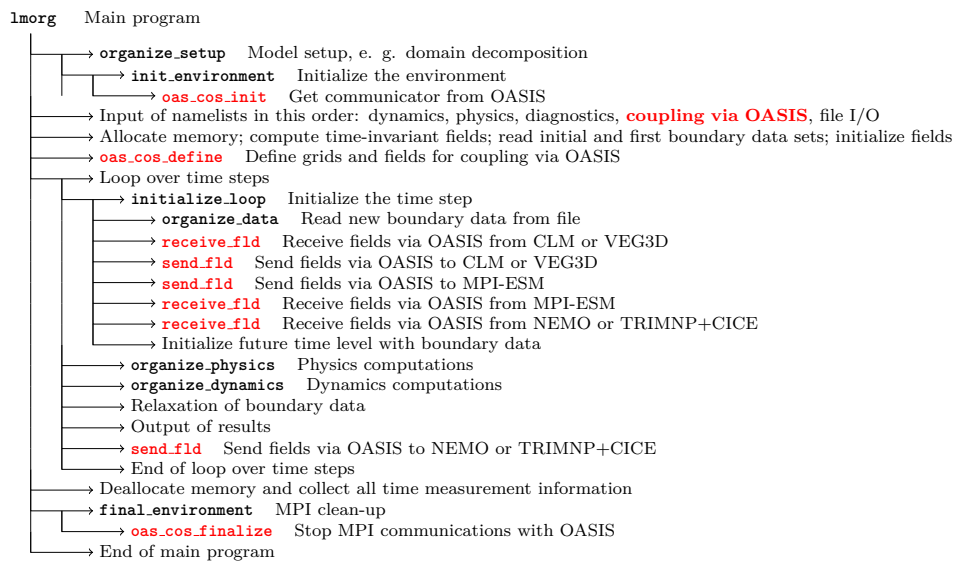


Figure 7: **Simplified flow diagram of the main program of the regional climate model COSMO-CLM, version 4.8_clm19_uoi.** The red highlighted parts indicate the locations at which the additional computations necessary for coupling are executed and the calls to the OASIS interface take place. Where applicable, the component models to which the respective calls apply are given.



Figure 8: As Fig. 7 but for the global atmosphere model ECHAM of MPI-ESM.

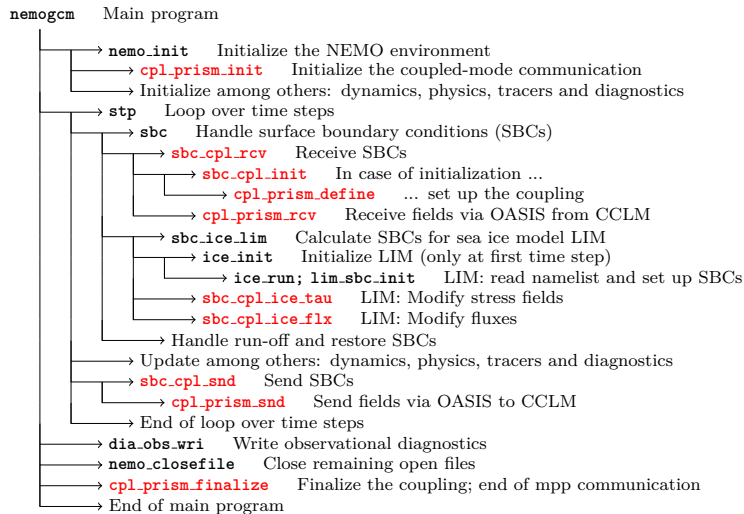


Figure 9: As Fig. 8 but for the ocean model NEMO version 3.3.

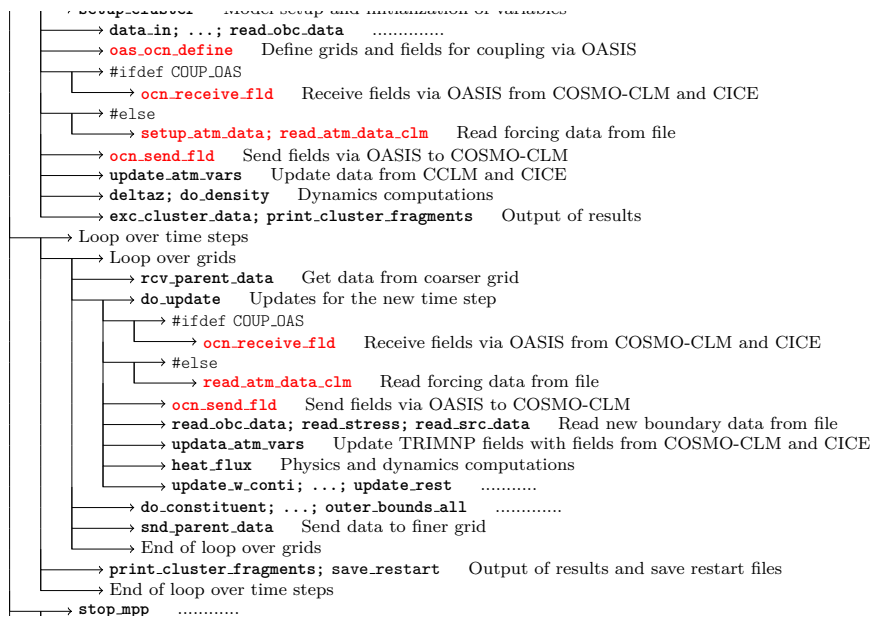


Figure 10: As Fig. 8 but for the ocean model TRIMNP.

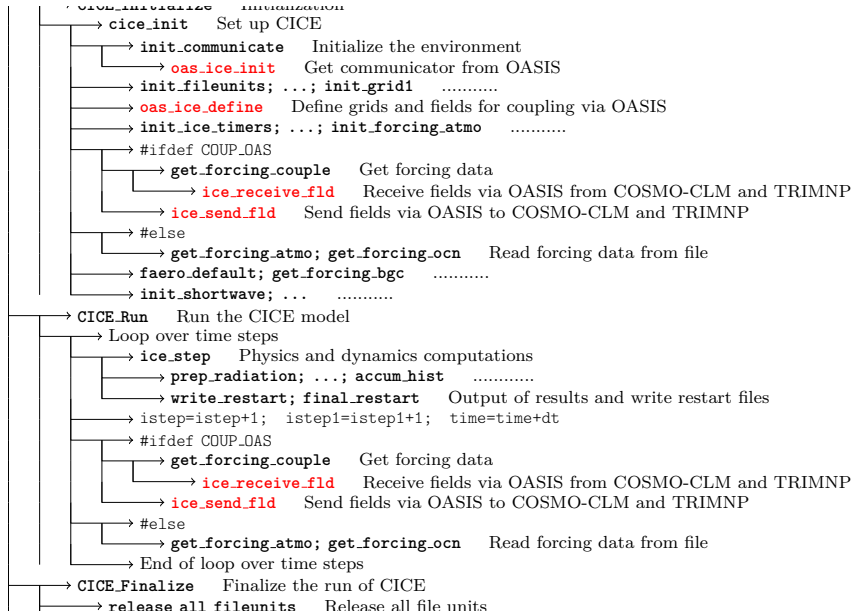


Figure 11: As Fig. 8 but for the sea ice model CICE.

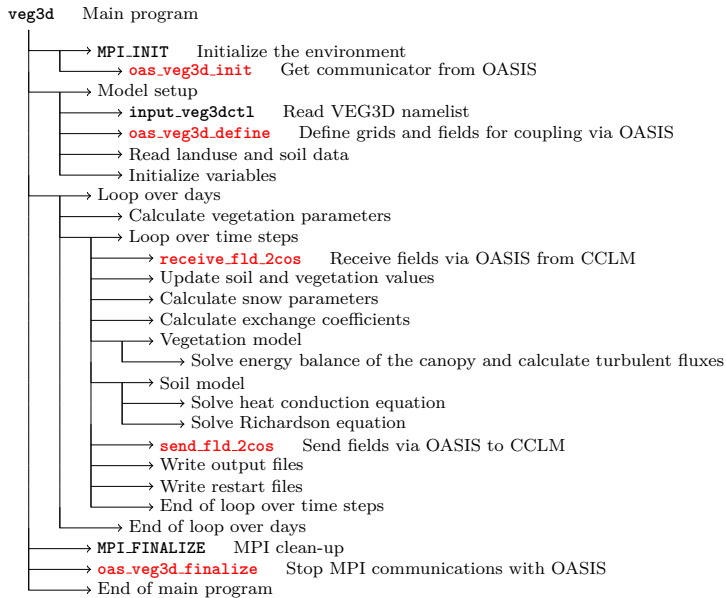


Figure 12: As Fig. 8 but for the soil-vegetation model VEG3D.

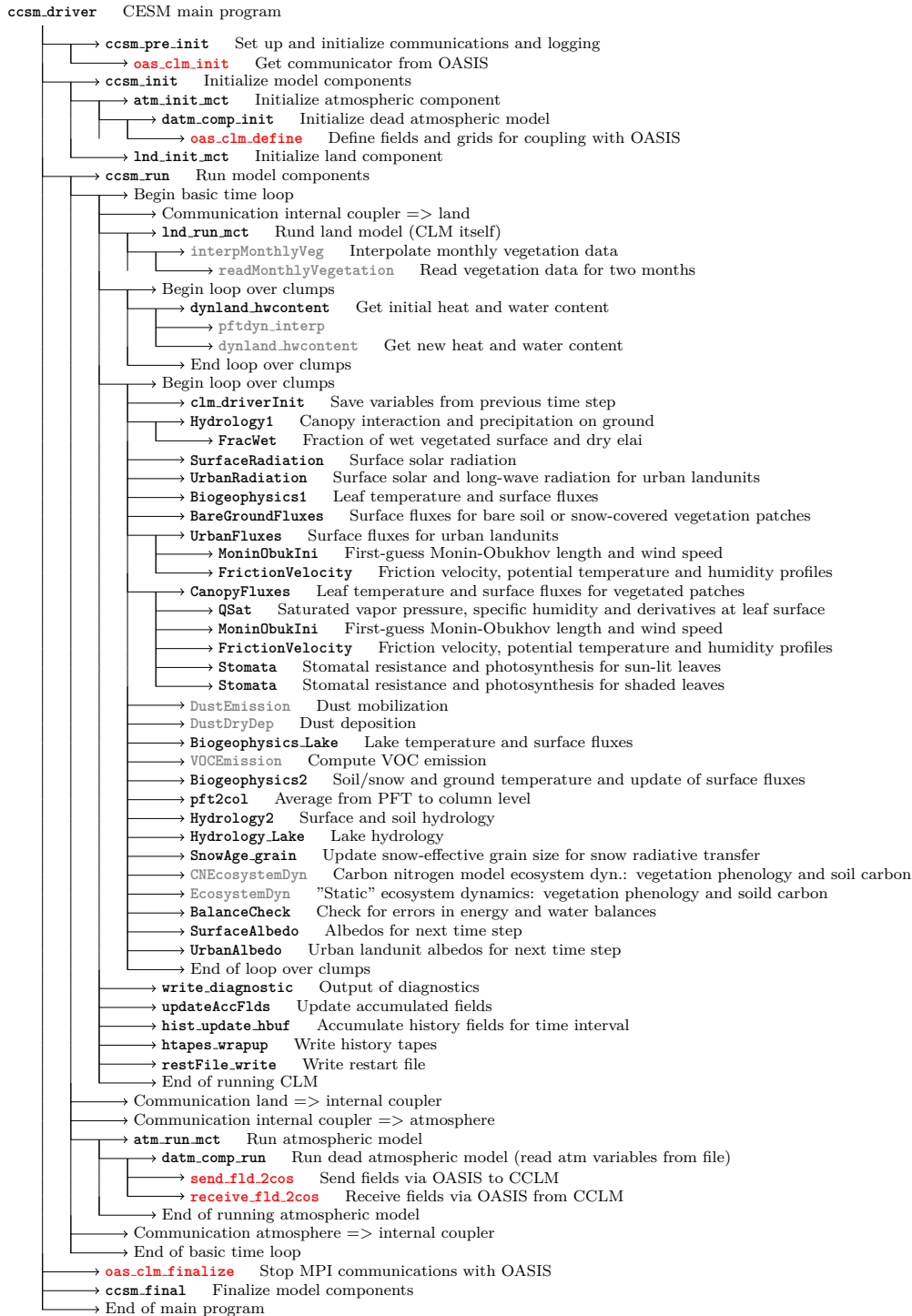


Figure 13: As Fig. 8 but for the Community Land Model (CLM). The gray highlighted routines are optional.